# A THEORETICAL INVESTIGATION OF THERMAL WAVES

by

**Jay Irwin Frankel**

Dissertation submitted to the faculty of the
**Virginia Polytechnic Institute and State University**
in partial fulfillment of the requirements for the degree of

**DOCTOR OF PHILOSOPHY**

in

Mechanical Engineering

APPROVED:

Dr. Brian Vick, Chairman

Dr. J. R. Thomas, Jr.

Dr. M. C. Edlund

Dr. L. W. Johnson

Dr. D. J. Nelson

August 1986
Blacksburg, Virginia

# A THEORETICAL INVESTIGATION OF THERMAL WAVES

by

Jay I. Frankel

ABSTRACT

A unified and systematic study of one-dimensional heat conduction based on thermal relaxation is presented. Thermal relaxation is introduced through the constitutive equation (modified Fourier's law) which relates this heat flux and temperature. The resulting temperature and flux field equations become hyperbolic rather than the usual classical parabolic equations encountered in heat conduction. In this formulation, heat propagates at a finite speed and removes one of the anomalies associated to parabolic heat conduction, i.e., heat propagating at an infinite speed. In situations involving very short times, high heat fluxes, and cryogenic temperatures, a more exact constitutive relation must be introduced to preserve a finite speed to a thermal disturbance.

The general one-dimensional temperature and flux formulations for the three standard orthogonal coordinate systems are presented. The general solution, in the temperature domain, is developed by the finite integral transform technique. The basic physics and mathematics are demonstrated by reviewing Taitel's problem. Then attention is turned to the effects of radially dependent systems, such as the case of a cylinder and sphere. Various thermal disturbances are studied showing the

unusual physics associated with dissipative wave equations. The flux formulation is shown to be a viable alternative domain to develop the flux distribution. Once the flux distribution has been established, the temperature distribution may be obtained through the conservation of energy.

Linear one-dimensional composite regions are then investigated in detail. The general temperature and flux formulations are developed for the three standard orthogonal coordinate systems. The general solution for the flux and temperature distributions are obtained in the flux domain using a generalized integral transform technique. Additional features associated with hyperbolic heat conduction are displayed through examples with various thermal disturbances.

A generalized expression for temperature dependent thermal conductivity is introduced and incorporated into the one-dimensional hyperbolic heat equation. An approximate analytical solution is obtained and compared with a standard numerical method.

Finally, recommendations for future analytical and experimental investigations are suggested.

ACKNOWLEDGEMENTS

The author wishes to thank his parents, grandparents, and his brother Gary for their continual support and encouragement. The author wishes to dedicate this effort to his wife, Valerie and their soon to be born child. He also wishes to give special thanks to his advisor and friend Dr. Brian Vick for his support and many colorful conversations. The author expresses much thanks to Dr. J. R. Thomas, Jr., Dr. D. J. Nelson, Dr. M. C. Edlund, and Dr. L. W. Johnson for serving on his committee. Finally, he wishes to thank Mrs. Lynne Sawyer for her meticulous efforts in typing this dissertation.

TABLE OF CONTENTS

Page

TABLE OF CONTENTS (cont'd)

TABLE OF CONTENTS (cont'd)

LIST OF FIGURES

LIST OF FIGURES (cont'd)

LIST OF FIGURES (cont'd)

LIST OF TABLES

NOMENCLATURE

$a_1, a_{N+1}$ , constants relating type of boundary condition

$a_j(\lambda_m, \xi)$ , function associated with degenerate kernel

$A_{m\ell k}$ , set of constants defined in Eq. (5.3.13b)

$b_1, b_{N+1}$ , constants relating type of boundary condition

$b_j(\lambda_m, \xi)$ , function associated with degenerate kernel

$B_{\ell m}$ , set of constants defined by Eq. (4.3.14)

$B_j$ , boundary operator j = i,o (inner,outer)

$c$ , propagation speed

$c_i$ , propagation speed for region i

$c_j(\lambda_m, \xi)$ , dependent variable defined by Eq. (4.3.20b)

$C_p$ , specific heat

$C_{1j}, C_{2j}$ , dimensionless boundary coefficients, j = i,o

$C^*_{1j}, C^*_{2j}$ , boundary coefficients, j = i,o

$G(\eta, \xi/\eta_o, \xi_o)$ , Green's function

$\overline{G}_m(\lambda_m, \xi_o)$ , transform of Green's function

$L$ , modified heat flux linear operator

$L^*$ , formal adjoint of L

$k$ , thermal conductivity

$k_o$ , thermal conductivity at initial reference temperature

$k_i$ , thermal conductivity for region i

$K(\xi, \xi_o; \lambda_m)$ , degenerate kernel

$M_p$ , modified heat conduction linear operator

$N(\lambda_m)$ , normalization integral

$p$ , radial geometry indicator

$q(x,t)$ , heat flux

$N(\lambda_m)$ , normalization integral

$q_{w,j}(t)$ , prescribed flux boundary function, j=1, N+1

$q_i(x,t)$ , heat flux for region i

$Q_i(\eta,\xi)$ , dimensionless heat flux

$\overline{Q}_m(\xi)$ , transform of dimensionless heat flux

$S(\eta,\xi)$ , dimensionless heat source

$t$ , time variable

$T(x,t)$ , temperature

$T_o$ , initial temperature

$T_{ref}$ , reference temperature

$t$ , time variable

$T_o$ , initial temperature

$T_{w,j}(t)$ , prescribed temperature boundary functions, j=1, N+1

$T_i(x,t)$ , temperature for region i

$u(x,t)$ , volumetric heat source

$u_i(x,t)$ , volumetric heat source in region i

$U_o$ , total energy associated to u(x,t)

$V_m(\xi)$ , dimensionless transform disturbance function

$x$ , space variable

Greek Symbols

$\alpha$ , thermal diffusivity

$\alpha_o$ , thermal diffusivity at initial temperature $T_o$

$\alpha_i$ , thermal diffusivity for region i

$\beta_n$ , general thermal conductivity coefficient

$\beta'$ , thermal conductivity coefficient

$\delta$ , Dirac Delta Function

$\varepsilon$ , small increment

$\eta$ , dimensionless space variable

$\theta(\eta,\xi)$ , dimensionless temperature

$\theta_i(\eta,\xi)$ , dimensionless temperature for region i

$\overline{\theta}_m(\xi)$ , dimensionless transform

$\lambda_m$ , eigenvalues

$\xi$ , dimensionless time

$\rho$ , density

$\rho_i$ , density for region i

$\tau$ , relaxation time

$\tau_i$ , relaxation time for region i

$\phi(\eta,\xi)$ , auxiliary function

$\psi_m(\eta)$ , eigenfunction associated to eigenvalue $\lambda_m$

$\psi_{im}(\eta)$ , eigenfunction for region i

Superscripts

$*$ , dimensionless quantity

# Chapter 1

# INTRODUCTION

## 1.1 Basic Parabolic Heat Conduction

In classical heat conduction theory, the constitutive law governing heat flow in a homogeneous material is given by Fourier's law

$$q = -k \frac{\partial T}{\partial x} , \tag{1.1.1}$$

where $q(x,t)$ is the local heat flux, $k$ is the thermal conductivity, $T(x,t)$ is the temperature, and where $x$ and $t$ are the spatial and temporal variables, respectively. In words, Fourier's law states that the local heat flux is proportional to the negative of the temperature gradient. The thermal conductivity $k$, is a measurable material property which indicates the amount of heat that will flow per unit area when the temperature gradient is unity. This law is named in honor of J. B. J. Fourier who proposed it in 1822 from experimental observations at steady state conditions.

Phenomenologically speaking, diffusion is the experimental recognition that heat flows from a point of higher temperature to a point of lower temperature in a medium. In this continuum description of heat conduction, the mean free path of the particles are small compared with the other dimensions existing in the medium. In that way, a global (field) description may be formulated.

On the molecular level, the mechanism of diffusion is visualized as the exchange of kinetic energy between the molecules in the regions of high and low temperatures. In particular, it is attributed to

translational movements and collisions of molecules in gases, free electrons in metallic liquids and metals which lead to rapid energy transport, and to vibrational interactions in nonmetallic liquids and solids where molecules are more closely packed.

Engineering heat transfer analysis is based on two physical relationships, namely a constitutive law and a general law. The first law of thermodynamics represents the general law required in the formulation of a heat transfer problem. Performing a one-dimensional energy balance in a stationary medium in the usual manner [1], we get

$$- \frac{\partial q}{\partial x} + u = \rho \frac{de}{dt} , \tag{1.1.2}$$

where $u(x,t)$ is an arbitrary volumetric heat source, $\rho$ is the density, and e is the internal energy. For solids and incompressible fluids, the internal energy is assumed to be only a function of temperature and an equation of state may be written as

$$de = C_p \, dT \tag{1.1.3}$$

where $C_p$ is the specific heat at constant pressure. Substituting Eq. (1.1.3), for the internal energy, into the conservation of energy equation, we arrive at

$$- \frac{\partial q}{\partial x} + u = \rho C_p \frac{\partial T}{\partial t} \tag{1.1.4}$$

When the constitutive relation (flux law) as expressed in Eq. (1.1.1) is used to eliminate the heat flux in Eq. (1.1.4), we arrive at the usual parabolic temperature field equation

$$k \frac{\partial^2 T}{\partial x^2} + u = \rho C_p \frac{\partial T}{\partial t} . \qquad (1.1.5)$$

## 1.2 Controversy in Fourier's Law

Though Fourier's law represents one of the best models in mathematical physics, it possesses many anomalies, the most predominant being that it associates an infinite speed of propagation to a thermal disturbance. In other words, any thermal disturbance on a medium is instantaneously felt throughout the medium. An instantaneous propagation of heat is physically impossible since thermal energy is carried by molecular motion which propagates at finite speed. The usual assumption (or justification) is that the diffusion equation is correct only after a sufficient amount of time has elapsed. In view of this, the temperature field equation expressed in Eq. (1.1.5) may be considered a limiting form of a transport equation where the velocity of the particles are infinite.

Despite this apparent paradox, Fourier's law is quite accurate for most common engineering situations. However with the advent of laser and nuclear technologies, there appear to be situations where such a description of heat conduction is inappropriate. This law noticeably breaks down in circumstances involving very short times, large temperature gradients or at cryogenic temperatures (temperatures near

absolute zero) where diffusion theory cannot account for short-time inertial effects. Many applications require a more accurate determination of the temperature distribution. Applications such as laser welding, drilling, annealing, and cutting which may involve femtosecond to nanosecond pulses, explosive bonding, laser fusion reactors where fuel pellets are bombarded with short time pulsed laser sources, fast flux reactors, electrical discharge machining, rarefied supersonic flow, catalytic supported crystallites, and the study of heat and mass transfer in capillary-porous bodies are possible areas where the influence of a finite rate of propagation of heat may become appreciable. Since thermally induced stress waves [2] are directly related to the temperature distribution in uncoupled thermoelasticity, an accurate account of the temperature is important with respect to design engineering. A finite propagation velocity of a disturbance can also play an important role in problems involving coupled elastic-thermal-electromagnetic fields [3].

## 1.3 Basic Hyperbolic Heat Conduction

It is apparent in situations involving short times, cryogenic temperatures or large temperature gradients that a more exact constitutive law is required in describing the true nature of heat conduction. The dilemma of an infinite speed of propagation of a thermal disturbance can be resolved by introducing the concept of thermal relaxation. It was originally proposed by Maxwell [4] via kinetic considerations and later by Vernotte [5-7], Cattaneo [8], and Morse and Feshbach [9] on a heuristic basis that the constitutive law of

heat conduction should account for thermal relaxation or the finite buildup time for the onset of heat to flow. The proposed relation , commonly known as the modified Fourier's law, is

$$\tau \frac{\partial q}{\partial t} + q = - k \frac{\partial T}{\partial x} , \qquad (1.3.1)$$

where $\tau$ is the thermal relaxation time. Physically, $\tau$ represents the start-up time required for the commencement of heat flow after a temperature gradient has been imposed. The apparent paradox can be resolved by noting that Fourier's law may be interpreted as an approximation to Eq. (1.3.1).

In Eq. (1.3.1), we see that two independent material properties are present. The thermal conductivity k, can be measured accurately by various methods [10]. However, difficulties arise in obtaining accurate measurements of the relaxation time $\tau$ for most materials. In metals, the relaxation time apparently ranges from $10^{-14}$ seconds to $10^{-9}$ seconds. At cryogenic temperatures, the relaxation times become relatively large and thus permit an arena where thermal waves may be observed.

The introduction of the modified Fourier's law, as the particular law relating the heat flux to the temperature, also completes the analogy between electricity and heat transfer [11-13] as shown in Table 1.3.1. Previously, no heat transfer quantity had been proposed to be the equivalent of electrical inductance. Besides the usual analogy with electricity [14], conduction based on the modified Fourier's law now has an exact analogy with fluid mechanics [15], mass transfer [13],

turbulent heat transfer [13], and acoustics. Table 1.3.1 also displays the analogy with fluid mechanics, where one can consider Newtonian liquids as a viscoelastic body with zero relaxation time. Consequently as $\tau = \mu/K \to 0$, a liquid substance behaves like an ordinary viscous liquid.

When the modified Fourier's law is used in conjunction with the energy equation displayed in Eq. (1.1.4), a new heat equation (temperature field equation) is developed, namely

$$k \frac{\partial^2 T}{\partial x^2} + \left(u + \tau \frac{\partial u}{\partial t}\right) = \rho C_p \left(\frac{\partial T}{\partial t} + \tau \frac{\partial^2 T}{\partial t^2}\right) . \qquad (1.3.2)$$

The resulting temperature field equation is a dissipative wave equation which now associates a finite speed of propagation to heat flow. The speed of propagation becomes

$$c = \sqrt{k/(\rho C_p \tau)} , \qquad (1.3.3)$$

which is finite for positive relaxation times $\tau$. The speed c may be interpreted as the average thermal velocity of the molecules.

It is apparent that as the relaxation time $\tau$ approaches zero, the speed of propagation tends toward infinity. Also, the heat equation expressed in Eq. (1.3.2) reduces to the classical parabolic heat equation as $\tau \to 0$. Lastly, an additional term involving the time derivative of the volumetric source is present in Eq. (1.3.2) as a consequence of the finite propagation speed.

Simons [16] pointed out that no single equation for determining the

Table 1.3.1 Exact Analogies with Heat Conduction

| PHYSICS | CONSTITUTIVE EQUATIONS | | Diffusivity ($L^2/t$) | Relaxation time ($\tau$) |
|---|---|---|---|---|
| | flux = diffusivity $\cdot\nabla$ (potential) | (Relax. time) $\cdot$ rate of change of flux + flux = diff $\cdot\nabla$ (pot.) | | |
| Heat Conduction | Fourier's Law: $q = -\alpha \frac{\partial(\rho CT)}{\partial x}$ | Modified Fourier's Law: $\tau \frac{\partial q}{\partial t} + q = -\alpha \frac{\partial(\rho CT)}{\partial x}$ | $-\alpha$ | $\tau$ |
| Fluid Mechanics | Newtonian Fluids: $\tau_s = \nu \frac{\partial(\rho u)}{\partial y}$ | Viscoelastic Fluids: $\frac{\mu}{K} \frac{\partial \tau_s}{\partial t} + \tau_s = \nu \frac{\partial(\rho u)}{\partial y}$ | $\nu$ | $\frac{\mu}{K}$ |
| Electricity | Ohm's Law: $i = \frac{-1}{RC} \frac{\partial(VC)}{\partial x}$ | $\frac{L}{R} \frac{\partial i}{\partial t} + i = \frac{-1}{RC} \frac{\partial(VC)}{\partial x}$ | $\frac{-1}{RC}$ | $\frac{L}{R}$ |

$\rho CT$ = internal energy density

$\rho u$ = momentum density

$VC$ = charge density

temperature field equation is exact. He developed a hierarchy of field equations of continually higher orders of accuracy. Equation (1.3.3) is the lowest member of this hierarchy. He based his results on the rigorous Boltzmann equation for thermal carriers which involved only well-defined approximations.

As mentioned previously, in some materials at low absolute temperatures, thermal disturbances may be found as progressive waves with little attenuation or dispersion. This phenomenon is usually referred to as "second sound." The first observation of this effect was by Peshkov [17] using liquid helium at temperatures below 2.2 Kelvin. He later predicted [18] that a similar effect should be observable in crystalline solids provided that the scattering of phonons by impurities were sufficiently small [19]. Ackerman et al. [20] performed experiments on single crystals of $^4$He which confirmed Peshkov's predictions.

In light of these and recent experimental results indicating the existence of thermal waves, a sound theoretical (macroscopic) investigation is warranted. In fact, many theories have been advanced in hopes of accounting for a finite speed of propagation of a thermal disturbance. Though many theories appear, this dissertation will investigate the consequences of heat conduction based on thermal relaxation through the flux law. Before proceeding, a review of the literature is now presented.

# Chapter 2

# LITERATURE REVIEW AND SCOPE OF RESEARCH

## 2.1 History and Proposed Theories

Interest in obtaining a physically consistent heat equation has grown, largely due to the rise in situations where Fourier's law apparently breaks down. This section reviews the literature concerning various approaches toward the development of a more accurate heat equation.

Maxwell [4] proposed his famous dynamical theory of gases in 1867. It is interesting to note that the modified Fourier's law may be regarded as a truncated form of an extensive relation derived from Maxwell's kinetic theory involving ideal gases. In his formulation, Maxwell realized the magnitude of the inertial term appropriate to his problem and casually cast out the time derivative term, remarking "the rate of conduction will rapidly establish itself" [4, p. 86]. For his particular problem he was correct. This inertial term then lay dormant for many years.

Vernotte [5-7], Cattaneo [8], and Morse and Feshbach [9] proposed the modified Fourier's law through physical arguments. They reasoned that the particular law should account for thermal relaxation. Chester [21] expounded on the modified Fourier's law and discussed the evaluation of the relaxation times based on measurable macroscopic parameters. Chester also suggested that thermal waves may be detected in certain alkali halides (solid) experimentally.

Since these arguments were qualitative, many different approaches have been proposed to quantify Eq. (1.3.1). Maurer [22] developed a relaxation model for heat conduction in metals in the form of three postulates and an approximation which he then used to formulate and manipulate the simplified Boltzmann transport equation. He developed an expression for the macroscopic heat flux in metals due to free electrons. The equation consisted of two terms; the first being the usual Fourier model involving the temperature gradient and the second term being a relaxation term. Assuming that the energy consumed by thermal expansion is negligible and that the heat conduction due to free electrons is much greater than that due to the lattice, he arrived at Eq. (1.3.2).

Nettleton [23] addressed the problem of thermal relaxation in liquids. He concluded that the modified Fourier's law is consistent with the assumption that thermal energy is carried by elastic waves at very high frequency.

Kaliski [3] gave a thermodynamical justification to the hyperbolic heat equation expressed in Eq. (1.3.2). He showed that the damped wave equation model is compatible with the second law of thermodynamics. He further suggested that the velocity of propagation, c, may be obtained by measuring the angle of a Cerenkov thermal radiation cone measured by electrical means, making use of the effects of the coupled thermo-electrical fields. Luikov [13,24] also developed the hyperbolic heat conduction equation using methods of thermodynamics of an irreversible process in the investigation of heat and mass transfer.

Weymann [25] and Taitel [26] obtained Eq. (1.3.1) through a random walk argument. In Taitel's [26] and Temkin's [27] derivations, an infinite order temperature field equation was obtained. Simons [16] also obtained an hierarchy of equations. Truncating Taitel's equation at various points reduces it either to the classical parabolic or hyperbolic heat conduction equation, i.e. first and second order differential approximations. Taitel suggests that a discrete temperature field in time and space is closer to physical reality than the continuous description since both the parabolic and hyperbolic equations present nonphysical solutions: infinite speed of propagation and temperature overshoots, respectively.

An infinite speed of propagation associated with a thermal disturbance is in direct violation of special relativity. Van Kampen [28] and Kelly [29] performed relativistic appraisals for diffusion. Van Kampen [28] pointed out that no paradox really exists since the parabolic heat conduction equation is only an approximate field equation. In case of a gas, it is only valid if

$$\left| \frac{1}{T} \frac{\partial T}{\partial x} \right| \ll \frac{1}{\kappa} , \qquad (2.1.1)$$

where $\kappa$ is the mean free path of the molecules. Van Kampen believed that the hyperbolic temperature field equation, Eq. (1.3.2) as developed by Cattaneo [8] and Weymann [25] is poorly justified. He finds fault in that the finite velocity of heat is arrived at by breaking the expansion

r This expression is only justified as an approximation when

small compared to that of $\frac{\partial T}{\partial t}$. However, near the wavefront, the term $\frac{\partial^2 T}{\partial t^2}$ dominates, and therefore it is not permitted to ignore higher terms in the expansion [28]. Finally, Van Kampen remarks that the hyperbolic temperature field equation cannot be regarded as a proper generalization of the parabolic equation.

The development of the wave heat equation from molecular kinetic considerations was performed by Bubnov [30]. Berkovsky [31] mentions that a finite speed of propagation for heat flow may be obtained using classical parabolic heat conduction if a power-type dependence (in temperature) of heat capacity and thermal conductivity is adopted.

Chernyshov [32] assumed that the rate of increase in entropy and internal energy depends on the temperature and on the first partial derivative of the temperature with respect to the spatial and temporal variables. Using this assumption, he obtained a hyperbolic heat conduction equation, though with different boundary conditions than that of the thermal relaxation model. Domanski [33] compared the relaxation model of Vernotte [5-7] to the modified internal energy model of Chernyshov [32] for a specific problem. It was found that hyperbolic heat conduction based on thermal relaxation predicts higher temperatures than those of Chernyshov's modified internal energy model. The parabolic solution lies between the two hyperbolic solutions. Both hyperbolic heat equations produced identical wave speeds.

Another approach in resolving the infinite speed of propagation of a thermal disturbance is based on a general theory of thermodynamics with memory. Gurtin and Pipkin [34] developed a general theory of heat conduction in rigid nonlinear materials with memory where the thermal

wave speed is finite. The linearized equation produced an integro-differential equation in the temperature variable. The distinguishing feature of this theory is that it depends on the history of the temperature gradient. If a simple exponential function is chosen for the kernel of the integro-differential equation, the hyperbolic field equation of Eq. (1.3.2) is reproduced.

Using this theory, Amos and Chen [35] studied a particular problem concerning a half-space subject to a step change in surface temperature. In addition, MacCamy [36] studied asymptotic stability theorems for the solution of problems based on Gurtin and Pipkin's theory. Additional studies concerning this formulation were performed by Coleman and Mizel [37], and Coleman and Gurtin [38]. Hermann and Nachlinger [39] studied uniqueness and wave propagation of the nonlinear equation of Gurtin and Pipkin. Chen and Gurtin [40] extended Gurtin and Pipkin's [34] theory to include deforming media. Chen [41] also studied the properties of temperature rate waves of arbitrary forms.

Norwood [42,43] investigated various problems using the theory proposed by Gurtin and Pipkin [34]. Other variations of heat conduction theories with memory have been advanced by Nunziato [44] and Lindsay and Straughan [45].

Lord and Shulman [46] modified the coupled equations of thermo-elasticity to accommodate a finite thermal wave speed. Many theoretical investigations concerning the fully coupled systems have appeared [47-58]. In most real instances, uncoupling may be permitted when the coupling parameter [59] is small compared to unity. Kao [2] performed an analytical study concerning thermally induced non-Fourier stress

waves in a semi-infinite medium. In [2], Kao assumed that Vernotte's [5-7] wave equation described heat conduction exactly.

## 2.2 Theoretical Studies Considering Thermal Relaxation

This section reviews various analytical and approximate solution techniques that have been applied in solving problems in hyperbolic heat conduction based on the thermal relaxation.

Baumeister and Hamill [60,61] studied the effect of the propagation velocity of heat on the temperature and flux distributions in a semi-infinite body due to a step change in temperature at its surface. Brazel and Nolan [62] investigated the temperature distribution in a semi-infinite body subject to a single pulsed surface heat flux. According to Maurer and Thompson [63], Brazel and Nolan [62] set the surface heat flux equal to the temperature gradient which is inconsistent with the relaxation formulation. Domanski [33] compared the solutions resulting from the hyperbolic heat equation as derived from the modified Fourier's law to that of modifying the internal energy [32] for the surface heat flux problem. Chan, Low, and Mueller [64] considered a finite slab with a periodic heat flux boundary condition as a model for catalytic supported crystallites.

The effect of volumetric heating was first approached by Lorenzini and Spiga [65] using the thermal relaxation model. Unfortunately, they did not formulate the proper heat equation. They omitted the time derivative of the volumetric source as required by the relaxation model as shown in Eq. (1.3.2). Vick and Ozisik [66] and Ozisik and Vick [67] studied the temperature and flux distributions for a pulsed volumetric source in a semi-infinite and finite region slab, respectively.

Kao [68] studied the influence of surface curvature on the temperature distribution in a semi-infinite medium for various boundary conditions.

The study of hyperbolic equations using approximate analytical and purely numerical techniques include perturbation methods, finite differences, finite elements, predictor-corrector methods [69], Lax-Wendroff methods [70], the method of characteristics, and various other methods [71]. The hyperbolic heat equation has been investigated by these and other techniques for select linear and nonlinear problems.

Glass, Ozisik, McRae, and Vick [72] and Glass, Ozisik, and Vick [73,74] have investigated the effects of linear sources, variable thermal conductivity, and surface radiation, respectively, using McCormick's predictor-corrector method. Wiggert [75] considered an early-time transient analysis using the method of characteristics in a finite width slab.

A variational approach was taken by Carey and Tsai [76] in studying hyperbolic heat conduction with a reflecting back surface. They presented detailed results in their investigation for determining an effective numerical procedure. Finite elements were employed in space and alternative time integration schemes were studied.

Finkel'shtein [77] recently used a perturbation method for resolving the temperature distribution where relaxation time $\tau$ was the small parameter to be expanded. Various nonlinear problems have been formulated [78-80] where material properties are functions of the temperature.

Moving boundary value problems have been considered by Sadd and Didlake [81], de Scocio and Gualtieri [82], and Solomon et al. [83]. According to Solomon et al., Sadd and Didlake, and de Scocio and Gualtieri incorrectly formulated the Stefan condition of the phase change front.

The inverse problem in hyperbolic heat conduction has been addressed by Novikov [84,85]. Novikov [85] states that the linear hyperbolic inverse heat conduction problem is well-posed and requires solving a Volterra integral equation of the second kind.

## 2.3 Experimental Studies

Peshkov [17] is credited with discovering "second sound" in superfluid liquid helium in 1944. According to Ackerman and Guyer [86], Nerst in 1917 is credited with the earliest speculation on the existence of a propagating temperature wave. Nerst suggested that heat may have sufficient "inertia" to give rise to an oscillatory discharge in good thermal conductors at low temperatures.

Bertman and Sandiford [87] displayed an oscilloscope trace of a pulsed energy source propagating at constant speed in superfluid helium at about one degree Kelvin. Figure 2.3.1 displays a typical trace of heat flow as would be predicted by the two heat conduction approximations. Figure 2.3.1a plots the temperature of a sample material as a function of time at a given position where a diffusion-like process is occurring. In contrast, Fig. 2.3.1b demonstrates heat flow by wave propagation as taken from a superfluid liquid helium sample at one degree Kelvin. Bertman and Sandiford's experimental procedure is

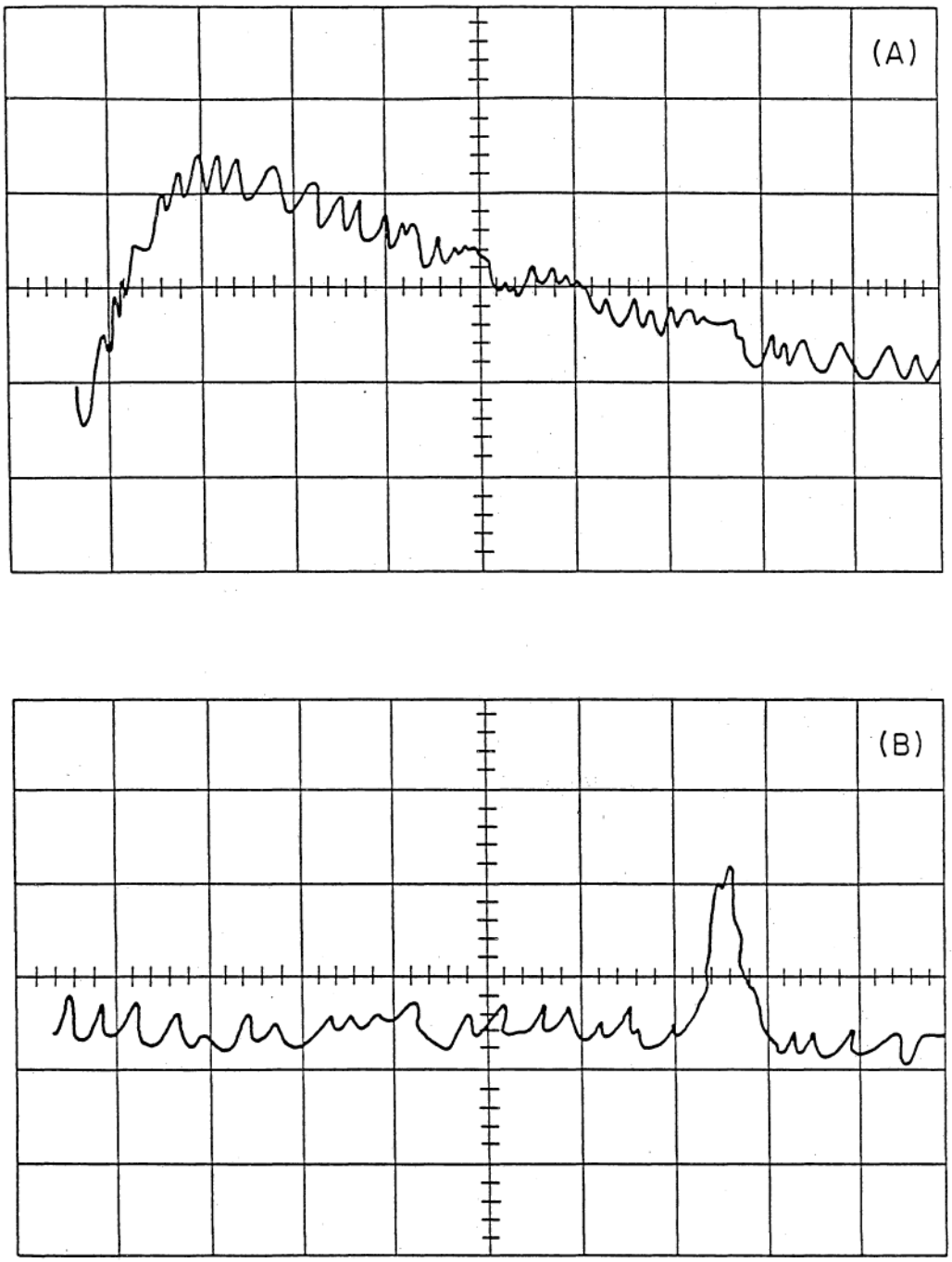


Figure 2.3.1 Typical Oscilloscope Trace Comparing Parabolic and Hyperbolic Heat Conduction.

outlined in [20,87].

Recently, much attention has been given to discovering thermal waves in solids. Ward and Wilkes [88] suggested the possibility that temperature waves may be detected in dielectric solids. Recall that Chester [21] and Peshov [18] have also conjectured that thermal waves may be detected in various solids. Solid helium has been the only solid [87,89] where thermal waves have been observed. Enz [90] discussed the pulse technique which is a typical experimental method used in the investigation of thermal waves. In addition to the pulse technique, Schlieren photography [91,92] of second-sound shock waves in superfluid helium has been used in observing this pheonomenon.

## 2.4 Purpose and Scope of Research

This exposition takes a unified and systematic approach in examining hyperbolic heat conduction in opaque materials. A comprehensive study is necessary to consolidate and understand heat conduction based on thermal relaxation. Limitations of the theory may then be objectively understood and stated.

The general one-dimensional temperature and flux formulations for the three standard orthogonal coordinate systems are presented. The general solution, in the temperature domain, is developed by the finite integral transform technique. The basic physics and mathematics are demonstrated by reviewing Taitel's problem. Then attention is turned to the effects of radially dependent systems, such as the case of a cylinder and sphere. Various thermal disturbances are presented showing the unusual physics associated with dissipative wave equations. The

flux formulation is shown to be a viable alternative domain to develop the flux distribution. Once the flux distribution has been established, the temperature distribution may be obtained through the conservation of energy.

Linear one-dimensional composite regions are then investigated in detail. The general temperature and flux formulations are developed for the three standard orthogonal coordinate systems. The general solution for the flux and temperature distributions are obtained in the flux domain using a generalized integral transform technique. Additional features associated with hyperbolic heat conduction are displayed through examples with various thermal disturbances.

A generalized expression for temperature dependent thermal conductivity is introduced and incorporated into the one-dimensional hyperbolic heat equation. An approximate analytical solution is obtained and compared with a standard numerical method.

Finally, recommendations for future analytical and experimental investigations are suggested.

# Chapter 3

# LINEAR THEORY

## 3.1 Introduction

This chapter develops a unified and comprehensive investigation of linear one region hyperbolic heat conduction for an isotropic and homogeneous medium using both the temperature and flux formulations. In addition, new concepts for classical parabolic heat conduction shall also be exhibited.

The general one-dimensional linear temperature field equation for the three standard orthogonal coordinate systems is developed along with its appropriate boundary and initial conditions. The general flux formulation is also presented as an alternative domain for developing the distributions.

Next, the general solution for the temperature distribution is resolved by using the finite integral transform technique [93]. The associated flux distribution is obtained through the time integration of the modified Fourier's law.

Taitel's [26] problem is revisited in order to display the unique features of hyperbolic heat conduction and to display the mathematical behavior involved in an infinite series solution of a hyperbolic equation. For completeness, the flux distribution is presented since Taitel omitted it in his discussion. Examples using various thermal disturbances in radially dependent systems are presented, discussed, and compared to the classical heat conduction solutions.

The controversial and peculiar nature of hyperbolic heat conduction is examined in radially dependent systems. As previously discussed, the nature of heat propagation based on thermal relaxation has been approached by many investigators. However, no systematic or complete study has been taken to investigate the ramifications of hyperbolic heat conduction in the various radial geometries (cylindrical and spherical).

Finally, an example using the flux formulation is presented. It is shown that the flux formulation is a more convenient domain in analyzing situations involving specified heat flux boundary conditions. The Green's function method is utilized in obtaining the flux distribution.

## 3.2 Relationships Between Temperature and Flux

Some clarification appears necessary concerning the relationships between temperature and flux before developing the field equations, and boundary and initial conditions. Let us start by remarking on the general and particular laws governing hyperbolic heat conduction in incompressible materials. For hyperbolic heat conduction, the two physical relations required are the conservation of energy (general law) and the modified Fourier's law (particular law). For clarity in this discussion, we write the one-dimensional equations below

$$-\frac{\partial q}{\partial x} + u = \rho C_p \frac{\partial T}{\partial t} , \tag{3.2.1}$$

$$\tau \frac{\partial q}{\partial t} + q = - k \frac{\partial T}{\partial x} . \tag{3.2.2}$$

Equation (3.2.1) is the mathematical expression for the conservation of energy while Eq. (3.2.2) is the modified Fourier's law. These equations are a coupled set of first order partial differential equations defining a hyperbolic system. The coupling occurs in the heat flux and temperature dependent variables. This primary system of equations may be used to eliminate either dependent variable to form a second order partial differential equation. A discussion clarifying the proper formulation of the boundary and initial conditions is warranted since this is usually taken for granted. The results of this discussion also apply to parabolic heat conduction.

First we note that convection is not considered in this dissertation since hyperbolic heat conduction is associated with small times, i.e., times prior to the movement of any mass. Only boundary conditions specifying temperature or heat flux is formulated in the linear theory.

Table 3.2.1 displays the equivalent boundary conditions in the two formulations, i.e., temperature and flux domains. This table shows that a specified temperature can be written in terms of flux through the general law, whereas a specified heat flux can be converted to the temperature domain via the particular law. Observe that a boundary condition of the first kind in temperature becomes a boundary condition of the second kind in flux and vice versa.

Table 3.2.2 displays the equivalent initial conditions of the two formulations. Here lies another point which generally has been obscured. The coupled first order partial differential equations, representing the primary mathematical description of heat conduction,

Table 3.2.1 Equivalent Boundary Conditions in Temperature and Flux Domains

| Specified domain of boundary condition | Map ⟶ | Equivalent boundary condition in desired domain |
|---|---|---|
| Specified temperature<br>$T(x_o,t) = f(t)$ | (general law)<br>Conservation of energy<br>$-\frac{\partial q}{\partial x} + u = \rho C_p \frac{\partial T}{\partial t}$ | Equivalent flux<br>$\frac{\partial q}{\partial x}(x_o,t) = u(x_o,t) - \rho C_p \frac{df(t)}{dt}$ |
| Specified flux<br>$q(x_o,t) = f(t)$ | (particular law)<br>Modified Fourier's law<br>$\tau \frac{\partial q}{\partial t} + q = -k \frac{\partial T}{\partial x}$ | Equivalent temperature<br>$-k \frac{\partial T}{\partial x}(x_o,t) = \tau \frac{df(t)}{dt} + f(t)$ |

Table 3.2.2 Equivalent Initial Conditions in Temperature and Flux Domains

| Specified domain of initial condition | Map ⟶ | Equivalent initial condition in desired domain |
|---|---|---|
| Specified flux<br>$q(x,t_o) = f(x)$ | (general law)<br>Conservation of energy<br>$-\frac{\partial q}{\partial x} + u = \rho C_p \frac{\partial T}{\partial t}$ | Equivalent temperature<br>$\frac{\partial T}{\partial t}(x,t_o) = \frac{1}{\rho C_p}\left[-\frac{df(x)}{dx} + u(x,t_o)\right]$ |
| Specified temperature<br>$T(x,t_o) = f(x)$ | (particular law)<br>Modified Fourier's law<br>$\tau \frac{\partial q}{\partial t} + q = -k \frac{\partial T}{\partial x}$ | Equivalent flux<br>$\frac{\partial q}{\partial t}(x,t_o) = -\frac{1}{\tau}\left[q(x,t_o) + k\frac{df(x)}{dx}\right]$ |

relates two dependent variables; namely, flux and temperature. From this set of equations, the natural specified initial conditions at time $t_o$ should be

$$T(x,t_o) = f(x) \tag{3.2.3a}$$

$$q(x,t_o) = g(x) \ , \ x\varepsilon D \ , \tag{3.2.3b}$$

where $f(x)$ and $g(x)$ are specified functions at $t = t_o$ in the domain D.

In contrast to Table 3.2.1, the equivalent initial condition table uses the opposite map from domain to domain. That is, a specified temperature initial condition requires the particular law to be transformed into the flux domain, whereas a specified flux initial condition requires the general law to be converted to the temperature domain. Obviously, these tables are valid for parabolic heat conduction where $\tau = 0$. An additional table would be required to include convection for classical parabolic heat conduction.

Another subtle point arises in obtaining the flux distribution from the temperature distribution. One may always obtain the flux distribution from the modified Fourier's law since both initial conditions in temperature and flux must be specified as shown in Eqs. (3.2.3a) and (3.2.3b). But notice that in some instances, the conservation of energy equation may be used to obtain the flux distribution if a flux boundary condition has been specified. Now, the governing equations for both the temperature and flux formulations are presented.

## 3.3 Temperature and Flux Formulations

The general one dimensional temperature field equation for an incompressible, isotropic, and homogeneous medium is now derived for the three standard orthogonal coordinate systems [94]. Referring to Fig. 3.3.1 and performing a general one-dimensional energy balance in the usual manner [1], we arrive at the mathematical expression for the conservation of energy, namely

$$-\frac{1}{x^p}\frac{\partial}{\partial x}(x^p q) + u(x,t) = \rho C_p \frac{\partial T}{\partial t}\,, \tag{3.3.1a}$$

where

$$p = \begin{cases} 0 & \text{slab} \\ 1 & \text{cylinder} \\ 2 & \text{sphere} \end{cases} \tag{3.3.1b}$$

and where $q(x,t)$ is the heat flux, $T(x,t)$ is the temperature, $u(x,t)$ is an arbitrary volumetric heat source, $\rho$ is the density, and $C_p$ is the specific heat. It is assumed, in arriving at Eq. (3.3.1a), that the internal energy is proportional to the temperature.

To obtain the temperature field equation, we eliminate $q(x,t)$ between Eqs. (3.2.2) and (3.3.1a) with the assumption of constant thermal properties to get

$$\frac{1}{x^p}\frac{\partial}{\partial x}\left[x^p \frac{\partial T}{\partial x}\right] + \frac{1}{k}\left[u + \tau \frac{\partial u}{\partial t}\right] = \frac{1}{\alpha}\frac{\partial}{\partial t}\left[T + \tau \frac{\partial T}{\partial t}\right]\,, \tag{3.3.2}$$

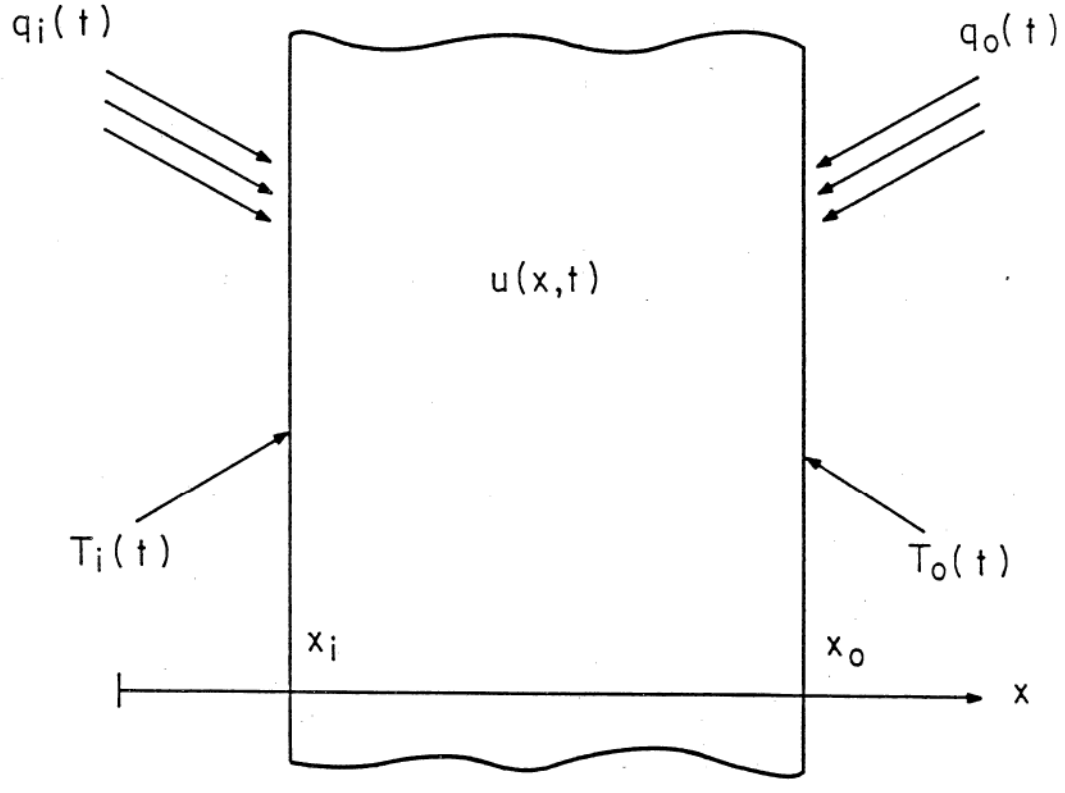


Figure 3.3.1 Schematic Displaying Possible Thermal Disturbances in a One-Region Geometry.

where p designates the geometry as expressed by Eq. (3.3.1b) and $\alpha \equiv k/\rho C_p$ is the thermal diffusivity. Equation (3.3.2) is a linear nonhomogeneous hyperbolic field equation in the temperature variable which now associates a finite speed of propagation to the heat flow.

The boundary and initial conditions required to complete the mathematical formulation in the temperature domain are now developed. Since convection is not considered in hyperbolic heat conduction, only boundary conditions of the first kind (specified temperature) and second kind (specified heat flux) is formulated in the temperature domain.

Referring to Fig. 3.3.1, we find

$$C_{2i}^* k \frac{\partial T}{\partial x} + C_{1i}^* T = -C_{2i}^* [\tau \frac{dq_i}{dt} + q_i(t)] + C_{1i}^* T_i(t), \quad x = x_i , \tag{3.3.3a}$$

and

$$C_{2o}^* k \frac{\partial T}{\partial x} + C_{1o}^* T = C_{2o}^* [\tau \frac{dq_o}{dt} + q_o(t)] + C_{1o}^* T_o(t), \quad x = x_o, \; t > 0 , \tag{3.3.3b}$$

where the general notation introduced above reduces to the prescribed temperature $T_i(t)$, $T_o(t)$ or heat flux $q_i(t)$, $q_o(t)$ boundary conditions depending on the various combinations of $C_{1j}^*$, $C_{2j}^*$ with j = i,o (inner, outer) and $C_{1j}^*$, $C_{2j}^*$ to equal 0 or 1. The number subscript designates the kind of boundary condition, a flux boundary (second kind) would have a $C_{2j}^*$ as its coefficient, while a temperature boundary condition (first

kind) would have a $C^*_{1j}$ as its coefficient. Specifically, a prescribed temperature at $x = x_i$ would require $C^*_{2i} = 0$, and $C^*_{1i} = 1$. While a specified heat flux would require $C^*_{2i} = 1$, and $C^*_{1i} = 0$. A similar interpretation can be made at $x = x_o$. By introducing this notation, we can consider all possible combinations of boundary conditions that can appear in developing the general solution. Finally, as $\tau \to 0$, we observe that the standard parabolic heat conduction equations are recovered.

The initial conditions are taken at the equilibrium state, which can be readily established as

$$T = T_o \quad , \tag{3.3.4a}$$

$$\frac{\partial T}{\partial t} = 0 \quad , \quad x\varepsilon[x_i, x_o] \quad , \quad t = 0. \tag{3.3.4b}$$

The temperature field is uniquely governed by Eq. (3.3.2) subject to boundary conditions Eq. (3.3.3) and initial conditions Eq. (3.3.4).

The general <u>one-dimensional flux field equation</u> for an incompressible, isotropic, and homogeneous medium is presently derived for the three standard orthogonal coordinate systems. Eliminating the temperature $T(x,t)$ between Eqs. (3.2.2) and (3.3.1a), we find

$$\frac{\partial}{\partial x}\left[\frac{1}{x^p}\frac{\partial}{\partial x}(x^p q)\right] + \frac{\partial u}{\partial x} = \frac{1}{\alpha}\frac{\partial}{\partial t}\left[\tau\frac{\partial q}{\partial t} + q\right] \quad , \tag{3.3.5}$$

$$x\varepsilon(x_i, x_o) \quad , \quad t > 0 \quad ,$$

where p designates the geometry as expressed by Eq. (3.3.1b), and $\alpha$ is

the thermal diffusivity. Notice that in this formulation only the spatial gradient of the volumetric heat source is involved whereas in the temperature formulation, the volumetric source and its time derivative appear as shown in Eq. (3.3.2).

As $\tau \to 0$, the classical parabolic heat flux field equation is recovered. It should be remarked that very little has been mentioned or devoted to the flux formulation in parabolic heat conduction.

When considering the required boundary and initial conditions required to complete the mathematical formulation in the flux domain, we again consider only specified temperatures and fluxes at the boundaries.

Referring to Fig. 3.3.1 and following the logic of Table 3.2.1, we arrive at

$$A^*_{1i} q - A^*_{2i} \frac{1}{x^p} \frac{\partial}{\partial x}(x^p q) = A^*_{1i} q_i(t) + A^*_{2i}\left[\rho C_p \frac{dT_i}{dt} - u\right] , \quad (3.3.6a)$$

$$x = x_i ,$$

$$A^*_{1o} q - A^*_{2o} \frac{1}{x^p} \frac{\partial}{\partial x}(x^p q) = -A^*_{1o} q_o(t) + A^*_{2o}\left[\rho C_p \frac{dT_o}{dt} - u\right] , \quad (3.3.6b)$$

$$x = x_o, \; t > 0.$$

Observe that Eqs. (3.3.6a-b) are identical to the boundary conditions which would appear in the flux formulation of parabolic heat conduction. Since the transformation of the temperature information to the flux domain is based on the general law, we see no appearance of the thermal relaxation time $\tau$.

The general notation introduced in Eq. (3.3.6) reduces to the prescribed flux ($q_i(t)$, $q_o(t)$) or temperature ($T_i(t)$, $T_o(t)$) boundary conditions depending on the various combinations of $A^*_{1j}$, $A^*_{2j}$ with j = i,o (inner,outer) and $A^*_{1j}$, $A^*_{2j}$ equal to 0 or 1. The number subscript designates the kind of boundary condition in the flux domain. A flux boundary condition (first kind) would have a $A^*_{1j}$ as its coefficient while a temperature boundary condition (second kind) would have a $A^*_{2j}$ as its coefficient. Specifically, a prescribed flux at $x = x_i$ would require $A^*_{1i} = 1$ and $A^*_{2i} = 0$, while a specified temperature would require $A^*_{1i} = 0$ and $A^*_{2i} = 1$. A similar interpretation can be made at $x = x_o$.

The initial conditions may be readily obtained through Table 3.2.2. At the equilibrium initial state, we find

$$q = 0 \ , \tag{3.3.7a}$$

$$\frac{\partial q}{\partial t} = 0 \ , \ x\varepsilon[x_i,x_o] \ , \ t = 0. \tag{3.3.7b}$$

The flux field is uniquely governed by Eq. (3.3.5) subject to the boundary and initial conditions expressed in Eqs. (3.3.6) and (3.3.7), respectively.

It should be mentioned that in the general three-dimensional flux formulation, a heat flux vector equation [95] is developed. That is

$$\nabla \cdot [\nabla \cdot \vec{q}(\bar{r},t)] - \nabla u(\bar{r},t) = \frac{1}{\alpha} \frac{\partial}{\partial t} [\tau \frac{\partial \vec{q}}{\partial t}(\bar{r},t) + \vec{q}(\bar{r},t)] \ , \tag{3.3.8}$$

where $\vec{q}(\bar{r},t)$ is the heat flux vector and $\bar{r}$ is the spatial vector. For the three dimensional case, Eq. (3.3.8) represents three simultaneous hyperbolic scalar equations for the heat flux components. In the following section, the general solution is developed and used to show the rather controversial behavior of linear hyperbolic heat conduction theory in a variety of situations.

## 3.4 General Solution Developed from Temperature Formulation

In this section, we use the temperature formulation to develop the general one dimensional temperature and flux distributions associated with hyperbolic heat conduction in an incompressible, isotropic, and homogeneous medium. The finite integral transform technique is utilized in determining the temperature distribution. This technique provides a general and systematic approach in determining the temperature distribution. Finally, the flux distribution may be resolved by either the energy conservation law Eq. (3.3.1) or by the modified Fourier's law Eq. (3.2.2).

### Dimensionless Quantities

For convenience in the subsequent analyses, we introduce the dimensionless quantities

$$\eta = \frac{1}{2}\frac{cx}{\alpha} \tag{3.4.1a}$$

$$\xi = \frac{1}{2}\frac{c^2 t}{\alpha} \tag{3.4.1b}$$

$$\theta(\eta,\xi) = \frac{T - T_o}{T_{ref}} \quad , \tag{3.4.1c}$$

$$Q(\eta,\xi) = \frac{q}{T_{ref}(\frac{ck}{\alpha})} \quad , \tag{3.4.1d}$$

$$S(\eta,\xi) = \frac{u}{T_{ref}(\frac{kc^2}{4\alpha^2})} \quad , \tag{3.4.1e}$$

where $T_{ref}$ is a reference temperature which appropriately characterizes the thermal disturbance of interest.

Introducing the dimensionless quantities expressed in Eq. (3.4.1) into Eqs. (3.3.2), (3.3.3) and (3.3.4), we obtain a system of dimensionless equations governing linear hyperbolic heat conduction in a one-dimensional medium. The dimensionless temperature field equation becomes

$$M_p[\theta(\eta,\xi)] = -[S(\eta,\xi) + \frac{1}{2}\frac{\partial S}{\partial \xi}] \quad , \tag{3.4.2}$$

where $M_p$ is the modified heat conduction linear operator

$$M_p \equiv \frac{1}{\eta^p}\frac{\partial}{\partial \eta}\left(\eta^p \frac{\partial}{\partial \eta}\right) - \frac{\partial^2}{\partial \xi^2} - 2\frac{\partial}{\partial \xi} \quad , \tag{3.4.3}$$

and p designates the geometry as defined in Eq. (3.3.1b). The general boundary conditions are succinctly expressed as

$$B_i[\theta(\eta,\xi)] = -C_{2i}[\frac{dQ_i}{d\xi} + 2Q_i(\xi)] + C_{1i}\theta_i(\xi), \ \eta = \eta_i \ , \tag{3.4.4a}$$

$$B_o[\theta(\eta,\xi)] = C_{2o}[\frac{dQ_o}{d\xi} + 2Q_o(\xi)] + C_{1o}\theta_o(\xi), \ \eta = \eta_o, \ \xi > 0 \ , \tag{3.4.4b}$$

where $B_i$ and $B_o$ represent the boundary operators defined as

$$B_i \equiv C_{2i} \frac{\partial}{\partial \eta} + C_{1i}, \quad \eta = \eta_i \quad , \tag{3.4.5a}$$

$$B_o \equiv C_{2o} \frac{\partial}{\partial \eta} + C_{1o}, \quad \eta = \eta_0 \quad . \tag{3.4.5b}$$

The dimensionless boundary coefficients $C_{1j}$, $C_{2j}$ , $j = i,o$ are the dimensionless counterparts to the general notation introduced in Eqs. (3.3.3) and again become 0 or 1 depending on the type of boundary condition. The dimensionless counterpart of the initial conditions expressed in Eq. (3.3.4) are

$$\theta = 0 \quad , \tag{3.4.6a}$$

$$\frac{\partial \theta}{\partial \xi} = 0 \quad , \quad \xi = 0 \quad . \tag{3.4.6b}$$

Finally, the dimensionless modified Fourier's law becomes

$$\frac{\partial Q}{\partial \xi} + 2Q = - \frac{\partial \theta}{\partial \eta} \quad . \tag{3.4.7}$$

The finite integral transform technique [93] is now utilized in determining the general temperature distribution $\theta(\eta,\xi)$. Once the temperature distribution has been established, the flux distribution can be obtained by solving Eq. (3.4.7) for the flux $Q(\eta,\xi)$.

The appropriate eigenvalue problem is obtained from considering the homogeneous version of the temperature equation (3.4.2) together with the homogeneous version of the boundary conditions expressed in Eq. (3.4.4). We immediately establish the eigenvalue problem as

$$\frac{d}{d\eta}\left[\eta^p \frac{d\psi_m}{d\eta}\right] + \lambda_m^2 \eta^p \psi_m(\eta) = 0 , \tag{3.4.8}$$

subject to

$$B_i[\psi_m] = 0 \quad , \quad \eta = \eta_i , \tag{3.4.9a}$$

$$B_o[\psi_m] = 0 \quad , \quad \eta = \eta_o , \tag{3.4.9b}$$

where p represents the geometry as defined in Eq. (3.3.1b) and $\eta^p$ represents the Sturm-Liouville weight function. The case where $\lambda_0 = 0$ is an allowable eigenvalue will require special and individual attention to preserve correctness in the analysis. This situation occurs when both boundary conditions are of the second kind.

The orthogonality condition for the eigenfunctions is

$$\int_{\eta=\eta_i}^{\eta_o} \eta^p \psi_m(\eta) \psi_n(\eta) \, d\eta = \begin{cases} 0 & , \quad m \neq n \\ N(\lambda_m) & , \quad m = n \end{cases} \tag{3.4.10a}$$

where the normalization integral $N(\lambda_m)$ is defined as

$$N(\lambda_m) = \int_{\eta=\eta_i}^{\eta_o} \eta^p \psi_m^2(\eta)\, d\eta \ . \qquad (3.4.10b)$$

Using the orthogonality relation, we can develop the integral transform pair [93,94],

Inversion Formula:

$$\theta(\eta,\xi) = \sum_m \frac{\psi_m(\eta)\, \bar{\theta}_m(\xi)}{N(\lambda_m)} \ , \qquad (3.4.11a)$$

Integral Transform:

$$\bar{\theta}_m(\xi) = \int_{\eta=\eta_i}^{\eta_o} \eta^p\, \theta(\eta,\xi)\, \psi_m(\eta)\, d\eta \ , \qquad (3.4.11b)$$

where the summation over m may range from m = 1,...,$\infty$ or m = 0,1,..., $\infty$, depending on whether $\lambda_0 = 0$ is an allowable eigenvalue.

We now remove all spatial dependence from our original temperature field equation, Eq. (3.4.2), by operating on it with

$$\int_{\eta=\eta_i}^{\eta_o} \eta^p\, \psi_m(\eta)\, d\eta \ , \qquad (3.4.12)$$

to obtain

$$\int_{\eta=\eta_i}^{\eta_o} M_p[\theta(\eta,\xi)]\, \eta^p\, \psi_m(\eta) d\eta = - \int_{\eta=\eta_i}^{\eta_o} \left[S(\eta,\xi) + \frac{1}{2}\frac{\partial S}{\partial \xi}\right] \eta^p\, \psi_m(\eta) d\eta \ . \ . \qquad (3.4.13)$$

After some manipulation, we arrive at the following ordinary differential equation (initial value problem) in the transform variable

$$\frac{d^2 \bar{\theta}_m}{d\xi^2} + 2 \frac{d \bar{\theta}_m}{d\xi} + \lambda_m^2 \bar{\theta}_m(\xi) = V_m(\xi) \ , \tag{3.4.14a}$$

where the transformed thermal disturbance function is

$$V_m(\xi) = \int_{\eta=\eta_i}^{\eta_o} \left[ S(\eta,\xi) + \frac{1}{2} \frac{\partial S}{\partial \xi} \right] \eta^p \psi_m(\eta) d\eta + \eta^p \left[ \frac{\partial \theta}{\partial \eta} \psi_m - \frac{d\psi_m}{d\eta} \theta \right]_{\eta=\eta_i}^{\eta_o} . \tag{3.4.14b}$$

The transformed initial conditions become

$$\bar{\theta}_m = 0 \ , \quad \xi = 0 \tag{3.4.15a}$$

$$\frac{d\bar{\theta}_m}{d\xi} = 0 \ , \quad \xi = 0. \tag{3.4.15b}$$

The above expression for $\bar{\theta}_m(\xi)$ is valid for all m = 0,1,... Substituting the boundary conditions expressed in Eqs. (3.4.4) and (3.4.9) into Eq. (3.4.14b), we get

$$V_m(\xi) = \int_{\eta=\eta_i}^{\eta_o} \left[ S(\eta,\xi) + \frac{1}{2} \frac{\partial S}{\partial \xi} \right] \eta^p \psi_m(\eta) d\eta + \eta_o^p \left[ C_{2o} \left( \frac{dQ_o}{d\xi} + 2Q_o(\xi) \right) \psi_m(\eta_o) - \frac{d\psi_m(\eta_o)}{d\eta} \theta_o(\xi) C_{1o} \right] + \eta_i^p \left[ C_{2i} \left( \frac{dQ_i}{d\xi} + 2Q_i(\xi) \right) \psi_m(\eta_i) + \frac{d\psi_m}{d\eta}(\eta_i) \theta_i(\xi) C_{1i} \right] \tag{3.4.16}$$

If $\lambda_0 = 0$, a careful evaluation for $V_0(\xi)$ will be required.

The solution to Eqs. (3.4.14) is easily obtained with the aid of the Laplace transform technique. We find

$$\bar{\theta}_m(\xi) = \int_{\xi_o=0}^{\xi} \frac{V_m(\xi_o) e^{-(\xi-\xi_o)} \sin\left[\sqrt{\lambda_m^2 - 1}\,(\xi-\xi_o)\right]}{\sqrt{\lambda_m^2 - 1}}\, d\xi_o \ , \ m = 0,1,\ldots \quad (3.4.17)$$

For the situation where $\lambda_0 = 0$ is an allowable eigenvalue, Eq. (3.4.17) further reduces to

$$\bar{\theta}_0(\xi) = \int_{\xi_o=0}^{\xi} V_0(\xi_o)\, e^{-(\xi-\xi_o)} \sinh(\xi - \xi_o)\, d\xi_o \ . \quad (3.4.18)$$

Finally, the temperature distribution can be constructed with the aid of the inversion formula expressed by Eq. (3.4.11a). The temperature distribution becomes

$$\theta(\eta,\xi) = \sum_m \frac{\psi_m(\eta)}{N(\lambda_m)} \cdot \int_{\xi_o=0}^{\xi} \frac{V_m(\xi_o)\, e^{-(\xi-\xi_o)} \sin\left[\sqrt{\lambda_m^2 - 1}\,(\xi-\xi_o)\right] d\xi_o}{\sqrt{\lambda_m^2 - 1}} \ , \quad (3.4.19)$$

$$\eta \in [\eta_i, \eta_o] \ , \ \xi \geq 0 \ .$$

The heat flux distribution is developed by solving the dimensionless form of the modified Fourier's law as expressed in Eq. (3.4.7) for $Q(\eta,\xi)$. Solving the first order differential equation yields

$$Q(\eta,\xi) = Q(\eta,0)\, e^{-2\xi} - \int_{\xi_o=0}^{\xi} e^{-2(\xi-\xi_o)} \frac{\partial\theta}{\partial\eta}(\eta,\xi_o)\, d\xi_o \ , \quad (3.4.20a)$$

subject to

$$Q = 0 \quad , \quad \xi = 0 \ , \tag{3.4.20b}$$

which represents the initial equilibrium state. Substituting Eq. (3.4.19) into Eq. (3.4.20a) yields the general heat flux distribution

$$Q(\eta,\xi) = - \sum_{m} \frac{d\psi_m(\eta)}{d\eta} \cdot \frac{1}{N(\lambda_m)} \cdot \frac{1}{\lambda_m^2} \tag{3.4.21}$$

$$\cdot \int_{\xi_o=0}^{\xi} V_m(\xi_o) \left\{ e^{-(\xi-\xi_o)} \left[ \frac{\sin\left(\sqrt{\lambda_m^2 - 1}\ (\xi-\xi_o)\right)}{\sqrt{\lambda_m^2 - 1}} \right.\right.$$

$$\left.\left. - \cos\left(\sqrt{\lambda_m^2 - 1}\ (\xi-\xi_o)\right)\right] + e^{-2(\xi-\xi_o)} \right\} d\xi_o \ .$$

$$\eta \in [\eta_i \ , \ \eta_o] \quad , \quad \xi \geq 0 \ .$$

The temperature and heat flux distributions, as predicted by linear hyperbolic heat conduction theory are now available from Eqs. (3.4.19) and (3.4.21), respectively in the three common geometries subjected to a variety of thermal disturbances. Controversial predictions in a one dimensional solid slab, cylinder, and sphere are demonstrated in the following sections.

## 3.5 Nature of the Physics and Mathematics

Taitel's [26] problem represents the simplest one region example which can illustrate the basic physics and mathematical difficulties associated with the study of hyperbolic heat conduction. Taitel presented results illustrating why hyperbolic heat conduction remains controversial, however his paper omitted many subtle details concerning the nature of the physics and mathematics. This section serves to introduce the characteristics of hyperbolic heat conduction (based on thermal relaxation) and to complete Taitel's problem.

Taitel [26] considered a finite width slab initially at the equilibrium state suddenly subject to a step change in temperature at both external boundaries. Since the problem is symmetric, one could consider half the slab and use an insulated boundary condition.

Using the dimensionless variables introduced previously, the step change in temperature at $\eta_i = 0$ corresponds to $\theta(0,\xi) = 1$ where $T_{ref} = T_w - T_o$ while the insulated boundary condition at $\eta = \eta_o$ is $\frac{\partial\theta}{\partial\eta}(\eta_o,\xi) = 0$. The general solution presented in Eq. (3.4.19) for the temperature distribution ($p = 0$) may now be utilized. The boundary coefficients become $C_{1i} = 1$, $C_{2i} = 0$ and $C_{1o} = 0$, $C_{2o} = 1$ and the source term $S(\eta,\xi)$ is set to zero since no volumetric heating is taking place.

The dimensionless temperature distribution becomes

$$\theta(\eta,\xi) = 1 - \frac{2}{\eta_o}\sum_{m=1}^{\infty}\frac{\sin\lambda_m\eta}{\lambda_m}\cdot e^{-\xi}\cdot\left[\frac{\sin\sqrt{\lambda_m^2-1}\,\xi}{\sqrt{\lambda_m^2-1}} + \cos\sqrt{\lambda_m^2-1}\,\xi\right], \qquad (3.5.1)$$

$$\eta\varepsilon[0,\eta_o] \ , \ \xi \geq 0 \ ,$$

and where the eigenvalues $\lambda_m$ are defined as

$$\lambda_m = \frac{(2m - 1)\pi}{2\eta_o} \ , \ m = 1,2,... \tag{3.5.2}$$

The flux distribution may be obtained from Eq. (3.4.21). Performing the indicated operations, we find

$$Q(\eta,\xi) = -\frac{2}{\eta_o} \sum_{m=1}^{\infty} \frac{\cos\lambda_m \eta}{\sqrt{\lambda_m^2 - 1}} \cdot e^{-\xi} \cdot \sin\sqrt{\lambda_m^2 - 1}\ \xi \ , \tag{3.5.3}$$

$$\eta\varepsilon[0,\eta_o] \ , \ \xi \geq 0 \ ,$$

where the eigenvalues $\lambda_m$ are defined in Eq. (3.5.2). Next, we present some numerical results displaying the nature of the physics and mathematics associated with the hyperbolic heat conduction and compare these results with the classical parabolic model.

Figure 3.5.1 shows the temperature distribution in a flat plate of width $\eta_o = .5$ for various times $\xi$. The distinct dissipative wave feature associated with hyperbolic heat conduction appears dominant. At $\xi = .2$, the wavefront approaches the back surface at $\eta = \eta_o = .5$. For $\xi < .5$, this solution is identical to the half-space problem since the wavefront is unaware of the insulated surface. This undisturbed region appears because no molecular communication has occurred ahead of

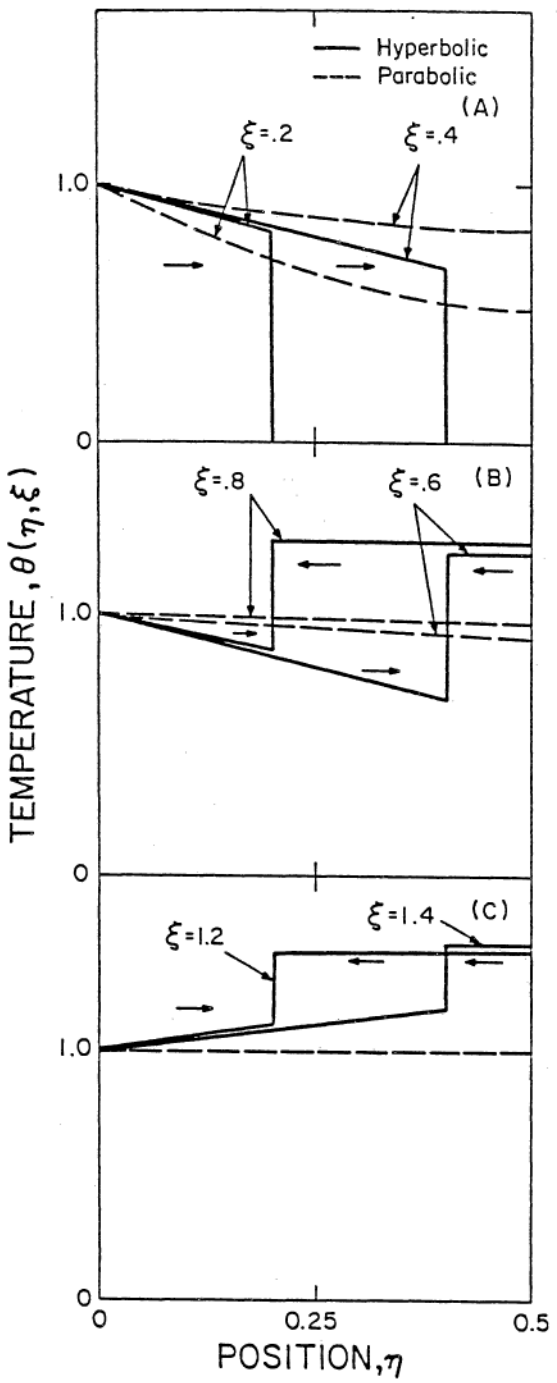


Figure 3.5.1 Hyperbolic and Parabolic Temperatrue Distributions for Various Times in Slab.

the front, i.e., a finite speed of propagation exists. In contrast, the solution to the classical parabolic heat equation displays a continuous distribution throughout the medium which will rise monotonically to the steady state value of unity.

A total reflection of the thermal wave occurs at $\xi = .5$ as the wave impacts the back surface at $\eta_o = .5$. The insulated boundary assures that no energy will be lost through this boundary so that a total reflection takes place. At $\xi = .6$, we notice two distinct wavefronts passing in opposite directions. A controversial feature of hyperbolic heat conduction is displayed here since the temperature of the wavefront moving to the left in Fig. 3.5.1b is greater than the temperature imposed at the wall at $\eta = 0$. This occurs because the energy emanating from $\eta = 0$ and moving toward the rear surface at $\eta_o = .5$ is added to the reflected energy moving toward $\eta = .8$. Meanwhile, the parabolic solution is already nearing its steady state value of unity.

At $\xi = 1.2$, we again see two wavefronts moving in the opposing directions. The wavefront liberated from $\eta = 0$ and moving to the right appears to be negating the reflected wave from $\eta_o = .5$. The corresponding flux distribution will provide further insight to this phenomenon.

The corresponding flux distribution, shown in Fig. 3.5.2, displays similar features to the temperature distribution. At $\xi = .2$ and .4, the distinct damped wave nature of the thermal relaxation model for heat conduction is apparent. In contrast, classical parabolic heat conduction presents a continuous flux distribution.

At $\xi = .5$, a total reflection of energy emerges from the impact at $\eta = \eta_o = .5$. A wiping away effect of energy (negation) is clearly

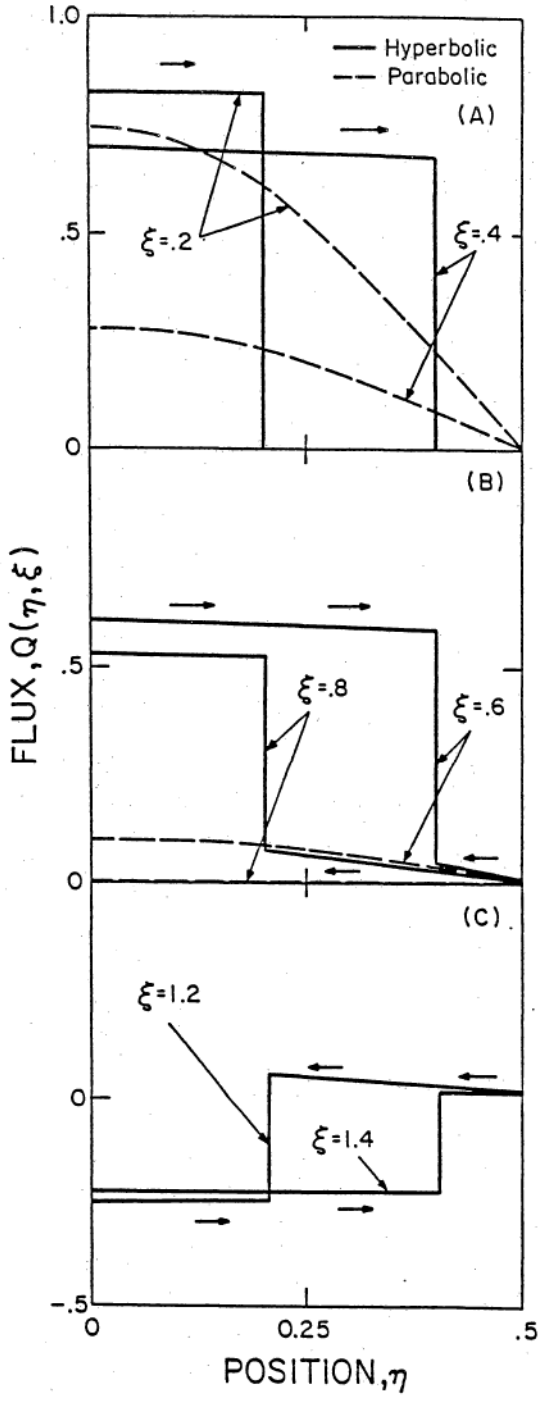


Figure 3.5.2 Hyperbolic and Parabolic Flux Distributions for Various Times in Slab.

evident at $\xi = .6$ as the positive and negative fluxes collide. Further negation of the heat flux waves appear at $\xi = .8$. In contrast, the parabolic heat flux solution approaches its steady state value of zero monotonically and quicker than the corresponding hyperbolic heat flux solution.

The initially reflected wave impacts at the origin at $\xi = 1.0$. Notice that at $\xi = 1.2$ a negative heat flux occurs behind the wavefront departing from the origin. This is another unusual feature which Taitel [26] failed to observe. A purely diffusive heat equation subject to these boundary conditions would never permit a negative flux since the energy entering the slab at $\eta = 0$ would diffuse until steady state had been reached.

The reason for the appearance of the negative wavefront may be understood through the behavior of the heat flux at $\eta = 0$ over time $\xi$. Figure 3.5.3 shows how the heat flux varies with time in order to maintain a constant wall temperature of unity for both the parabolic and hyperbolic heat conduction approximations.

Since a finite thermal wave speed is present in hyperbolic heat conduction, the flux required to maintain the wall temperature at unity is unaware of any reflected energy until $\xi = 1.0$. Up to $\xi = 1.0$, energy is added through the boundary in order to preserve the wall temperature at unity. At $\xi = 1.0$, just as the wavefront hits $\eta = 0$, energy must be removed quickly in order to maintain the wall temperature $\theta(0,\xi) = 1$. The appearance of a negative heat flux wave emanating from $\eta = 0$ at $\xi = 1.0$ is the adjustment required to maintain this boundary temperature. This process of addition and removal of energy at $\eta = 0$ will persist

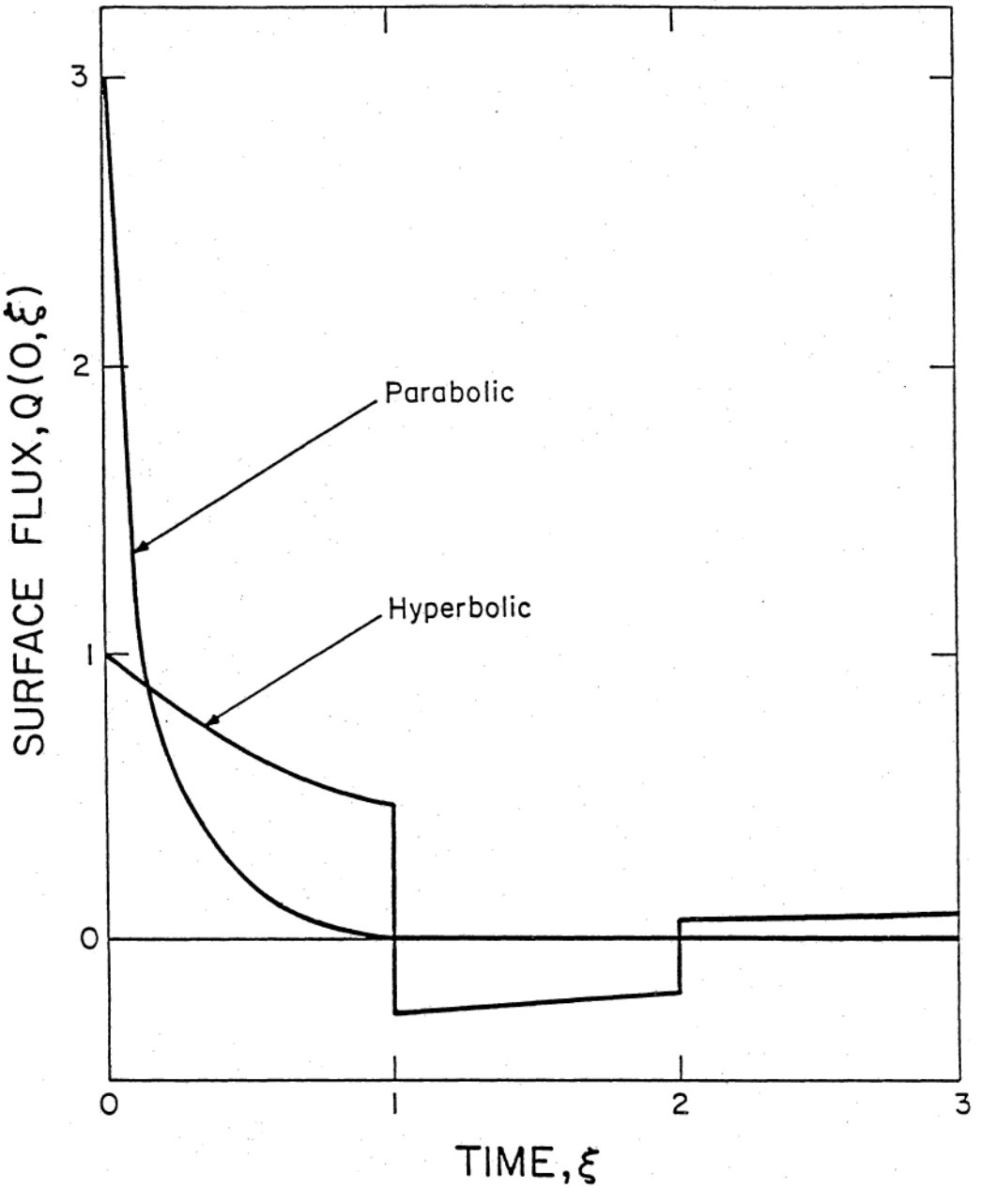


Figure 3.5.3 Behavior of the Flux at the Origin for Hyperbolic and Parabolic Heat Conduction in Slab.

;ntil steady state has been reached.

Some interesting and unusual mathematical features of hyperbolic heat conduction are now highlighted. In reality, the infinite series solutions for both the temperature and flux distributions shown in Eqs. (3.5.1) and (3.5.3) must be truncated after a finite number of terms. A slow convergence rate is associated with the infinite series solutions in hyperbolic heat conduction. One must consider between 300 and 5000 terms for the series to converge to 3-5 significant figures. Examination of the terms in the hyperbolic temperature series solution appears necessary in order to find a method to accelerate the convergence rate of the infinite series.

The difference in the convergence rates between the exact parabolic and hyperbolic solutions may be qualitatively understood by examining the infinite series representations. For this reason, we present the exact temperature solution for the equivalent parabolic heat conduction problem. The temperature distribution is

$$\theta(\eta,\xi) = 1 - \frac{2}{\eta_o} \sum_{m=1}^{\infty} e^{-\frac{\lambda_m^2 \xi}{2}} \frac{\sin\lambda_m \eta}{\lambda_m}, \qquad (3.5.4)$$

where $\lambda_m$'s are defined in Eq. (3.5.2). At first glance, the major difference occurs in the exponential term. The terms in the parabolic solution die out exponentially for increasing eigenvalues at a fixed time $\xi$, whereas those in the hyperbolic solution presented in Eq. (3.5.1) do not. Here lies the major reason for the slow convergence rate of hyperbolic infinite series solutions. A second more subtle reason may be understood by viewing the behavior of the terms of the

infinite series solution expressed in Eq. (3.5.1).

Figure 3.5.4 displays the $m^{th}$ term of the infinite series (not the partial sum) for the hyperbolic temperature solution for a typical set of parameters. At first glance, there appears to be a pattern occurring for large terms. Figure 3.5.5 is an enlargement of Fig. 3.5.4 showing the values of the $m^{th}$ term of the series, $m > 3$. A distinct periodic pattern appears within an exponential envelope. For a different set of parameters a different periodic pattern would be exhibited. The periodic pattern, which dies off slowly, causes the poor convergence. On the other hand, the parabolic series solution would display a very quick decay.

The behavior of the series solution for hyperbolic heat conduction restricts most acceleration methods for infinite series [96-102]. However, the Kummer transform [103, p. 171] works remarkably well when a closed form expression [104-106] may be indentified for the asymptotic series. The convergence rate then becomes comparable to the parabolic solution.

With this introduction, we now proceed to examine the behavior of linear one-dimensional hyperbolic heat conduction in radial systems.

## 3.6 Propagation of Thermal Waves in Radially Dependent Geometries

The effect of radial geometry and the unusual behavior of hyperbolic heat conduction is now investigated through some specific examples. The temperature and flux distributions for the one-dimensional cylinder ($p = 1$) and sphere ($p = 2$) are discussed for two situations. Radially dependent geometries are of practical importance in

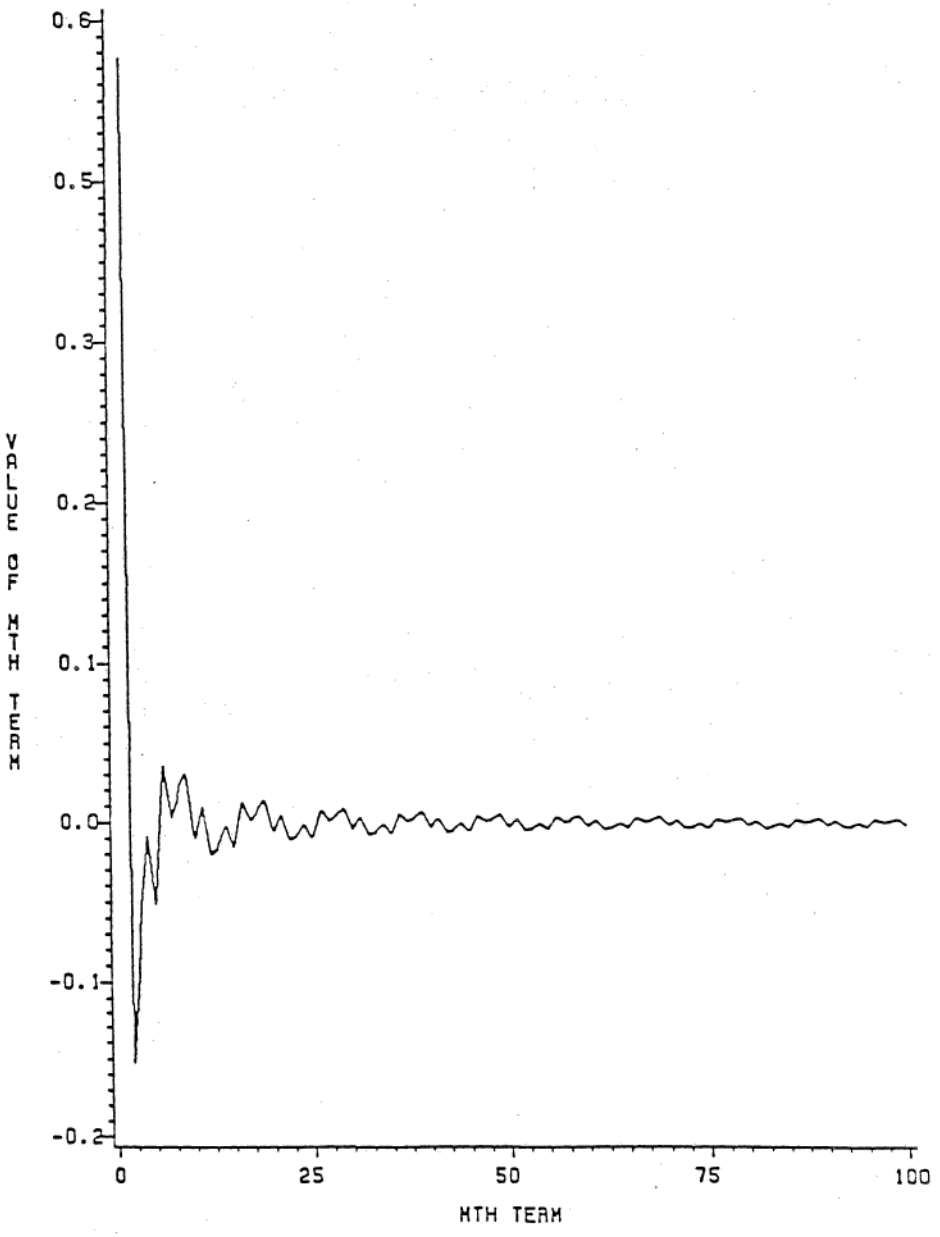


Figure 3.5.4 Terms in the Hyperbolic Temperature Series for $\eta_o = 1$, $\xi = .7$, $\eta = .5$.

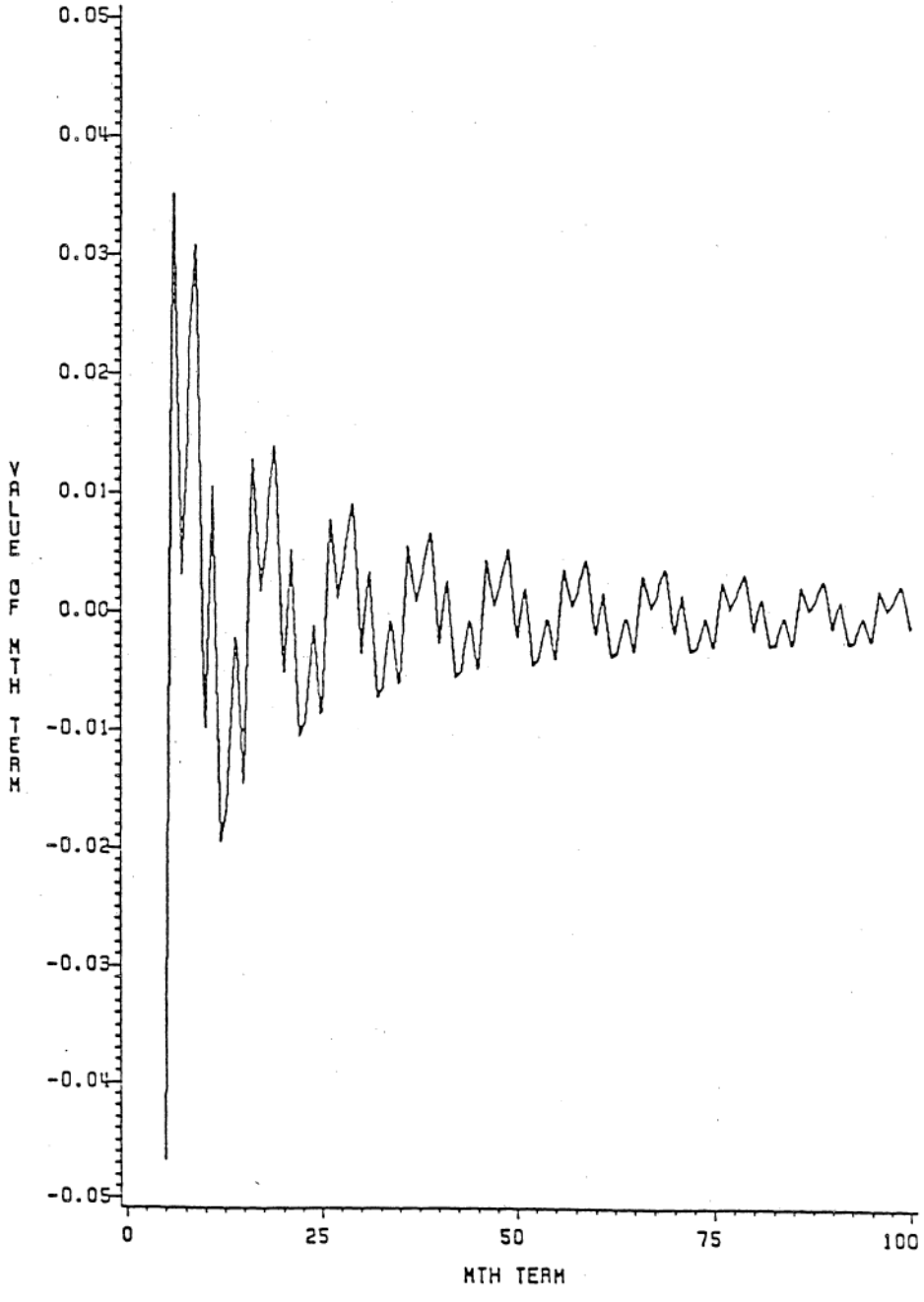


Figure 3.5.5 Enlargement of Fig. 3.5.4 Showing Distinct Periodic Pattern.

several areas of engineering and physics. For example, in laser fusion reactors, tiny fuel pellets are targeted with intense heat fluxes from extremely short pulses of laser radiation. This bombardment of energy induces implosion to take place, thus causing these pellets to achieve extremely high temperatures.

First, consider either a solid cylinder or sphere ($x_i = 0$) subject to a step change in temperature $T_w$ at $x = x_o$ for all time $t > 0$. For nondimensionalization, we choose $T_{ref} = T_w - T_o$, thus the dimensionless boundary temperature becomes $\theta(\eta_o,\xi) = 1$. In the dimensionless form, the boundary coefficients become $C_{2i} = C_{1o} = 1$ and $C_{2o} = C_{1i} = 0$. The temperature and flux distribution resulting from Eqs. (3.4.19) and (3.4.21), respectively, can be utilized once the eigenfunctions $\psi_m(\eta)$, eigenvalues $\lambda_m$, normalization integral $N(\lambda_m)$, and the transformed thermal disturbance function $V_m(\xi)$ have been resolved from Eqs. (3.4.8), (3.4.9), (3.4.10), and (3.4.14b) using the guidelines presented previously. A summary of the above mentioned components required to uniquely determine the temperature and flux distributions are displayed in Tables 3.6.1 and 3.6.2, and are designated as problems 1a and 1b.

The second situation involves a pulsed volumetric heat source $u(x,t)$ emanating in a finite volume about the center of the solid ($x_i = 0$). The energy released by this source is confined in the solid for all time by an insulated outer surface at $x = x_o$. We express this source as

Table 3.6.1 Reference Temperature, Boundary Conditions, Source Functions, and Transformed Thermal Disturbance Function for Cases Under Investigation

| Case # | Problems Description | Reference Temperature | Boundary Conditions | Source, $S(\eta,\xi)$ | Transformed Thermal Disturbance, $V_m(\xi)$ |
|---|---|---|---|---|---|
| 1a | solid cylinder, $T_w$ | $T_w - T_o$ | $\frac{\partial\theta}{\partial\eta}(0,\xi) = 0$<br>$\theta(\eta_o,\xi) = 1$ | 0 | $\lambda_m \eta_o J_1(\lambda_m \eta_o)$, |
| 1b | solid sphere, $T_w$ | $T_w - T_o$ | $\frac{\partial\theta}{\partial\eta}(0,\xi) = 0$<br>$\theta(\eta_o,\xi) = 1$ | 0 | $\lambda_m \eta_o (-1)^{m+1}$ |
| 2a | solid cylinder, pulsed source | $\frac{c^2 U_o}{2\alpha k \pi}$ | $\frac{\partial\theta}{\partial\eta}(0,\xi) = 0$<br>$\frac{\partial\theta}{\partial\theta}(\eta_o,\xi) = 0$ | $\frac{\delta(\xi)}{\Delta\eta^2}$ , $\eta < \Delta\eta$<br>0 , $\eta > \Delta\eta$ | $[\delta(\xi) + \frac{1}{2}\frac{d\delta}{d\xi}] \frac{J_1(\lambda_m \Delta\eta)^*}{\lambda_m \Delta\eta}$ |
| 2b | solid sphere, pulsed source | $\frac{3 c^3 U_o}{16\pi k \alpha^2}$ | $\frac{\partial\theta}{\partial\eta}(0,\xi) = 0$<br>$\frac{\partial\vartheta}{\partial\eta}(\eta_o,\xi) = 0$ | $\frac{\delta(\xi)}{\Delta\eta^3}$ , $\eta < \Delta\eta$<br>0 , $\eta > \Delta\eta$ | $[\delta(\xi) + \frac{1}{2}\frac{d\delta}{d\xi}] \frac{[\frac{\sin(\lambda_m \Delta\eta)}{\Delta\eta} - \lambda_m \cos(\lambda_m \cos(\lambda_m \Delta\eta)]^{**}}{(\lambda_m \Delta\eta)^2}$ |

*For $\lambda_o = 0$ , $V_o(\xi) = \frac{1}{2}[\delta(\xi) + \frac{1}{2}\frac{d\delta}{d\xi}]$

**For $\lambda_o = 0$ , $V_o(\xi) = \frac{1}{2}[\delta(\xi) + \frac{1}{2}\frac{d\delta}{d\xi}]$

Table 3.6.2 Eigenvalues, Eigenfunctions, and Normalization Integrals for Cases under Investigation

| Case # | Eigenvalues $\lambda_m$ are Positive Roots of | Eigenfunctions, $\psi_m(\eta)$ | Normalization Integral, $N(\lambda_m)$ |
|---|---|---|---|
| 1a | $J_o(\lambda_m \eta_o) = 0$ | $J_o(\lambda_m \eta)$ | $\frac{\eta_o^2}{2} J_1^2(\lambda_m \eta_o)$ |
| 1b | $\sin(\lambda_m \eta_o) = 0$ | $\frac{\sin(\lambda_m \eta)}{\eta}$ | $\frac{\eta_o}{2}$ |
| 2a* | $J_1(\lambda_m \eta_o) = 0$ | $J_o(\lambda_m \eta)$ | $\frac{\eta_o^2}{2} J_0^2(\lambda_m \eta_o)$ |
| 2b** | $\tan(\lambda_m \eta_o) - \lambda_m \eta_o = 0$ | $\frac{\sin(\lambda_m \eta)}{\eta}$ | $\frac{\eta_o}{2} \sin^2(\lambda_m \eta_o)$ |

*$\lambda_m = 0$ is an eigenvalue with $\psi_o(\eta) = 1$, $N(\lambda_o) = \frac{\eta_o^2}{2}$

**$\lambda_o = 0$ is an eigenvalue with $\psi_o(\eta) = 1$, $N(\lambda_o) = \frac{\eta_o^3}{3}$

$$u(x,t) = \begin{cases} \dfrac{U_o\,\delta(t)}{\Delta V} & , \quad 0 \leq x \leq \Delta x \\ 0 & , \quad \Delta x < x \leq x_o \end{cases} \tag{3.6.1a}$$

where

$$U_o = \int_{t=0}^{\infty} \int_{V} u(x,t)\, dV dt \quad < \infty \quad . \tag{3.6.1b}$$

The term $U_o$ represents the total amount of energy generated in the entire region over all time and $\Delta V$ is the volume in which the pulsed source is released. In general, the dimensionless form of this source function can be expressed as

$$S(\eta,\xi) = \begin{cases} \dfrac{\delta(\xi)}{\Delta\eta^{p+1}} & , \quad 0 \leq \eta \leq \Delta\eta \\ 0 & , \quad \Delta\eta < \eta \leq \eta_o \end{cases} \tag{3.6.2}$$

where p represents the geometry as expressed in Eq. (3.3.1b). The natural choices for the reference temperatures are

$$T_{ref} = \begin{cases} \dfrac{U_o c}{k} & , \quad \text{slab} \\ \dfrac{U_o c^2}{2\alpha k \pi} & , \quad \text{cylinder} \\ \dfrac{3U_o c^3}{16\pi\alpha^2 k} & , \quad \text{sphere} \quad . \end{cases} \tag{3.6.3}$$

The boundary coefficients required are $C_{2i} = C_{2o} = 1$, $C_{1i} = C_{1o} = 0$. Problems 2a and 2b in Tables 3.6.1 and 3.6.2 contain the required components for the temperature and flux distribution to uniquely specify the

solution for the pulsed source problem.

Numerical results are now discussed for the two problems considered. These results will show the unique and controversial phenomena exhibited by linear one-dimensional hyperbolic heat conduction with radial dependence. Also, a comparison between classical parabolic and hyperbolic heat conduction will be displayed to show the contrasting features between the two heat conduction approximations.

Figure 3.6.1 displays the temperature distributions resulting from Problem 1 where a solid cylinder and sphere are subject to a step change of wall temperature at $\eta_o = 1$. Tables 3.6.1 and 3.6.2 contain all the analytical ingredients to uniquely construct the exact solutions. Figure 3.6.1a displays the slab, cylinder, and sphere temperature distributions contrasting the effect of geometry as the initial wave progresses to the origin. At $\xi = .5$, it is apparent that some focusing (amplification) in temperature is occurring in the spherical medium. The slab and cylinder temperatures are below the thermal disturbance value of unity imposed at the boundary. It is also clear that an undisturbed region lies ahead of the wavefront as a consequence of a finite wavespeed imposed from the thermal relaxation model. At $\xi = 1.0$, the converging cylindrical and spherical shock wave produce singularities at the origin as a finite amount of energy is packed into zero volume. The spherical temperature shock wave grows quicker because of geometrical considerations, i.e., the volume of sphere goes as $\eta^3$ whereas the volume of the cylinder goes as $\eta^2$.

Though the appearance of a converging thermal wave appears unusual, many other branches of science and engineering have studied the focusing

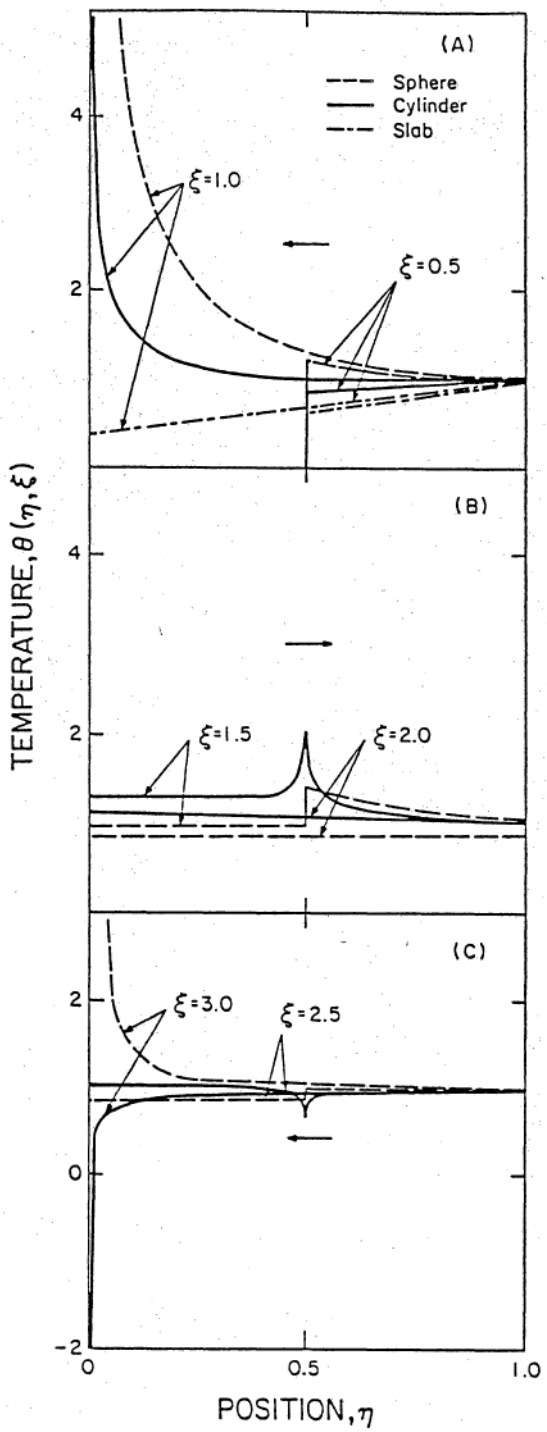


Figure 3.6.1 Temperature Distributions for Sphere, Cylinder, and Slab Resulting from Step Change in Wall Temperature.

of shock waves in radial systems. For example, the growth of converging shock waves in compressible fluids has been experimentally [107,108] studied since 1950. Also numerical [109,110] and purely mathematical [111] studies have been performed concerning the focusing of waves to form singularities. Reference 107 is particularly interesting, where Perry and Kantrowitz display Schlieren photographs taken from their experiments verifying that cylindrical shock waves focus in air. That is, a finite amount of amplification of the incoming shock wave occurred.

The results presented in Fig. 3.6.1, from linear theory, do not suggest that temperature singularities physically exist. Even discounting the limitations of linear theory of heat conduction and not accounting for mechanical deformation effects, the continuum assumption would break down as the converging shock wave reaches radii of the order of several mean free paths. Some focusing of energy should be physically expected as shown in [107], however the magnitude cannot be assessed from linear uncoupled theory.

The converging cylindrical and spherical shocks then rebound after impacting at the origin at $\xi$ 1.0. Figure 3.6.1b displays the rebounding waves at $\xi = 1.5$ and 2.0.

Another interesting feature of hyperbolic heat conduction is shown in the spherical temperature distribution as the returning wave reaches the imposed temperature boundary at $\eta_o = 1$ where a temperature jump results at this boundary. The temperature peaks decrease in magnitude as the rebounding wave travels through increasing radius $\eta$.

After a reflection at $\xi = 2.0$, Fig. 3.6.1c shows the temperature

distributions of the focusing waves heading back toward the origin. These distributions are flatter since some diffusion has take place. But also notice that the cylindrical wave peaks to a negative temperature singularity at $\xi = 3.0$, whereas the spherical wave focuses quicker and toward a positive temperature singularity. The reason for this strange downward spike can be understood by exmaining the heat flux at $\eta_o = 1$ over time.

Figure 3.6.2 displays the behavior of the heat flux at the boundary $\eta_o = 1$ over time as required to maintain the wall temperature at unity. As the initial wave enters the medium and moves toward the origin, energy is added to the system in order to maintain the wall temperature at unity. Since a finite speed of propagation is now present, the surface heat flux is unaware of any net changes until $\xi = 2$ when the returning wave impinges. As the returning cylindrical wave impacts the specified (fixed) wall temperature boundary condition at $\xi = 2$, a sudden glut of energy must be removed to maintain a constant wall temperature. This is clearly seen in Fig. 3.6.2 by the appearance of a sudden peak at $\xi = 2$. In contrast, the rebounding spherical temperature wave is below the specified wall temperature, therefore a sudden addition of energy must be provided. This process will proceed until steady state has been reached.

Figure 3.6.3 displays the flux distributions corresponding to Fig. 3.6.1. Again, focusing of the incoming thermal waves is clearly shown in Fig. 3.6.2 where the spherical geometry produces the most severe distributions. At $\xi = 1.0$, a flux jump at the origin appears for the slab, cylinder, and sphere. Actually, a flux jump at the boundary

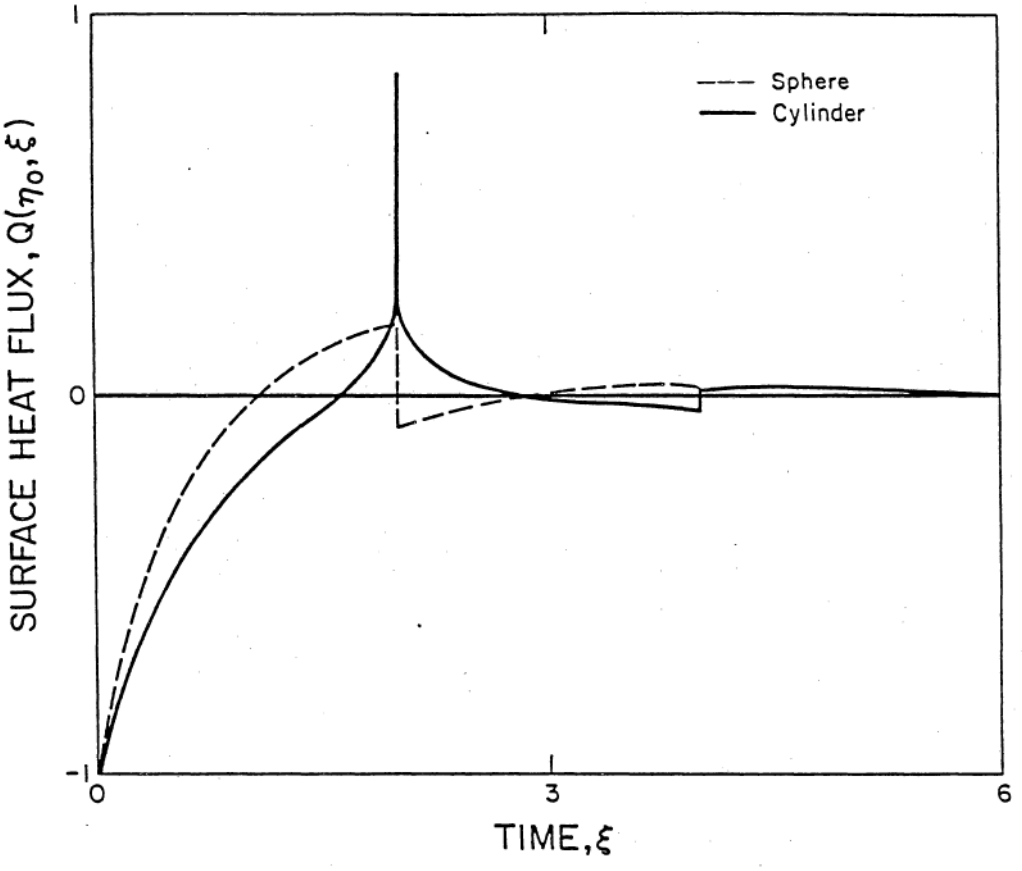


Figure 3.6.2 Variation of Heat Flux at Boundary where Thermal Disturbance is Imposed for Cylinder and Sphere.

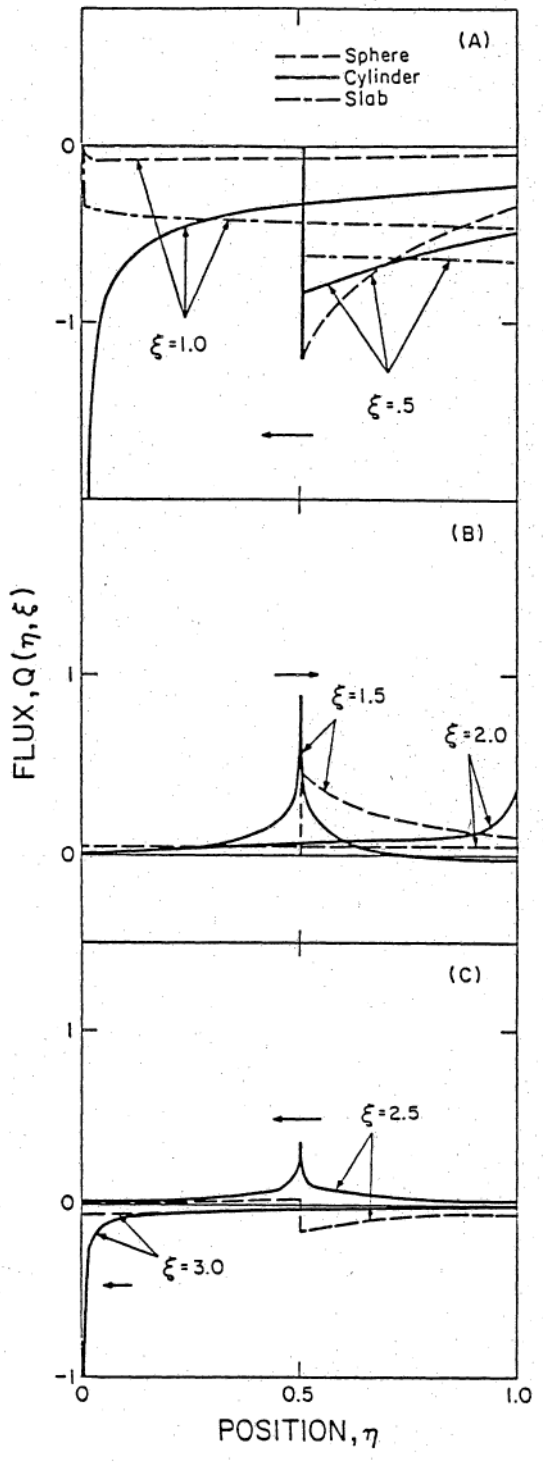


Figure 3.6.3 Flux Distributions for Sphere, Cylinder, and Slab Resulting from Step Change in Wall Temperature.

conditions will occur at the instances where the wavefront impinges these conditions. At all other times the flux at $\eta_i = 0$ and $\eta_o = 1$ will be smooth. Next, we consider a problem of a more fundamental nature involving a pulsed source.

Problem 2 considers a volumetric heat source released about the origin at $\xi = 0^+$ and confined for all time within the solid (radially dependent) medium. The insulated boundary imposed at $\eta_o = 1$ assures that no energy will be lost through the boundary. Tables 3.6.1 and 3.6.2 contain all the ingredients required to construct the exact solution for this set of conditions.

Figure 3.6.4 displays the contrasting heat conduction approximations (parabolic, hyperbolic) for a cylinder subject to a pulsed volumetric source released in a volume of radial width $\Delta\eta = 0.1$. The hyperbolic heat conduction approximation displays an unusual temperature waveform at $\xi = .5$. An undisturbed region lies ahead of the wavefront indicating that a finite speed of propagation of energy exists. The origins of the unusual temperature distribution can be traced to the initially released source confined between $\eta\varepsilon[0,\Delta\eta]$. When the source is released at $\xi = 0^+$, no preferred direction for the energy propagation is distinguished. The net effect is that the pulse width stretches to $2\Delta\eta$ as some of the energy initially moves toward increasing $\eta$ while the remaining energy moves toward the origin. The two temperature spikes are consequences of the initial splitting of energy. The positive temperature peak results from the initial release of energy moving in the increasing $\eta$ direction while the negative temperature peak is the residue of the reflected portion of energy (from $\eta = 0$) which had experi-

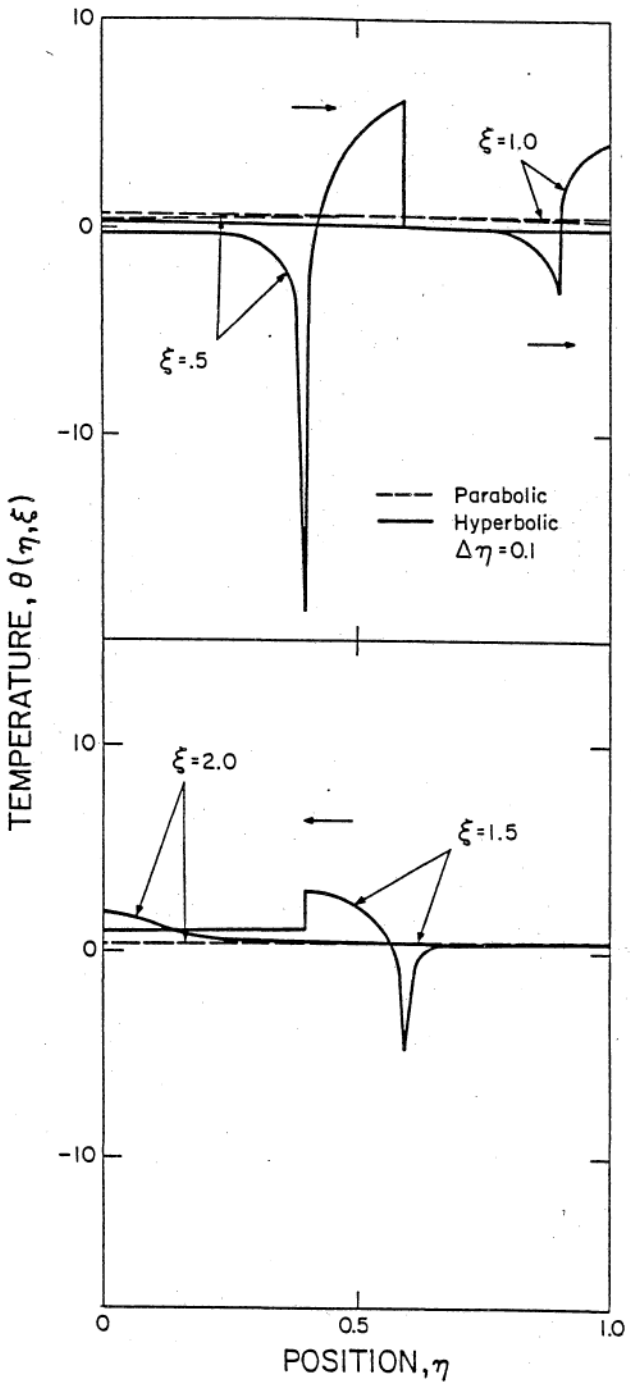


Figure 3.6.4 Parabolic and Hyperbolic Temperature Distributions Resulting from Pulsed Volumetric Heat Source in a Cylinder.

enced a singularity at the origin.

At $\xi = 1.0$, a total reflection of energy occurs since no energy can be lost at $\eta_o = 1$. At $\xi = 1.5$, the waveform is moving toward the origin at a constant speed. The effects of diffusion are apparent from the residual temperature behind the waveform as it moves through the medium. In contrast, the parabolic solution predicts lower temperatures, although both approximations yield identical steady state values.

The corresponding flux distributions are shown in Fig. 3.6.5. Similar wavelike features are present in the hyperbolic heat conduction flux distributions. The hyperbolic model predicts much higher fluxes than the corresponding parabolic solution. The effect of diffusion is displayed behind the propagating pulse.

Figure 3.6.6 shows the temperature distributions for a cylinder and sphere of radius $\eta_o = 1$ subject to a pulsed source of width $\Delta\eta = 0.1$. Tables 3.6.1 and 3.6.2 contain all the information to construct the exact temperature and flux distributions. The propagation of the cylindrical and spherical shock waves behave in a similar manner. The temperature wave disperses as the energy content per volume decreases for increasing $\eta$ as seen at times $\xi = .5$ and 1.0. Both geometries display identical trends as the rebounding wave ($\xi = 1.5$ and 2) focuses toward the origin. As mentioned previously, no direction of propagation is preferred when the source is initially released in the medium. Therefore, the trailing end of the pulses, as seen at $\xi = .5$ and 1.0, represents the portion of energy which initially went to a singular value at the origin whereas the leading edge represents the energy directed toward increasing $\eta$. The steady state temperature for the two geome-

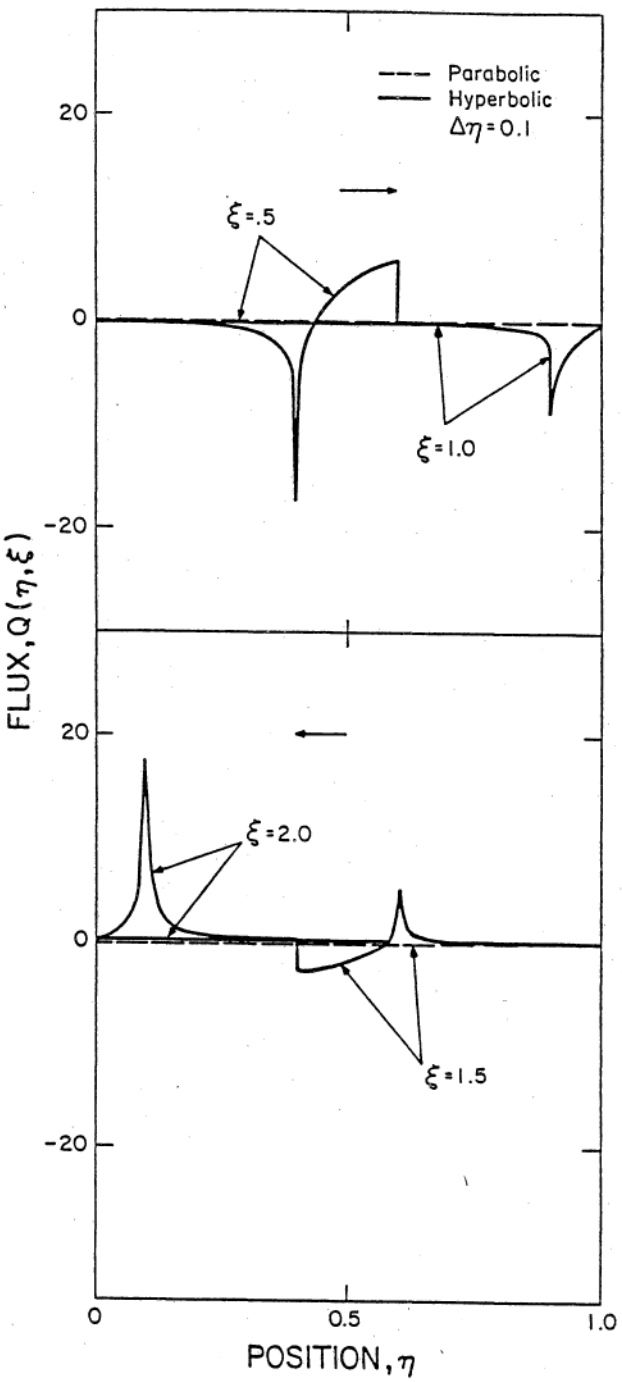


Figure 3.6.5 Parabolic and Hyperbolic Flux Distributions Resulting from Pulsed Volumetric Heat Source in a Cylinder.

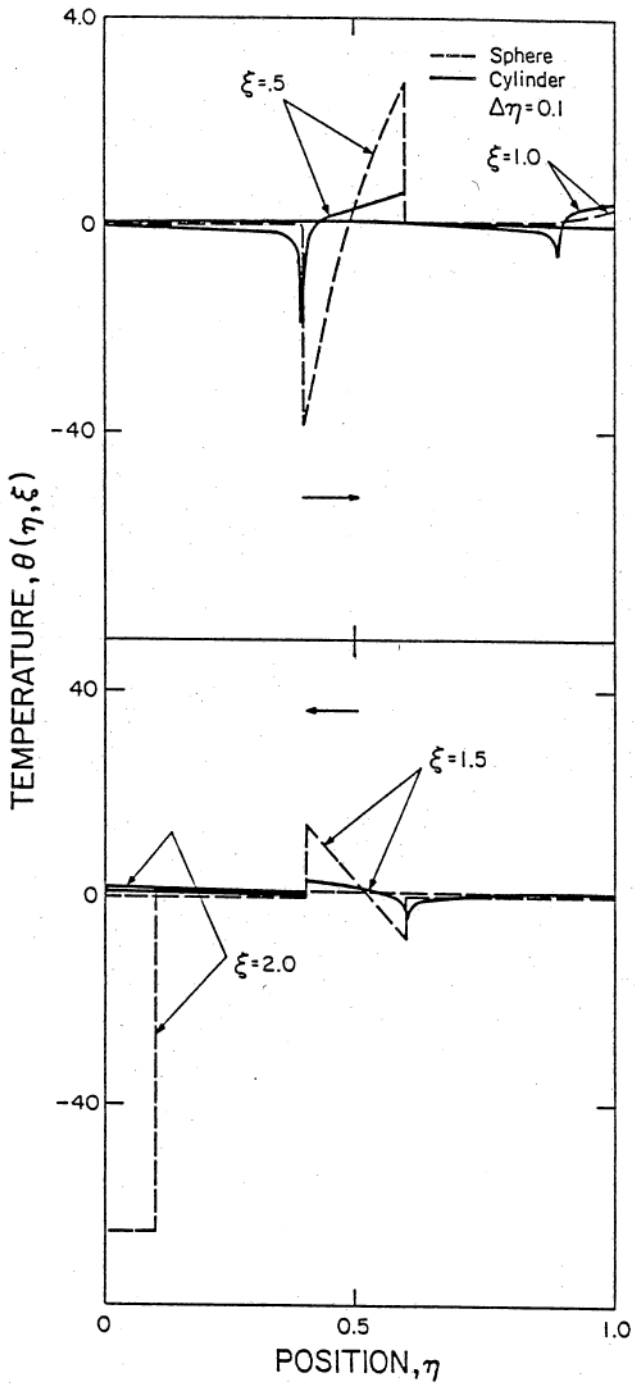


Figure 3.6.6 Temperatrue Distributions for Cylinder and Sphere Subjected to Pulsed Source Originating about the Origin.

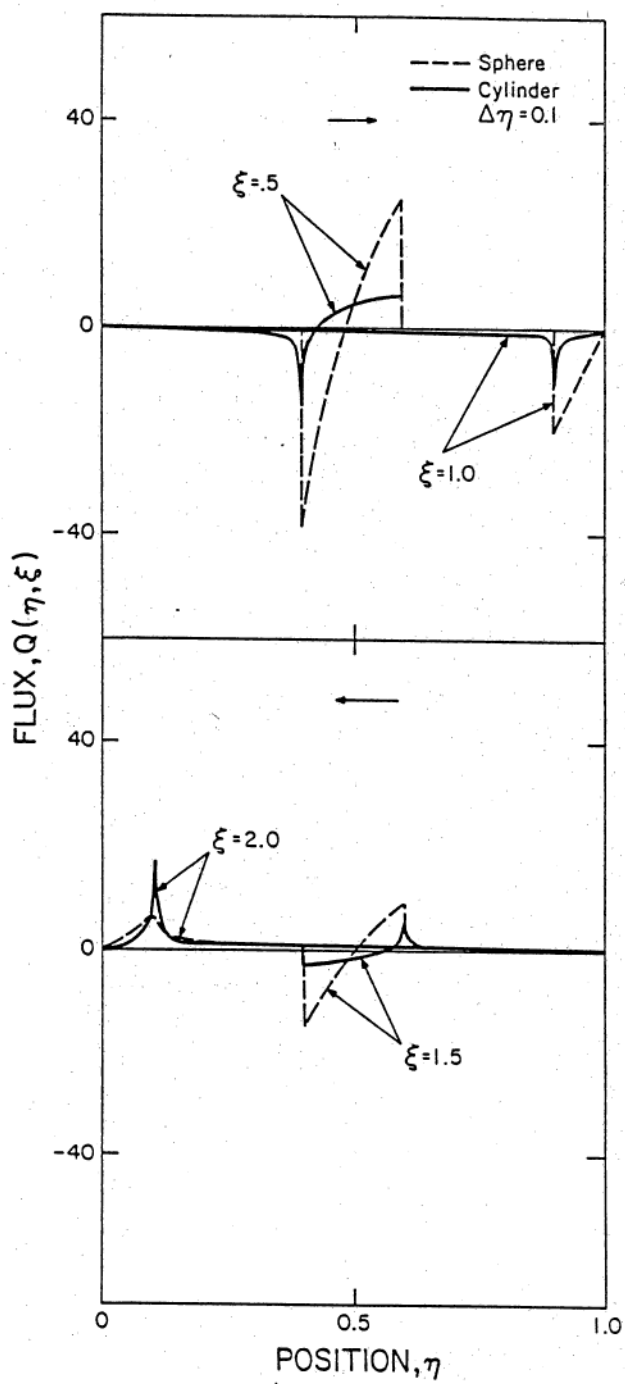


Figure 3.6.7 Flux Distributions for Cylinder and Sphere Subjected to Pulsed Source Originating about the Origin.

tries will not yield indentical results since the volumes are dissimilar. Finally, Fig. 3.6.7 displays the corresponding flux distribution which exhibits similar trends as discussed previously.

## 3.7 Pulsed Surface Heat Flux Problem Resolved in Flux Domain

The development of the general flux formulation for heat conduction based on the modified Fourier's law is presented in Section 3.3. The one-dimensional flux formulation produces a hyperbolic field equation which is certainly more convenient to use in situations involving specified flux conditions than the usual temperature formulation. It should be recalled that boundary conditions involving specified temperatures may also be transformed into the flux domain as shown by Table 3.2.1. The recovery of the temperature distribution may be obtained through integrating of the energy conservation law with respect to time.

In this section, the Green's function approach is used to develop a general solution for hyperbolic heat conduction in a finite slab ($p = 0$). The utility of the flux formulation and the unusual nature of heat conduction based on thermal relaxation are demonstrated by developing analytical expressions for the heat flux and temperature distributions in a finite slab exposed to a pulsed surface heat flux.

Consider a slab initially at the equilibrium temperature $T_o$. At time $t = 0$, both external surfaces are suddenly exposed to arbitrary time dependent heat fluxes while the entire slab is in the presence of a general volumetric heat source. In this situation, the general three dimensional flux formulation developed Section 3.3 for a slab ($p = 0$) reduces to

$$\frac{\partial^2 q}{\partial x^2}(x,t) - \frac{\partial u}{\partial x}(x,t) = \frac{1}{\alpha}\left[\tau \frac{\partial^2 q}{\partial t^2}(x,t) + \frac{\partial q}{\partial t}(x,t)\right] , \qquad (3.7.1)$$

$$x\varepsilon(0,\ell), t>0.$$

where $x_i = 0$ and $x_o = \ell$.

The boundary and initial conditions may be expressed as

$$q(0,t) = q_o(t) , \qquad (3.7.2a)$$

$$q(\ell,t) = -q_\ell(t) , \quad t>0 , \qquad (3.7.2b)$$

and

$$q(x,0) = 0 , \qquad (3.7.3a)$$

$$\frac{\partial q}{\partial t}(x,0) = 0, \quad x\varepsilon[0,\ell] . \qquad (3.7.3b)$$

Formally, as $\tau \to 0$, Eq. (3.7.1) reduces to the classical parabolic heat flux formulation. The convenience of the flux formulation for a problem involving specified heat flux boundary conditions now becomes apparent. That is, a simple boundary condition such as Eq. (3.7.2a) replaces a more involved boundary condition

$$-k \frac{\partial T}{\partial x}(0,t) = \tau \frac{dq_o}{dt}(t) + q_o(t) . \qquad (3.7.4)$$

This conversion of flux information to the temperature variable is shown in Table 3.2.1.

For convenience in the subsequent analysis, we introduce the dimensionless variables expressed in Eq. (3.4.1) into Eqs. (3.7.1-3.7.3) to

obtain the dimensionless system governing the flux distribution. The dimensionless heat flux field equation becomes

$$\frac{\partial^2 Q}{\partial \xi^2}(\eta,\xi) + 2\frac{\partial Q}{\partial \xi}(\eta,\xi) = \frac{\partial^2 Q}{\partial \eta^2}(\eta,\xi) - \frac{1}{2}\frac{\partial S}{\partial \eta}(\eta,\xi) \quad , \quad \eta\varepsilon(0,\eta_\ell) \quad , \xi > 0 \quad , \tag{3.7.5}$$

$$Q(0,\xi) = Q_o(\xi) \quad , \tag{3.7.6a}$$

$$Q(\eta_\ell,\xi) = - Q_\ell(\xi) \quad , \quad \xi > 0 \quad , \tag{3.7.6b}$$

and

$$Q(\eta,0) = 0 \quad , \tag{3.7.7a}$$

$$\frac{\partial Q}{\partial \xi}(\eta,0) = 0 \quad , \quad \eta\varepsilon[0,\eta_\ell] \quad . \tag{3.7.7b}$$

The dimensionless one-dimensional (p = 0) energy balance for Eq. (3.3.1a) (p = 0) becomes

$$- \frac{\partial Q}{\partial \eta}(\eta,\xi) + 1/2\, S(\eta,\xi) = \frac{\partial \theta}{\partial \xi}(\eta,\xi) \quad , \tag{3.7.8}$$

which can be integrated to give the temperature distribution as

$$\theta(\eta,\xi) = \theta(\eta,0) - \int_{\xi'=0}^{\xi} [\frac{\partial Q}{\partial \eta}(\eta,\xi') - 1/2\, S(\eta,\xi')]d\xi' \quad . \tag{3.7.9}$$

Next we develop the general solution to the system of equations (3.7.5-3.7.7) by the Green's function method and apply the results for a

pulsed surface heat flux.

The formal starting point in the development of the Green's function method is the application of Green's second formula over the domain of interest [112-115] on Eq. (3.7.5) to get

$$\lim_{\varepsilon\to 0}\int_{\xi_o=0}^{\xi+\varepsilon}\int_{\eta_o=0}^{\eta_\ell} G(\eta,\xi|\eta_o,\xi_o)L_o[Q(\eta_o,\xi_o)]d\eta_o d\xi_o$$

$$= \lim_{\varepsilon\to 0}\{(BC + IC) + \int_{\xi_o=0}^{\xi+\varepsilon}\int_{\eta_o=0}^{\eta_\ell} Q(\eta_o,\xi_o) \tag{3.7.10}$$

$$\cdot L_o^*[G(\eta,\xi|\eta_o,\xi_o)]d\eta_o d\xi_o\} .$$

Here $G(\eta,\xi|\eta_o,\xi_o)$ is the appropriate Green's function where the arguments are written to represent the "effect/cause" relationship. We introduce $\varepsilon > 0$ in order to invoke causality at a later time in the analysis.

For any given linear operator $L_o$, the contribution of the boundary and initial conditions are represented symbolically by BC and IC, respectively. Also, $L_o^*$ is the formal adjoint operator of the operator $L_o$. The operator L is chosen as the modified heat flux linear operator

$$L \equiv \frac{\partial^2}{\partial\eta^2} - \frac{\partial^2}{\partial\xi^2} - 2\frac{\partial}{\partial\xi} , \tag{3.7.11}$$

since we are interested in the solution to Eq. (3.7.5) which can be expressed as

$$L[Q(\eta,\xi)] = \frac{1}{2}\frac{\partial S}{\partial \eta}(\eta,\xi) \ , \ \eta\varepsilon(0,\eta_\ell) \quad , \quad \xi > 0 \ . \tag{3.7.12}$$

Integrating the LHS of Eq. (3.7.10) by parts, and using the linear operator given by Eq. (3.7.11) with the understanding that $L_o$ represents differentiation with respect to the cause variables $\eta_o$ and $\xi_o$, we obtain the following explicit expression

$$\begin{aligned}
&\lim_{\varepsilon\to 0} \int_{\xi_o=0}^{\xi+\varepsilon} \int_{\eta_o=0}^{\eta_\ell} G(\eta,\xi|\eta_o,\xi_o) L_o[Q(\eta_o,\xi_o)]\, d\eta_o\, d\xi_o \\
&= \lim_{\varepsilon\to 0}\Big\{ \int_{\xi_o=0}^{\xi+\varepsilon} \Big[G\frac{\partial Q}{\partial \eta_o}\Big|_0^{\eta_\ell} - \frac{\partial G}{\partial \eta_o} Q\Big|_0^{\eta_\ell}\Big] d\xi_o \\
&\quad + \int_{\eta_o=0}^{\eta_\ell} \Big[-G\frac{\partial Q}{\partial \xi_o} + Q\Big(\frac{\partial G}{\partial \xi_o} - 2G\Big)\Big]_0^{\xi+\varepsilon} d\eta_o \\
&\quad + \int_{\xi_o=0}^{\xi+\varepsilon} \int_{\eta_o=0}^{\eta_\ell} Q(\eta_o,\xi_o) L_o^*[G(\eta,\xi|\eta_o,\xi_o)]\, d\eta_o\, d\xi_o\Big\} \ ,
\end{aligned} \tag{3.7.13}$$

where the integration shows that the formal adjoint operator of $L_o$ is

$$L_o^* = \frac{\partial^2}{\partial \eta_o^2} - \frac{\partial^2}{\partial \xi_o^2} + 2\frac{\partial}{\partial \xi_o} \ . \tag{3.7.14}$$

We observe that $L_o^* \neq L_o$, that is, the operator $L_o$ is not formally self adjoint.

The Green's function is chosen such that

$$L_o^*[G(\eta,\xi|\eta_o,\xi_o)] = \delta(\eta_o - \eta)\delta(\xi_o - \xi) \ , \tag{3.7.15}$$

subject to homogeneous boundary conditions

$$G(\eta,\xi|0,\xi_o) = 0 \ , \tag{3.7.16a}$$

$$G(\eta,\xi|\eta_\ell,\xi_o) = 0 \ , \tag{3.7.16b}$$

with the additional requirement that

$$G(\eta,\xi|\eta_o,\xi_o) = 0 \ , \ \xi < \xi_o \ , \tag{3.7.17a}$$

$$\frac{\partial G(\eta,\xi|\eta_o,\xi o)}{\partial \xi_o} = 0 \ , \ \xi < \xi_o \ . \tag{3.7.17b}$$

Conditions (3.7.17a-b) represent the causality principle, which is merely a statement that no effect can be experienced prior to a cause. Using the Green's function as governed by Eqs. (3.7.15-3.7.17) and taking the limit as $\varepsilon \to 0$ in Eq. (3.7.13), gives the general representation of the heat flux distribution $Q(\eta,\xi)$ as

$$Q(\eta,\xi) = 1/2 \int_{\xi_o=0}^{\xi} \int_{\eta_o=0}^{\eta_\ell} G(\eta,\xi|\eta_o,\xi_o) \frac{\partial S(\eta_o,\xi_o)}{\partial \eta_o} d\eta_o d\xi_o$$

$$+ \int_{\xi_o=0}^{\xi} \left[ \frac{\partial G(\eta,\xi|\eta_\ell,\xi_o)}{\partial \eta_o} Q(\eta_\ell,\xi_o) \right.$$

$$\left. - \frac{\partial G(\eta,\xi|0,\xi_o)}{\partial \eta_o} Q(0,\xi_o) \right] d\xi_o$$

$$+ \int_{\eta_o=0}^{\eta_\ell} \left[-G(\eta,\xi|\eta_o,0)\,\frac{\partial Q(\eta_o,0)}{\partial \xi_o}\right. \tag{3.7.18}$$

$$\left. + Q(\eta_o,0)\left(\frac{\partial G(\eta,\xi|\eta_o,0)}{\partial \xi_o} - 2G(\eta,\xi|\eta_o,0)\right)\right] d\eta_o \ ,$$

$$\eta\in[0,\eta_\ell],\ \xi\geq 0 \ .$$

The only remaining ingredient needed for a complete specification of the function Q is the determination of the Green's function itself, which will be resolved by the finite integral transform technique.

The finite integral transform technique [93] is now utilized to determine the Green's function. The appropriate eigenvalue problem, obtained from the associated homogeneous version of the system of Eqs. (3.7.15-3.7.17) is given by

$$\frac{d^2}{d\eta_o^2}\psi_m(\lambda_m,\eta_o) + \lambda_m^2\psi_m(\lambda_m,\eta_o) = 0 \ , \tag{3.7.19}$$

subject to

$$\psi_m(\lambda_m,0) = 0 \ , \tag{3.7.20a}$$

$$\psi_m(\lambda_m,\eta_\ell) = 0 \ . \tag{3.7.20b}$$

The solution is of this problem gives the eigenfunctions

$$\psi_m(\lambda_m,\eta_o) = \sin\lambda_m\eta_o, \tag{3.7.21}$$

where the eigenvalues are defined as

$$\lambda_m = \frac{m\pi}{\eta_\ell} \ , \ m = 1,2,3,... \tag{3.7.22}$$

The <u>orthogonality</u> relation is written in terms of the inner product as

$$\left(\psi_m(\lambda_m,\eta_o) \ , \ \psi_n(\lambda_n,\eta_o)\right) \equiv \int_{\eta_o=0}^{\eta_\ell} \psi_m(\lambda_m,\eta_o)\psi_n(\lambda_n,\eta_o)d\eta_o$$

$$= \begin{cases} N(\lambda_m) \ , \ m = n \\ 0 \quad\quad , \ m \neq n \end{cases} \tag{3.7.23a}$$

where $N(\lambda_m)$ is the normalization integral given by

$$N(\lambda_m) = \frac{\eta_\ell}{2} \ . \tag{3.7.23b}$$

With the aid of the orthogonality relation, we can now define the finite integral transform pair as

<u>Inversion Formula</u>:

$$G(\eta,\xi|\eta_o,\xi_o) = \sum_{m=1}^{\infty} \frac{\psi_m(\lambda_m,\eta_o)\overline{G}_m(\lambda_m,\xi_o)}{N(\lambda_m)} \ , \tag{3.7.24}$$

<u>Integral Transform</u>:

$$\bar{G}_m(\lambda_m,\xi_o) = \int_{\eta_o=0}^{\eta_\ell} \psi_m(\lambda_m,\eta_o)G(\eta,\xi|\eta_o,\xi_o)d\eta_o \ . \qquad (3.7.25)$$

In order to determine the transform, $\bar{G}_m(\lambda_m,\xi_o)$, we operate on Eq. (3.7.15) with

$$\int_{\eta_o=0}^{\eta_\ell} \psi_m(\lambda_m,\eta_o)d\eta_o \ , \qquad (3.7.26)$$

and incorporate the homogeneous boundary conditions of Eqs. (3.7.16) and (3.7.20) in order to obtain the following ordinary differential equation for $\bar{G}_m(\lambda_m,\xi_o)$

$$\frac{d^2\bar{G}_m(\lambda_m,\xi_o)}{d\xi_o^2} - 2\frac{d\bar{G}_m(\lambda_m,\xi_o)}{d\xi_o} + \lambda_m^2\bar{G}_m(\lambda_m,\xi_o) = -\delta(\xi_o-\xi)\psi_m(\lambda_m,\eta), \qquad (3.7.27)$$

subject to the transformed initial conditions

$$\bar{G}_m(\lambda_m,\xi_o) = 0 \ , \ \xi<\xi_o \ , \qquad (3.7.28a)$$

$$\frac{d\bar{G}_m(\lambda_m,\xi_o)}{d\xi_o} = 0 \ , \ \xi<\xi_o \ . \qquad (3.7.28b)$$

After some careful manipulation, the solution to Eqs. (3.7.27) and (3.7.28) can be expressed as

$$\bar{G}_m(\lambda_m,\xi_o) = -\frac{\psi_m(\lambda_m,\eta)e^{-(\xi-\xi_o)}}{\sqrt{\lambda_m^2-1}} \cdot \sin\sqrt{\lambda_m^2-1}\,(\xi-\xi_o) \ , \ \xi>\xi_o. \qquad (3.7.29)$$

Substituting Eq. (3.7.29) into the inversion formula, Eq. (3.7.24), we

obtain the Green's function as

$$G(\eta,\xi|\eta_o,\xi_o) = -\sum_{m=1}^{\infty} \frac{\psi_m(\lambda_m,\eta)\psi_m(\lambda_m,\eta_o)e^{-(\xi-\xi_o)}\sin\sqrt{\lambda_m^2-1}\,(\xi-\xi_o)}{N(\lambda_m)\sqrt{\lambda_m^2-1}}, \tag{3.7.30}$$

$$\xi > \xi_0 \ , \ \eta\varepsilon[0,\eta_\ell] \ ,$$

where the eigenfunctions $\psi_m(\lambda_m,\eta)$, $\psi_m(\lambda_m,\eta_o)$ are defined by Eq. (3.7.21) the eigenvalues are expressed by Eq. (3.7.22).

Since the Green's function is now known, the heat flux distribution $Q(\eta,\xi)$ for any arbitrary volumetric heat source and boundary conditions as expressed by Eq. (3.7.6) can be obtained from Eq. (3.7.18). The dimensionless temperature distribution can be determined by using Eq. (3.7.9). A specific example is investigated to display the utility of this heat flux formulation to bring forth some unique features of heat conduction based on the hyperbolic formulation.

Here we consider a flat plate of thickness $\ell$, subject to a pulsed heat flux at the surface $x = 0$ which has an intensity $q_o$ for a duration of $\Delta t$ seconds. The surface at $x = \ell$ is insulated for all time $t > 0$. The body is initially in equilibrium at the uniform temperature $T_o$ and contains no volumetric heat source. Previous investigations [62,63] of the hyperbolic surface heat flux problem, based on the temperature formulation, have not considered the heat flux distribution in any manner. Boundary conditions involving heat flux have been incorrectly formulated [62] by using Fourier's law at the boundaries in conjunction with the hyperbolic model inside the region, resulting in an inconsistent formulation leading to questionable results.

For this specific case, a convenient reference temperature is chosen as

$$T_{ref} = \frac{q_o}{ck/\alpha} \, . \tag{3.7.31}$$

The dimensionless heat flux field equation, Eq. (3.7.5), reduces to

$$\frac{\partial^2 Q}{\partial \eta^2}(\eta,\xi) = \frac{\partial^2 Q}{\partial \xi^2}(\eta,\xi) + 2\frac{\partial Q}{\partial \xi}(\eta,\xi), \quad \eta\epsilon(0,\eta_\ell) \, , \quad \xi > 0 \, . \tag{3.7.32}$$

The boundary conditions are expressed as

$$q_o(0,t) = q_o[H(t) - H(t - \Delta t)] \, , \tag{3.7.32a}$$

$$q_o(\ell,t) = 0, \; t > 0 \, , \tag{3.7.32b}$$

or in dimensionless form as

$$Q(0,\xi) = H(\xi) - H(\xi - \Delta\xi) \, , \tag{3.7.34a}$$

$$Q(\eta_\ell,\xi) = 0 \, , \; \xi > 0 \, , \tag{3.7.34b}$$

where H represents the Heavyside step function. It is interesting to note that the proper boundary condition, corresponding to Eq. (3.7.32a) in the temperature formulation would be

$$\frac{\partial T}{\partial x}(0,t) = -\frac{q_o}{k}\left[H(t) - H(t - \Delta t) + \tau\delta(t) - \tau\delta(t - \Delta t)\right] \, . \tag{3.7.35}$$

The solution to the pulsed heat flux problem is now obtained from the general formula solution Eq. (3.7.18), by using the Green's function, Eq. (3.7.30), the boundary and initial conditions given by Eqs. (3.7.34) and (3.7.7), respectively, and a zero source. Performing the indicated operations and after a lengthy but straightforward set of manipulations, the heat flux distribution becomes

$$Q(\eta,\xi) = \left(1 - \frac{\eta}{\eta_\ell}\right)\cdot\left(H(\xi) - H(\xi - \Delta\xi)\right) +$$

$$- \frac{2}{\eta_\ell} \sum_{m=1}^{\infty} \frac{\sin\lambda_m \eta}{\lambda_m} e^{-\xi}\cdot\left[\frac{\sin\sqrt{\lambda_m^2-1}\ \xi}{\sqrt{\lambda_m^2 - 1}} + \cos\sqrt{\lambda_m^2 - 1}\ \xi\right]H(\xi) +$$

$$+ \frac{2}{\eta_\ell} \sum_{m=1}^{\infty} \frac{\sin\lambda_m \eta}{\lambda_m} \cdot e^{-(\xi-\Delta\xi)}\cdot\left\{\frac{\sin\sqrt{\lambda_m^2-1}\ (\xi-\Delta\xi)}{\sqrt{\lambda_m^2 - 1}} + \cos\sqrt{\lambda_m^2-1}\ (\xi-\Delta\xi)\right\}$$

$$\cdot H(\xi-\Delta\xi), \eta\in[0,\eta_\ell]\ ,\ \xi \geq 0\ . \qquad (3.7.36)$$

The dimensionless temperature distribution is now obtained by substituting Eq. (3.7.36) into Eq. (3.7.9), with no source term, and again performing the indicated operations to arrive at [105, p. 62]

$$\theta(\eta,\xi) = \left[\frac{\xi}{\eta_\ell} + \eta^2 - 2\eta + \frac{2\eta_\ell}{3}\right]\cdot\left(H(\xi) - H(\xi-\Delta\xi)\right) +$$

$$-\frac{4}{\eta_\ell}\sum_{m=1}^{\infty}\frac{e^{-\xi}\cos\lambda_m\eta}{\lambda_m^2}\cdot\left\{\frac{(2-\lambda_m^2)}{2\sqrt{\lambda_m^2-1}}\sin\sqrt{\lambda_m^2-1}\,\xi\right.$$

$$\left.+\cos\sqrt{\lambda_m^2-1}\,\xi\right\}H(\xi)+\frac{\Delta\xi}{\eta_\ell}\cdot H(\xi-\Delta\xi) \qquad (3.7.37)$$

$$+\frac{4}{\eta_\ell}\sum_{m=1}^{\infty}\frac{e^{-(\xi-\Delta\xi)}\cos\lambda_m\eta}{\lambda_m^2}\cdot$$

$$\cdot\left\{\cos\sqrt{\lambda_m^2-1}\,(\xi-\Delta\xi)+\frac{(2-\lambda_m^2)}{2\sqrt{\lambda_m^2-1}}\sin\sqrt{\lambda_m^2-1}\,(\xi-\Delta\xi)\right\}H(\xi-\Delta\xi)\,,$$

$$\eta\in[0,\eta_\ell]\,,\ \xi\geq 0\,.$$

The heat flux and temperature distributions, as predicted by the hyperbolic and parabolic heat conduction equations, are now numerically examined for the surface pulsed heat flux problem.

Numerical results displaying the development of the heat flux and temperature distributions arising from a pulsed surface heat flux of duration $\Delta\xi = 0.2$ on a slab of thickness $\eta_\ell = 1$ are now presented. The hyperbolic and parabolic solutions are then compared showing the distinct differences in the two heat conduction approximations.

An interesting comparison can be made between linear parabolic and hyperbolic heat conduction concerning the rate of convergence of their respective infinite series solutions. In parabolic heat conduction, the bilinear series solutions converge very rapidly. This rapid convergence rate is attributed to the decaying exponential term which contains the eigenvalues. However, in hyperbolic heat conduction no such term exists

as demonstrated in Eqs. (3.7.36) and (3.7.37) displaying the heat flux and temperature, respectively. These bilinear forms require hundreds of terms to obtain three significant figures of accuracy. However, techniques such as the Kummer transform may be incorporated to accelerate the rate of convergence of these series solutions.

Figure 3.7.1 displays the heat flux distribution for both the hyperbolic and parabolic cases at various times $\xi$. The hyperbolic solution shows that for $\xi < \eta_\ell = 1$, an undisturbed region exists ahead of the wavefront. Since no molecular communication has occurred ahead of the front, the behavior of the heat flux is the same as would exist in the half space problem. Certainly a finite speed of propagation is now associated with the rate of heat flow in the medium. As the wave propagates forward, energy is deposited in the wake by diffusion. The absolute magnitude of the wavefront decreases exponentially with increasing time due to the dissipation of energy by diffusion. On the other hand, the parabolic solution predicts that heat will propagate with an infinite speed and will be felt instantaneously throughout the medium after a thermal disturbance has been introduced.

When the wavefront impacts the insulated surface at $\xi = \eta_\ell = 1$, the energy will reflect back toward the origin at $\eta = 0$. This process of reflections at the surfaces will persist until the diffusion phenomena dominates. In contrast, the parabolic heat flux distribution displays monotonic decay to its steady-state value, i.e., it only predicts heat flow from $\eta = 0$ to $\eta = 1$ for all time $\xi$.

The corresponding temperature distributions ($\Delta\xi = .2$) are shown in Figure 3.7.2. Again, the distinct wave nature associated with hyper-

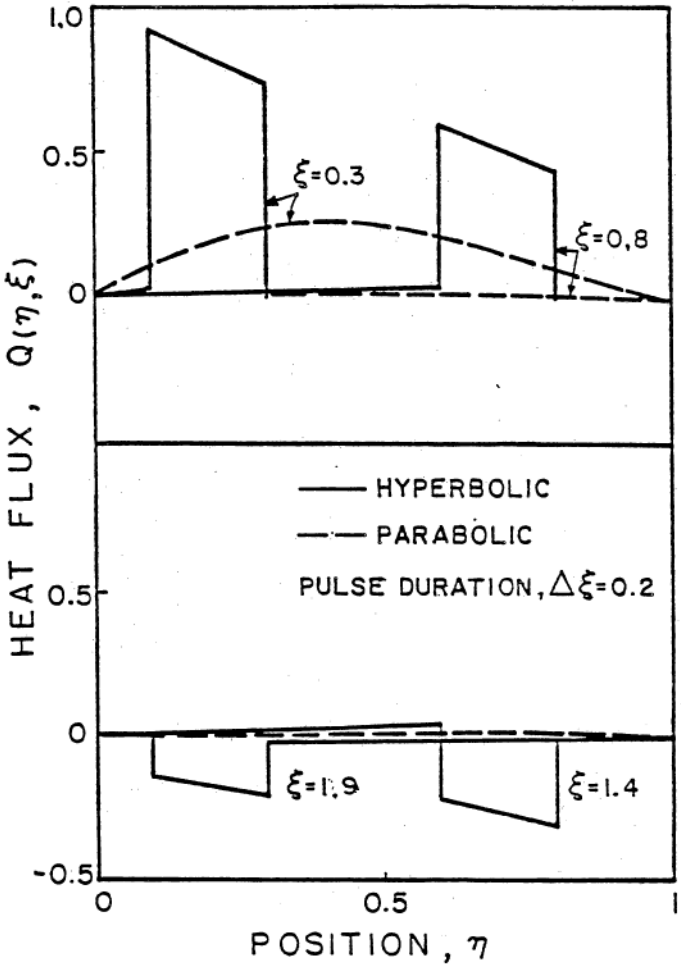


Figure 3.7.1 Heat Flux Distribution Resulting from a Pulsed Surface Heat Flux in a Slab of Thickness $\eta_\ell = 1$.

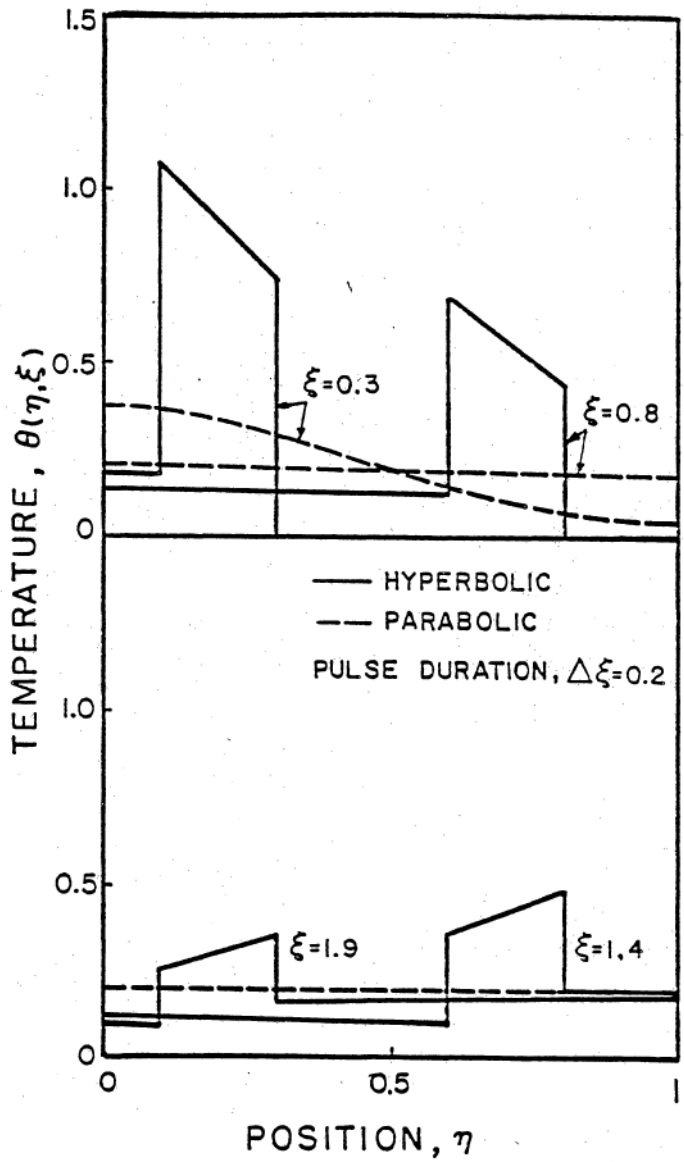


Figure 3.7.2 Temperature Distribution Resulting from a Pulsed Surface Heat Flux in a Slab of Thickness $\eta_\ell = 1$.

bolic heat conduction dominates. Diffusion causes the temperature wave to exponentially decay with time in the direction of propagation. Since energy has been deposited behind the wavefront, a small residual temperature is present. The parabolic solution displays a rapid decay to its steady state value of $\Delta\xi/\eta_{\ell}$. These two figures distinctly show the dominant wave feature associated to the hyperbolic heat conduction approximation.

## 3.8 Conclusions

This chapter discusses linear one-dimensional hyperbolic heat conduction in one region media. The relationships between temperature and flux are examined in detail to show that information may be systematically transferred from one domain to the other domain using the general and particular laws of conduction.

A general one-dimensional temperature and heat flux formulation for the three standard orthogonal coordinate systems is presented. The flux formulation is shown to be a viable alternative to the classical temperature formulation. As the relaxation time goes to zero, the equivalent parabolic temperature and flux formulations are recovered. The general temperature distribution for the three standard orthogonal coordinate systems is derived using the finite integral transform technique in the temperature domain. Once the temperature distribution has been established, the flux distribution is resolved from the modified Fourier's law.

Taitel's [26] problem is revisited to introduce the unique physics and mathematical difficulties associated with hyperbolic heat conduc-

tion. Next, an investigation of the propagation of thermal waves in radially dependent systems is given. Examples concerning a step change in surface temperature and a pulsed heat source in both a cylinder and sphere are discussed. These examples clearly show that linear one dimensional hyperbolic heat conduction predicts temperature singularities as an incoming wave front approaches the origin of a solid cylinder or sphere. These singularities occur as a result of a wavefront of finite energy concentration being packed into a region of zero volume. Also, temperatures below the initial equilibrium temperature occur in the wake of a thermal pulse; a phenomenon reminiscent of the wake following a pressure pulse in the field of acoustics.

The utility of the flux formulation and the unusual nature of heat conduction based on the thermal relaxation model are demonstrated by developing analytical expressions for the heat flux and temperature distributions in a finite slab exposed to arbitrary surface heat fluxes.

The Green's function method, as developed from Green's second formula, is applied to determine the heat flux distribution in a finite slab. A general expression for the heat flux distribution subject to any volumetric energy source and boundary conditions of the first kind (in flux) has been established. The determination of the Green's function has been obtained by the finite integral transform technique in the cause variable without introducing the standard reciprocity relation. Certainly, the development of the Green's function in this manner is more natural from the mathematical point of view.

The wave feature of the hyperbolic heat conduction approximation has been demonstrated in the finite thickness slab subject to a pulsed

surface heat flux. The realization of a finite speed of propagation of the thermal waves has been confirmed through this example. This, of course, is in contrast to the parabolic approximation which predicts an infinite speed of heat propagation.

# Chapter 4

# COMPOSITE REGIONS

## 4.1 Introduction

In this chapter, we study the effects and ramifications of linear hyperbolic heat conduction in a composite medium. Composites are generally of great interest to engineers and physicists since they appear in numerous situations including: laminated fins [126-130], reactor walls [131-133], laser annealing [134], stratified fluids, as well as many other applications. Multiregion linear parabolic heat conduction is well-studied and has generally been analyzed by classical eigenfunction expansion techniques [93,125,135-143].

In hyperbolic heat conduction, the study of the interaction of dissimilar materials provides additional insight and understanding into the unusual behavior of heat conduction based on the modified Fourier's law. Also, some recent experimental results in superfluid helium [91,92] indicate that a partial reflection is present as energy impacts an interface of two dissimilar materials. Presently, no general formulations and subsequently no general analyses exist for hyperbolic heat conduction in composite media.

The development of the general one-dimensional temperature and flux formulations for the standard three orthogonal coordinate systems are presented [144,145]. Then, the general one-dimensional flux and temperature distributions are developed from the flux domain using a generalized finite integral transform technique. Once the flux distribution is ascertained, the temperature distribution may be resolved from the conservation of energy.

Finally, two numerical examples are considered. The first example deals with a two region slab with a temperature jump at one of the exterior boundaries while the second considers a two region slab with a pulsed volumetric source emanating from one region. The stark differences between parabolic and hyperbolic heat conduction are also displayed.

## 4.2 General Temperature and Flux Formulations

The governing one-dimensional temperature and heat flux field equations are now formulated for the three standard orthogonal coordinate systems. Referring to Fig. 4.2.1 and performing an energy balance [93] in the usual manner, one arrives at the following mathematical statement for the conservation of energy in any region i in the multi-region medium

$$\frac{-1}{x^p}\frac{\partial}{\partial x}\left(x^p q_i\right) + u_i(x,t) = (\rho C_p)_i \frac{\partial T_i}{\partial t}\,, \qquad x\in[x_i,x_{i+1}]\,,\ t>0,\ i=1,2,\ldots,N, \tag{4.2.1}$$

where

$$p = \begin{cases} 0 & \text{slab} \\ 1 & \text{cylinder} \\ 2 & \text{sphere}\,. \end{cases}$$

The modified Fourier's law may be written as

$$\tau_i \frac{\partial q_i}{\partial t} + q_i = -k_i \frac{\partial T_i}{\partial x}\,,\quad i=1,2,\ldots,N, \tag{4.2.2}$$

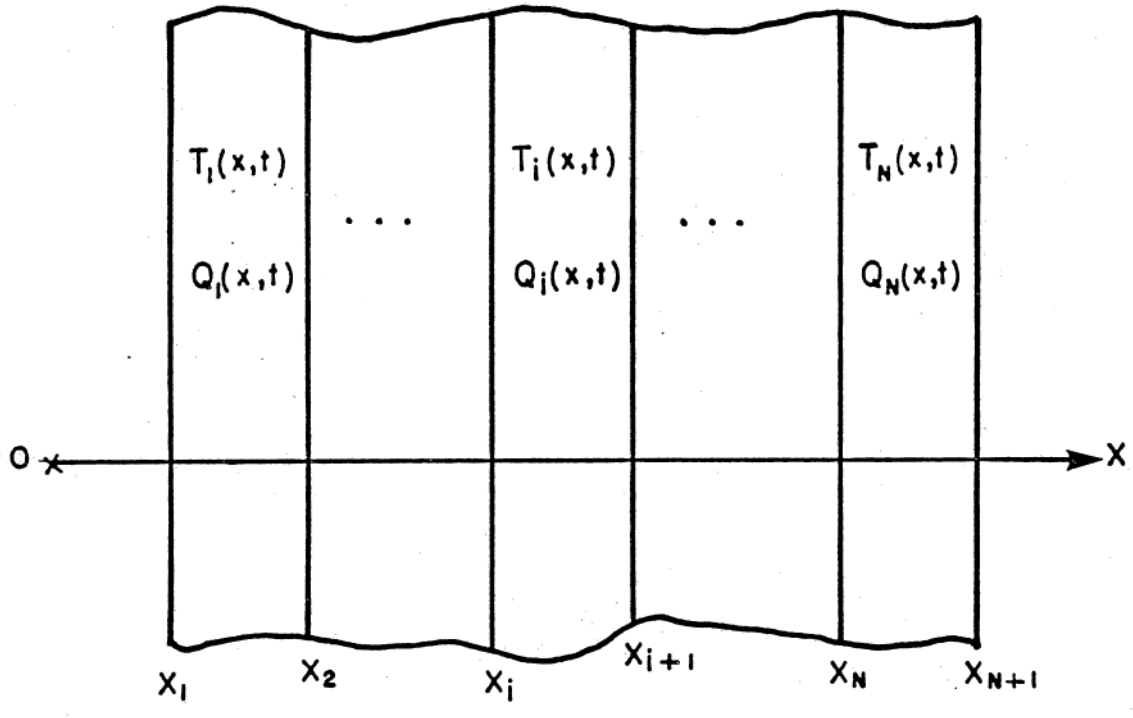


Figure 4.2.1 Geometry and Coordinates for N-region Composite.

for each region i.

Eliminating $q_i(x,t)$ between Eqs. (4.2.1) and (4.2.2) yields the following temperature field equation for any region i

$$\frac{1}{x^p}\frac{\partial}{\partial x}\left(x^p \frac{\partial T_i}{\partial x}\right) + \frac{1}{k_i}\left[u_i + \tau_i \frac{\partial u_i}{\partial t}\right] = \frac{1}{\alpha_i}\left[\tau_i \frac{\partial^2 T_i}{\partial t^2} + \frac{\partial T_i}{\partial t}\right] , \qquad (4.2.3)$$

$$x\varepsilon(x_i, x_{i+1}),\ t > 0,\ i = 1,2,\ldots,N .$$

Clearly as the relaxation time $\tau_i$ approaches zero, the standard parabolic case [93] is recovered.

The heat flux field equation is obtained by eliminating the temperature $T_i(x,t)$ between Eqs. (4.2.1) and (4.2.2). The flux field equation becomes

$$\frac{\partial}{\partial x}\left[\frac{1}{x^p}\frac{\partial}{\partial x}\left(x^p q_i\right)\right] - \frac{\partial u_i}{\partial x} = \frac{1}{\alpha_i}\left[\tau_i \frac{\partial^2 q_i}{\partial t^2} + \frac{\partial q_i}{\partial t}\right] , \qquad (4.2.4)$$

$$x\varepsilon[x_i, x_{i+1}],\ t > 0,\ i = 1,2,\ldots,N .$$

As seen in Eqs. (4.2.3) and (4.2.4), the volumetric heat generation term $u_i(x,t)$ appears in different combinations in the two formulations. In some circumstances, it may be more convenient to choose one formulation over the other merely on the basis of this term. Another interesting feature of hyperbolic heat conduction in composites is that the associated homogeneous version of field equations (4.2.3) and (4.2.4), are not separable in the classical sense. For instance, if the product

solution

$$q_i(x,t) = \psi_{im}(x)\Gamma_m(t) \ , \tag{4.2.5}$$

is substituted into the homogeneous version of Eq. (4.2.4), separability is not achieved as in the parabolic composites [93]. The reason for the nonseparability is the presence of the coefficient $\tau_i$ as a multiplier to the second order time derivative. Since $\tau_i$ assumes different values for different regions, a separated solution in the form given by Eq. (4.2.5) cannot be matched at the interfaces for all times. That is, the function $\Gamma_m(t)$ cannot be independent of all material properties as required by the classical eigenfunction expansion technique [93]. A generalized finite integral transform technique will be developed to overcome this difficulty.

The appropriate boundary conditions associated with the temperature formulation are now developed. Convective heat transfer is not considered since hyperbolic heat conduction is valid for small times, i.e., times prior to the onset of mass movement. The mode of heat transfer between liquid-solid regions is limited to conduction. For a specified temperature or heat flux at an external surface, the appropriate boundary condition becomes

$$-a_1 k_1 \frac{\partial T_1}{\partial x} + b_1 T_1 = a_1\left[\tau_1 \frac{dq_{w,1}}{dt} + q_{w,1}(t)\right] + b_1 T_{w,1}(t) \ , \tag{4.2.6a}$$

$$x = x_1 \ ,$$

$$a_{N+1}k_N \frac{\partial T_N}{\partial x} + b_{N+1}T_N = a_{N+1}\left[\tau_N \frac{dq_{w,N+1}}{dt} + q_{w,N+1}(t)\right] + b_{N+1}T_{w,N+1}(t) \ , \quad x = x_{N+1} \ , \tag{4.2.6b}$$

where the general notation introduced above reduces to the prescribed temperature $T_{w,j}(t)$ or heat flux $q_{w,j}(t)$, $j = 1, N + 1$ boundary conditions depending on the various combination of the coefficients $a_j$ and $b_j$. For example, if a prescribed temperature at $x = x_1$ were specified, then $a_1 = 0$, $b_1 = 1$, would be required. If however a specified heat flux is given, the coefficients would simply be $a_1 = 1$, $b_1 = 0$. A similar interpretation can be made when considering the boundary condition at $x = x_{N+1}$.

At the interface of two adjacent regions, two boundary conditions are required; namely, continuity of temperature, which implies perfect thermal contact, and continuity of heat flux. Continuity of temperature is expressed as

$$T_i = T_{i+1} \ , \ x = x_{i+1} \ , \ i = 1,2,\ldots,N - 1 \ , \tag{4.2.6c}$$

while continuity of heat flux is

$$q_i = q_{i+1} \ , \ x = x_{i+1}, \ i = 1,2,\ldots,N - 1 \ , \tag{4.2.6d}$$

Carefully eliminating both $q_i$, $q_{i+1}$ from Eq. (4.2.6d), using Eqs. (4.2.2) for each region i yields

$$-k_i\left[\tau_{i+1}\frac{\partial^2 T_i}{\partial x \partial t} + \frac{\partial T_i}{\partial x}\right] = -k_{i+1}\left[\tau_i \frac{\partial^2 T_{i+1}}{\partial x \partial t} + \frac{\partial T_{i+1}}{\partial x}\right], \quad x = x_{i+1}, \; i = 1,2,\ldots,N-1, \tag{4.2.6e}$$

where $\tau_i \neq \tau_{i+1}$. If $\tau_i = \tau_{i+1}$, the usual parabolic heat conduction boundary condition is obtained

$$-k_i \frac{\partial T_i}{\partial x} = -k_{i+1}\frac{\partial T_{i+1}}{\partial x}, \quad x = x_{i+1}, \quad i = 1,2,\ldots,N-1, \; t > 0 . \tag{4.2.6f}$$

Equation (4.2.6e) represents a new linear, second order boundary condition with mixed spatial and time derivatives which has not yet appeared in heat conduction. This new expression introduces additional complexity since it is nonseparable. As the relaxation times $\tau_i$ and $\tau_{i+1}$ approach zero, we see that Eq. (4.2.6e) is consistent with the parabolic formulation.

For convenience, the initial state of the medium is taken at the equilibrium temperature $T_o$. The inital conditions are readily established as

$$T_i = T_o, \; \frac{\partial T_i}{\partial t} = 0, \; t = 0, \; x\varepsilon[x_i, x_{i+1}], \; i = 1,2,\ldots,N , \tag{4.2.7a,b}$$

Once the temperature distribution has been determined, the heat flux distribution may be obtained by solving the modified Fourier's law, Eq. (4.2.2), for the heat flux distribution in each region i or by solving the energy conservation equation, Eq. (4.2.1) for $q_i(x,t)$ if a flux boundary had been specified.

For a specified temperature or heat flux at an external surface, the appropriate boundary conditions in the heat flux variable are expressed as

$$a_1 q_1 - b_1 \frac{1}{x^p} \frac{\partial}{\partial x}(x^p q_1) = a_1 q_{w,1}(t) + b_1\left[(\rho C_p)_1 \frac{dT_{w,1}}{dt} - u_1\right] \quad , \quad x = x_1 \, , \tag{4.2.8a}$$

and

$$a_{N+1} q_N - b_{N+1} \frac{1}{x^p} \frac{\partial}{\partial x}(x^p q_N) = - a_{N+1} q_{w,N+1}(t) + b_{N+1}\left[(\rho C_p)_N \frac{dT_{w,N+1}}{dt} - u_N\right] \quad , \quad x = x_{N+1}, \tag{4.2.8b}$$

where the coefficients $a_j, b_j$, $j = 1, N+1$ have the same interpretation as the coefficients associated with temperature boundary conditions (4.2.6a,b). In Eqs. (4.2.8a,b), the conservation law (4.2.1) was used to convert a prescribed temperature boundary into the flux domain. If a

prescribed surface temperature involves a step change in the surface temperature, then the terms involving the time derivative on the right hand side of Eqs. (4.2.8a,b) will involve delta functions and the use of generalized functions will be necessary to preserve a correct in the formulation.

The statement of continuity of temperature at an interface can be formulated in the heat flux domain by taking the partial derivative with respect to time of Eq. (4.2.6c) and incorporating Eq. (4.2.1) to obtain

$$\frac{1}{(\rho C_p)_i}\left[-\frac{1}{x^p}\frac{\partial}{\partial x}(x^p q_i) + u_i\right] = \frac{1}{(\rho C_p)_{i+1}}\left[-\frac{1}{x^p}\frac{\partial}{\partial x}(x^p q_{i+1}) + u_{i+1}\right] . \tag{4.2.8c}$$

Equation (4.2.8c) represents a separable but nonhomogeneous boundary condition which is valid for both parabolic and hyperbolic heat conduction. Continuity of heat flux at the interfaces is simply expressed by Eq. (4.2.6d).

Considering the medium initially at the equilibrium state, the initial conditions are

$$q_i = 0, \frac{\partial q_i}{\partial t} = 0, \; t = 0, \; i = 1,2,\ldots,N. \tag{4.2.9a,b}$$

Once the flux distribution has been established, the temperature distribution may be resolved by a time integration of the energy balance, Eq. (4.2.1), or by the spatial integration of the modified Fourier's law, Eq. (4.2.2) for each region i if a specified temperature

boundary condition is given.

## 4.3 General Solutions Developed in the Flux Domain

In this section, the development of the general one-dimensional flux and temperature distributions associated with linear hyperbolic heat conduction in a composite medium is presented. The previous formulation reveals that the field equations for temperature and heat flux, given by Eqs. (4.2.3) and (4.2.4), respectively, have similar form except for the nonhomogeneous source contribution. However, the statement of continuity of heat flux at the interfaces is quite convenient in the flux domain, as given by Eq. (4.2.6d) while the equivalent statement in the temperature variable, as given by Eq. (4.2.6e), represents a nonseparable condition with mixed partial derivatives. Due to this added mathematical complexity, we choose to develop an analytical solution directly in the heat flux domain and then recover the temperature distribution by a time integration of the energy conservation law, Eq. (4.2.1). A generalized finite integral transform technique is developed, capable of yielding very accurate results for nonseparable hyperbolic partial differential equations. This generalized transform technique reduces to the exact solution for situations where separability can be achieved, that is, when the relaxation times are identical in each region.

For convenience, we nondimensionalize the governing equations with respect to region 1 using the following dimensionless quantities

$$\eta = \frac{c_1 x}{2\alpha_1} \quad , \quad \xi = \frac{c_1^2 t}{2\alpha_1} \, , \tag{4.3.1a,b}$$

where $c_1^2 = \alpha_1/\tau_1$ and

$$Q_i(\eta,\xi) = \frac{q_i}{T_{ref}\left(\frac{k_1 c_1}{\alpha_1}\right)} , \tag{4.3.1c}$$

$$\theta_i(\eta,\xi) = \frac{T_i - T_o}{T_{ref}} , \tag{4.3.1d}$$

$$S_i(\eta,\xi) = \frac{u_i}{T_{ref}\left(\frac{k_1 c_1^2}{4\alpha_1^2}\right)} , \tag{4.3.1e}$$

and the dimensionless property ratios

$$k_i^* = \frac{k_i}{k_1} , \quad \alpha_i^* = \frac{\alpha_i}{\alpha_1} , \quad c_i^* = \left(\frac{c_i}{c_1}\right)^2 , \quad \tau_i^* = \frac{\alpha_i^*}{c_i^*} , \tag{4.3.2a-d}$$

$$i = 1,2,\ldots,N .$$

The reference temperature $T_{ref}$ is chosen to characterize the thermal disturbance of interest. Also, $T_o$ represents the initial temperature associated with the equilibrium initial state.

Introducing the dimensionless quantities expressed above into Eqs. (4.2.4), (4.2.8) and (4.2.9) produces the general one-dimensional system governing the dimensionless flux distribution. The dimensionless flux field equation for a general one dimensional composite is

$$L_{p,i}[Q_i(\eta,\xi)] = \frac{1}{2}\frac{\partial S_i}{\partial \eta} + \frac{2}{\alpha_i^*}\frac{\partial Q_i}{\partial \xi} , \tag{4.3.3a}$$

where $L_{p,i}$ is the operator defined as

$$L_{p,i} \equiv \frac{\partial}{\partial \eta}\left[\frac{1}{\eta^p}\frac{\partial}{\partial \eta}(\eta^p)\right] - \frac{\tau_i^*}{\alpha_i^*}\frac{\partial^2}{\partial \xi^2} , \tag{4.3.3b}$$

where p represents the particular geometry as expressed in Eq. (4.2.1) and i represents the region. The particular form of $L_{p,i}$ is naturally suggested by the dominant wave nature of the system under consideration. The dimensionless boundary conditions become

$$a_1^* Q_1 + b_1^*\left[-\frac{1}{\eta^p}\frac{\partial}{\partial \eta}(\eta^p Q_1)\right] = a_1^* Q_{w,1}(\xi) + b_1^*\left[-\frac{S_1}{2} + \frac{d\theta_{w,1}(\xi)}{d\xi}\right] , \tag{4.3.4a}$$
$$\eta = \eta_1 ,$$

$$Q_i = Q_{i+1} , \tag{4.3.4b}$$

$$\frac{\alpha_i^*}{k_i^*}\left[-\frac{1}{\eta^p}\frac{\partial}{\partial \eta}(\eta^p Q_i) + \frac{S_i}{2}\right] = \frac{\alpha_{i+1}^*}{k_{i+1}^*}\left[-\frac{1}{\eta^p}\frac{\partial}{\partial \eta}(\eta^p Q_{i+1}) + \frac{S_{i+1}}{2}\right] , \tag{4.3.4c}$$
$$\eta = \eta_{i+1} , \quad i = 1,2,\ldots,N-1,$$

and

$$-a_{N+1}^* Q_N + b_{N+1}^*\left[-\frac{1}{\eta^p}\frac{\partial}{\partial \eta}(\eta^p Q_N)\right] = a_{N+1}^* Q_{w,N+1}(\xi)$$
$$+ b_{N+1}^*\left[-\frac{S_N}{2} + \frac{k_N^*}{\alpha_N^*}\frac{d\theta_{w,N+1}}{d\xi}\right] , \quad \eta = \eta_{N+1} , \quad \xi > 0 , \tag{4.3.4d}$$

where the boundary coefficients $a_j^*, b_j^*$ , j = 1, N+1 are the dimensionless counterparts of the general notation introduced in Eqs. (4.2.8). The dimensionless initial conditions become

$$Q_i(\eta,0) = 0 \ , \tag{4.3.5a}$$

$$\frac{\partial Q_i}{\partial \xi}(\eta,0) = 0, \quad i = 1,2,\ldots,N \ . \tag{4.3.5b}$$

Eqs. (4.3.3-4.3.5) constitute the complete mathematical formulation to uniquely determine the dimensionless flux distribution once the thermal disturbances have been specified. Finally, the dimensionless equation governing the conservation of energy is

$$-\frac{1}{\eta^p}\frac{\partial}{\partial \eta}\left[\eta^p Q_i\right] + \frac{S_i(\eta,\xi)}{2} = \frac{k_i^*}{\alpha_i^*}\frac{\partial \theta_i}{\partial \xi} \ , \tag{4.3.6}$$

$$\eta \in [\eta_i,\eta_{i+1}] \ , \ \xi \geq 0 \ , \ i = 1,2,\ldots,N.$$

We shall now develop a generalized finite integral transform technique capable of yielding accurate numerical results.

Since Eqs. (4.3.3-4.3.5) constitute a system which is nonseparable in the classical sense, as described with regard to Eq. (4.2.5), standard analytical solution techniques such as the finite integral transform technique fail. However, suppose we view the right hand side of

Eq. (4.3.3a) as an effective heat source or nonhomogeneity. We then develop the solution method by considering the auxiliary problem

$$L_{p,i}[\phi(\eta,\xi)] = 0,\ \eta\varepsilon(\eta_i,\eta_{i+1}),\ \xi > 0,\ i = 1,2,\ldots,N\ , \qquad (4.3.7)$$

which is the classical (separable) wave equation.

The eigenfunctions $\psi_{im}(\eta)$ and eigenvalues $\lambda_m$ are chosen by considering Eq. (4.3.7) and the homogeneous version of Eq. (4.3.4), where $Q_i(\eta,\xi)$ is replaced by $\phi_i(\eta,\xi)$.

The appropriate eigenvalue problem then becomes

$$\frac{d}{d\eta}\left[\frac{1}{\eta^p}\frac{d}{d\eta}(\eta^p\psi_{im})\right] + \frac{\lambda_m^2\tau_i^*}{\alpha_i^*}\psi_{im}(\eta) = 0\ , \qquad (4.3.8a)$$

subject to the boundary conditions

$$a_1^*\psi_{1m} + b_1^*\left[-\frac{1}{\eta^p}\frac{d}{d\eta}(\eta^p\psi_{1m})\right] = 0\ ,\ \eta = \eta_1\ , \qquad (4.3.8b)$$

$$\frac{\alpha_i^*}{k_i^*}\left[-\frac{1}{\eta^p}\frac{d}{d\eta}(\eta^p\psi_{im})\right] = \frac{\alpha_{i+1}^*}{k_{i+1}^*}\left[-\frac{1}{\eta^p}\frac{d}{d\eta}(\eta^p\psi_{i+1,m})\right]\ , \qquad (4.3.8c)$$

$$\psi_{im} = \psi_{i+1,m}\ ,\ \eta = \eta_{i+1}\ ,\ i = 1,2,\ldots,N-1\ , \qquad (4.3.8d)$$

$$a_{N+1}^*\psi_{N,m} + b_{N+1}^*\left[-\frac{1}{\eta^p}\frac{d}{d\eta}(\eta^p\psi_{N,m})\right] = 0\ ,\ \eta = \eta_{N+1}\ , \qquad (4.3.8e)$$

where $a^*_j$, $b^*_j$ , $j = 1,\ N+1$ are the boundary coefficients introduced in Eq. (4.3.4). The eigenvalue problem presented above is of the same type as that encountered in parabolic heat conduction [93].

The eigenfunctions obey the following important orthogonality relation (see Appendix 1)

$$\sum_{i=1}^{N} \frac{\tau_i^*}{k_i^*} \int_{\eta=\eta_i}^{\eta_{i+1}} \eta^p \psi_{im}(\eta)\psi_{in}(\eta)d\eta = \begin{cases} 0 & , \ m \neq n \\ N(\lambda_m) & , \ m = n \ , \end{cases} \tag{4.3.9a}$$

where the normalization integral is defined as

$$N(\lambda_m) = \sum_{i=1}^{N} \frac{\tau_i^*}{k_i^*} \int_{\eta=\eta_i}^{\eta_{i+1}} \eta^p \psi_{im}^2(\eta)d\eta \ . \tag{4.3.9b}$$

Using this orthogonality relation, we now develop the integral transform pair (see Appendix 1) as

Inversion Formula

$$Q_i(\eta,\xi) = \sum_{m}^{\infty} \frac{\psi_{im}(\eta)\bar{Q}_m(\xi)^*}{N(\lambda_m)} \ , \tag{4.3.10a}$$

Integral Transform

$$\bar{Q}_m(\xi) = \sum_{i=1}^{N} \frac{\tau_i^*}{k_i^*} \int_{\eta=\eta_i}^{\eta_{i+1}} \eta^p \psi_{im}(\eta)Q_i(\eta,\xi)d\eta \ , \tag{4.3.10b}$$

$$m = 0,1,2,\ldots,\xi \geq 0 \ .$$

Having defined the integral transform pair in Eqs. (4.3.10) we

*If exterior BC's are of second kind, m starts at 0.

remove all spatial dependence from Eq. (4.3.3a) by operating on it with

$$\frac{\alpha_i^*}{k_i^*} \int_{\eta=\eta_i}^{\eta_{i+1}} \eta^p \psi_{im}(\eta) d\eta \ , \tag{4.3.11}$$

and sum over all regions i = 1,2,...,N. After some manipulation, the following ordinary differential equation (IVP) for each m appears

$$\frac{d^2\bar{Q}_m(\xi)}{d\xi^2} + \lambda_m^2 \bar{Q}_m(\xi) = A_m(\xi) - 2 \frac{d}{d\xi} \sum_{i=1}^{N} \frac{1}{k_i^*} \int_{\eta=\eta_i}^{\eta_{i+1}} Q_i(\eta,\xi) \eta^p \psi_{im}(\eta) d\eta \ , \tag{4.3.12a}$$

where

$$A_m(\xi) = \sum_{i=1}^{N} \frac{\alpha_i^*}{k_i^*} \left[ \psi_{im} \frac{\partial}{\partial \eta} (\eta^p Q_i) - Q_i \frac{d(\eta^p \psi_{im})}{d\eta} \right]_{\eta=\eta_i}^{\eta_{i+1}} \tag{4.3.12b}$$

$$- \frac{1}{2} \sum_{i=1}^{N} \frac{\alpha_i^*}{k_i^*} \int_{\eta=\eta_i}^{\eta_{i+1}} \frac{\partial S_i}{\partial \eta} \eta^p \psi_{im}(\eta) d\eta \ .$$

An expression for $A_m(\xi)$ can be written in terms of the boundary conditions explicitly (see Appendix 2).

Substituting the inversion formula, Eq. (4.3.10a) with the new dummy index $\ell$, into Eq. (4.3.12a) yields

$$\frac{d^2\bar{Q}_m(\xi)}{d\xi^2} + \lambda_m^2\bar{Q}(\xi) = A_m(\xi) - 2 \sum_{\ell} \frac{B_{\ell m}}{N(\lambda_\ell)} \cdot \frac{d\bar{Q}_\ell(\xi)}{d\xi} , \qquad (4.3.13a)$$

subject to the transformed initial conditions

$$\bar{Q}_m(0) = 0 , \qquad (4.3.13b)$$

and

$$\frac{d\bar{Q}_m(0)}{d\xi} = 0 . \qquad (4.3.13c)$$

The constants $B_{\ell m}$ are defined as

$$B_{\ell m} = \sum_{i=1}^{N} \frac{1}{k_i^*} \int_{\eta=\eta_i}^{\eta_{i+1}} \eta^p \psi_{im}(\eta)\psi_{i\ell}(\eta)d\eta , \qquad (4.3.14)$$

where this integral may be evaluated analytically (see Appendix 3).

The solution for the integral transform $\bar{Q}_m(\xi)$, as described in Eq. (4.3.13a), involves solving an infinite set of coupled ordinary differential equations with constant coefficents subject to the initial conditions expressed by Eqs. (4.3.13b,c). As shown in [144], $A_m(\xi)$ may contain generalized functions, e.g. the Dirac Delta function, which may cause some difficulty if Eqs. (4.3.13) were solved directly by some numerical method.

Before proceeding with the general solution, we observe the similarity between the definition of $B_{\ell m}$ expressed in Eq. (4.3.14) and the orthogonality relation expressed in Eq. (4.3.9b) For the situation in which all the regions in the composite have identical relaxation times,

i.e., $\tau_i^* = 1$ for all i, the coefficients defined in Eq. (4.3.14) reduce to

$$B_{\ell m} = \begin{cases} 0 & , \ell \neq m \\ N(\lambda_m) & , \ell = m \ . \end{cases} \tag{4.3.15}$$

For this case, Eq. (4.3.13a) for the transforms become uncoupled and can be solved directly to get

$$\bar{Q}_m(\xi) = \int_{\xi_o=0}^{\xi} \frac{A_m(\xi_o)}{\sqrt{\lambda_m^2 - 1}} \, e^{-(\xi-\xi_o)} \sin\left[\sqrt{\lambda_m^2 - 1}\,(\xi - \xi_o)\right] d\xi_o \ , \tag{4.3.16}$$

$$\text{valid for } \tau_i^* = 1, \ i = 1,2,\ldots,N \ .$$

For the more general case of regions with different relaxation times, Eqs. (4.3.13) must be solved simultaneously. Although the solution to these coupled equations may be formally expressed in an exact analytical form, the large number of terms [95] typically required for hyperbolic systems makes this approach unfeasible when numerical results are required. As an alternative, we propose to convert Eqs. (4.3.13) into an equivalent set of linear Volterra integral equations of the second kind. Using the Laplace transform technique and incorporating convolution, we arrive at

$$\bar{Q}_m(\xi) = f_m(\xi) - 2 \sum_{\ell} \frac{B_{\ell m}}{N(\lambda_\ell)} \cdot \int_{\xi_o=0}^{\xi} \bar{Q}_\ell(\xi_o)\cos\lambda_m(\xi-\xi_o)d\xi \ , \qquad (4.3.17a)$$

where

$$f_m(\xi) = \int_{\xi_o=0}^{\xi} \frac{A_m(\xi_o)}{\lambda_m} \sin\lambda_m(\xi - \xi_o)\, d\xi_o \ . \qquad (4.3.17b)$$

The 'kernel' present in Eq. (4.3.17a), namely $\cos\lambda_m(\xi - \xi_o)$, is degenerate [146-149], that is, it can be written as a finite sum of products of two linearly independent functions, one which depends on $\xi$ and the other on $\xi_o$. We express this kernel as

$$K(\xi,\xi_o;\lambda_m) = \cos\lambda_m(\xi - \xi_o) = \sum_{j=1}^{2} a_j(\lambda_m\xi)b_j(\lambda_m,\xi_o) \ , \qquad (4.3.18)$$

where the following form is chosen

$$\begin{aligned} a_1(\lambda_m,\xi) &= \cos\lambda_m\xi \quad , \quad a_2(\lambda_m\xi) = \sin\lambda_m\xi \ , \\ b_1(\lambda_m,\xi_o) &= \cos\lambda_m\xi_o \quad , \quad b_2(\lambda_m,\xi_o) = \sin\lambda_m\xi_o \ . \end{aligned} \qquad (4.3.19a\text{-}d)$$

The method of Bownds [150-152] is now utilized in evaluating the integral equation representation of $\bar{Q}_m(\xi)$ as described by Eq. (4.3.17). Briefly, this method transforms a general decomposable (degenerate) Volterra integral equation into a first order initial value problem in a new smoother variable. This technique is reminiscent of the usual solution technique applied to degenerate kernels in linear Fredholm theory [146,149]. The Method of Bownds may also be applied

directly to semidegenerate integral equations. If a kernel is not exactly decomposable, a kernel approximation can be made to form a degenerate kernel [153]. The numerical solution of this new smoother variable is obtained by a Runge-Kutta scheme, then the original transform variable $\bar{Q}_m(\xi)$ is reconstructed. Runge-Kutta and other inital value schemes are a paradigm to numerical analysis and many individual schemes are available with unique features. Fixed step size explicit integrators like the standard 4th order Runge-Kutta or (5,6) method of Butcher may be directly applied. Various explicit, semi-explicit, and implicit Runge-Kutta's [154-157] are available containing characteristics which may be exploited.

Writing Eq. (4.3.17a) in terms of the finite sum expressed in Eq. (4.3.18) yields

$$\bar{Q}_m(\xi) = f_m(\xi) - \sum_{j=1}^{2} a_j(\lambda_m,\xi)c_j(\lambda_m,\xi) \ , \qquad (4.3.20a)$$

where

$$c_j(\lambda_m,\xi) = 2 \sum_{\ell} \frac{B_{\ell m}}{N(\lambda_\ell)} \cdot \int_{\xi_o=0}^{\xi} b_j(\lambda_m,\xi_o)\, \bar{Q}_\ell(\xi_o)\, d\xi_o \ , \qquad (4.3.20b)$$

$$j = 1,2 \ , \ \xi \geq 0.$$

Once $c_j(\lambda_m,\xi)$, $j = 1,2$ is determined numerically, the transform $\bar{Q}_m(\xi)$ is found from Eq. (4.2.20a).

The equations governing the new functions $c_j(\lambda_m,\xi)$ are obtained by differentiating Eq. (4.2.20b) and substituting Eq. (4.2.20a) into the

result to get

$$\frac{dc_j(\lambda_m,\xi)}{d\xi} = 2\sum_{\ell} \frac{B_{\ell m}}{N(\lambda_\ell)} \cdot b_j(\lambda_m\xi) \cdot \left[f_\ell(\xi) - \sum_{k=1}^{2} a_k(\lambda_\ell,\xi)c_k(\lambda_\ell,\xi)\right] ,$$

$$j = 1,2 \quad , \quad \xi \geq 0 . \tag{4.3.21a}$$

The required initial conditions are obtained by evaluating Eq. (4.3.20b) at $\xi = 0$ to get,

$$c_j(\lambda_m,0) = 0 \ , \ j = 1,2 . \tag{4.3.21b}$$

We solve this set of equations, after truncating the $\ell$ series after a finite number of terms, by a Runge-Kutta method. Once the $c_j$'s are known, the integral transforms $\bar{Q}_m(\xi)$ are found from Eq. (4.3.20a) for each m. Finally, the flux distribution is resolved using the inversion formula expressed by Eq. (4.3.10a). If $\tau_i^* = 1$ for all regions, the exact analytical solution is obtained by substituting Eq. (4.3.16) into the inversion formula expressed by Eq. (4.3.10a) to get

$$Q_i(\eta,\xi) = \sum_{m} \frac{\psi_{im}(\eta)}{N(\lambda_m)} \int_{\xi_o=0}^{\xi} \frac{A_m(\xi_o)}{\sqrt{\lambda_m^2 - 1}} \cdot e^{-(\xi-\xi_o)} \sin[\sqrt{\lambda_m^2}-1(\xi-\xi_o)]d\xi_o ,$$

$$i = 1,2,\ldots,N \ , \ \xi \geq 0 . \tag{4.3.22}$$

In general, one must use the conservation of energy, as expressed in Eq. (4.2.1) to determine the temperature distribution in each region i. However, in circumstances where a specified temperature boundary

condition exists, one may also use the modified Fourier's law [144]. A time integration of Eq. (4.2.1) yields

$$\theta_i(\eta,\xi) = \theta_i(\eta,0) - \frac{\alpha_i^*}{k_i^*} \int_{\xi_o=0}^{\xi} \frac{1}{\eta^p} \frac{\partial}{\partial \eta} [\eta^p Q_i(\eta,\xi_o)] d\xi_o + \frac{\alpha_i^*}{k_i^*} \int_{\xi_o=0}^{\xi} \frac{S_i(\eta,\xi_o) d\xi_o}{2} , \quad \xi \geq 0 , \quad \ell = 1,2,\ldots,N , \tag{4.3.23}$$

where $\theta_i(\eta,0) = 0$ , $i = 1,2,\ldots,N$, from consideration of the equilibrium initial state.

In general, we substitute the inversion formula into Eq. (4.3.23) to get

$$\theta_i(\eta,\xi) = \frac{\alpha_i^*}{k_i^*}\left[\frac{-1}{\eta^p} \cdot \sum_m \frac{(\eta^p \psi_{im})'}{N(\lambda_m)} \cdot \int_{\xi_o=0}^{\xi} \bar{Q}_m(\xi_o) d\xi_o + \int_{\xi_o=0}^{\xi} \frac{S_i(\eta,\xi_o)}{2} d\xi_o \right] , \quad i = 1,2,\ldots,N. \tag{4.3.24}$$

For the general case of regions with different relaxation times ($\tau_i^* \neq 1$ for at least one i), a relation for the integral of the transform can be developed using known functions and the numerically resolved $c_j$'s. After some manipulation, we find

$$\int_{\xi_o=0}^{\xi} \bar{Q}_m(\xi_o)d\xi_o = \int_{\xi_o=0}^{\xi} f_m(\xi_o)d\xi_o + \sum_{j=1}^{2} \frac{c_j(\lambda_m,\xi)}{\lambda_m^2} \frac{da_j(\lambda_m,\xi)}{d\xi} . \tag{4.3.25a}$$

If $\tau_i^* = 1$ for all i, an exact evalution of the integral of the transform leads to

$$\int_{\xi_o=0}^{\xi} \bar{Q}_m(\xi_o)d\xi_o = -\frac{1}{\lambda_m^2} \int_{\xi_o=0}^{\xi} A_m(\xi_o) \left\{ e^{-(\xi-\xi_o)} \left[ \frac{\sin\sqrt{\lambda_m^2 - 1}\,(\xi-\xi_o)}{\sqrt{\lambda_m^2-1}} \right.\right. \tag{4.3.25b}$$

$$\left.\left. + \cos\sqrt{\lambda_m^2 - 1}(\xi-\xi_o) \right] - 1 \right\} d\xi_o \quad , \quad \tau_i^* = \tau_{i+1}^* \quad , \quad i = 1,2,\ldots,N.$$

Therefore, the temperature distribution in each region is known from Eqs. (4.3.24) and (4.3.25a) for the general case and is known from Eq. (4.3.24) and (4.3.25b) when $\tau_i^* = 1$ for all i. If $\lambda_o = 0$ (m = 0) is an allowable eigenvalue in the flux formulation, care must be taken in evaluating $A_o(\xi)$, $f_o(\xi)$, and the integral of the transform.

The flux and temperature distributions are now completely available for the three standard orthogonal coordinate systems. When $\tau_i^* = 1$ for all i, an exact analytic solution was developed and will serve to check the numerical scheme. Next we will study two examples considering a two region slab. The corresponding parabolic solution is also displayed to

show the distinct differences in the two heat conduction approximations.

## 4.4 Two Region Slab with Step Change in Wall Temperature

Consider a two region slab (N = 2, p = 0) initially at the equilibrium temperature $T_o$. At t = 0, the surface at $x = x_1 = 0$ is suddenly raised to the constant temperature $T_{w,1}$, while the back surface at $x = x_3$ remains insulated for all time $t > 0$. For simplicity, we do not consider the presence of any volumetric heat sources ($u_i(x,t) = 0$, i = 1,2).

For this problem, the boundary condition in the flux formulation corresponding to a step change in temperature ($a_1 = 0$, $b_1 = 1$) reduces Eq. (4.2.8a) to

$$-\frac{\partial q_1}{\partial x} = (\rho C_p)_1 \frac{dT_{w,1}(t)}{dt} = (\rho C_p)_1 T_{w,1}\delta(t) \ , \ x = x_1 = 0 \ , \quad (4.4.1a)$$

where the delta function has resulted from the time derivative of the step change of surface temperature. The remaining interface ($u_1 = u_2 = 0$) and outer surface ($b_3 = 0$, $a_3 = 1$) boundary conditions are

$$q_1 = q_2 \ , \ x = x_2 \ , \quad (4.4.1b)$$

$$\frac{1}{(\rho C_p)_1}\frac{\partial q_1}{\partial x} = \frac{1}{(\rho C_p)_2}\frac{\partial q_2}{\partial x} \ , \ x = x_2 \ , \quad (4.4.1c)$$

and

$$q_2 = 0 \ , \ x = x_3 \ , \ t > 0 \ , \quad (4.4.1d)$$

The initial conditions are represented in Eq. (4.2.9a,b) where N = 2 and the reference temperature is chosen a $T_{ref} = T_{w,1} - T_o$. The corresponding dimensionless boundary coefficients become $a_1^* = 0$, $b_1^* = 1$ and $a_3^* = 1$, $b_3^* = 0$. The eigenfunctions $\psi_m(\eta)$, eigenvalues $\lambda_m$ and the exact evaluation of $\beta_{\ell m}$, as defined in Eq. (4.3.14), are provided in Appendix 4. The transforms $\bar{Q}_m(\xi)$ are then resolved and the flux distribution is reconstructed using the inversion formula presented in Eq. (4.3.10a).

In this particular example [144], the temperature distribution may be obtained from the spatial integration of the modified Fourier's law expressed in Eq. (4.2.2) as an alternative to the previously derived general expression using the conservation of energy equation. Performing the spatial integration in Eq. (4.2.2) yields

$$\theta_i(\eta,\xi) = \theta_i(\eta_i,\xi) - \frac{1}{k_i^*} \int_{\eta_o=\eta_i}^{\eta} \left[\frac{\alpha_i^*}{c_i^*} \frac{\partial Q_i(\eta_o,\xi)}{\partial \xi} + 2Q_i(\eta_o,\xi)\right] d\eta_o \,, \tag{4.4.2}$$

$$\eta \varepsilon [\eta_i, \eta_{i+1}],\ i = 1,2\ ,\ \xi \geq 0.$$

Substituting the inversion formula, Eq. (4.3.10a), into Eq. (4.4.2), and interchanging the orders of operations yields

$$\theta_i(\eta,\xi) = \theta_i(\eta_i,\xi) - \frac{1}{k_i^*} \left\{ \sum_{m=1}^{\infty} \frac{\int_{\eta_o=\eta_i}^{\eta} \psi_{im}(\eta_o) d\eta_o}{N(\lambda_m)} \cdot \left[\frac{\alpha^*_i}{c_i^*} \frac{d\bar{Q}_m}{d\xi} + \bar{2}Q_m\right]\right\} \,, \tag{4.4.3}$$

$$\eta \varepsilon [\eta_i, \eta_{i+1}],\ i = 1,2,\ \xi \geq 0.$$

At this point, every quantity is known in Eq. (4.4.3) except for $\frac{d\bar{Q}_m(\xi)}{d\xi}$. An expression may be developed in terms of the known values for $c_j(\lambda_m,\xi)$. Differentiating Eq. (4.3.20a) and using Eq. (4.3.21a) for $\frac{dc_j(\lambda_m,\xi)}{d\xi}$ in the result and finally making use of Eq. (4.3.18) yields

$$\frac{d\bar{Q}_m(\xi)}{d\xi} = \frac{\alpha_1^* \theta_w \cos\lambda_m \xi}{k_1^*} - \sum_{j=1}^{2} \frac{da_j(\lambda_m,\xi)}{d\xi} c_j(\lambda_m,\xi)$$

(4.4.4)

$$-2 \sum_{\ell=1}^{\infty} \frac{B_{\ell m}}{N(\lambda_\ell)} \left[\frac{\alpha_1^* \theta_w \sin\lambda_\ell \xi}{k_1^* \lambda_\ell} - \sum_{k=1}^{2} a_k(\lambda_\ell,\xi) c_k(\lambda_\ell,\xi)\right] ,$$

$$\xi \geq 0, \; m = 1,2,\ldots .$$

Substituting Eqs. (4.3.20a) and (4.4.4) into Eq. (4.4.3) and evaluating permits the dimensionless temperature distribution to be known in terms of the numerically evaluated $c_j(\lambda_m,\xi)$ functions.

The flux and temperature distributions are now completely available for any combination of dimensionless properties. As remarked earlier, the special case where $\tau_1^* = \tau_2^*$ is the test case for both the mathematical and numerical scheme and gives credence to the general flux formulation. This special case was resolved by the finite integral transform technique [93] in the temperature formulation.

Numerical results displaying the nature of hyperbolic heat conduction in a two region slab are now presented. Since the properties are nondimensionalized with respect to region 1, we get $\tau_1^* = \alpha_1^* = k_1^* = 1$.

This composite is divided equally into two regions where $\eta_3 = 1$. At $\eta = 0$, the surface is suddenly exposed to a dimensionless surface temperature $\theta_w = 1$, for all time $\xi > 0$. All computations were performed on an IBM 370 in double precision.

Figure 4.4.1 displays the flux distribution for both hyperbolic and parabolic heat conduction at various times $\xi$. The details of the parabolic solution can be found in reference [93] and are not presented here. The special case where $k_2^* = 2$, $\alpha_2^* = 1$, $\tau_2^* = 1$ is presented, which represents regions with identical thermal diffusivities and relaxation times but with the thermal conductivity of region 2 twice that of region 1. The product of the density and specific heat in region 2 is therefore twice that of region 1. At $\xi = 0.2$, the hyperbolic solution clearly shows its wave nature by displaying an undisturbed region ahead of the front. On the other hand, the parabolic solution indicates that the thermal disturbance has been felt in the entire region. Also at this time, the heat flux at $\eta = 0$ is greater for the parabolic solution. The curves displaying the hyperbolic flux distribution actually represent both the exact solution, as developed from the temperature formulation with $\tau_1^* = \tau_2^*$, and our numerical procedure described previously which calculates the integral transform $\bar{Q}_m(\xi)$ numerically in the flux formulation. The solutions are indistinguishable, thus our flux formulation appears correct and our numerical procedure yields extremely accurate results. The time step used in the Runge Kutta scheme is $\Delta\xi = 0.05$ which is a rather large time step. This time step could be made smaller though no more accuracy would appear to three significant figures. We used 250 terms in the infinite series represented by Eq. (4.3.10a) for

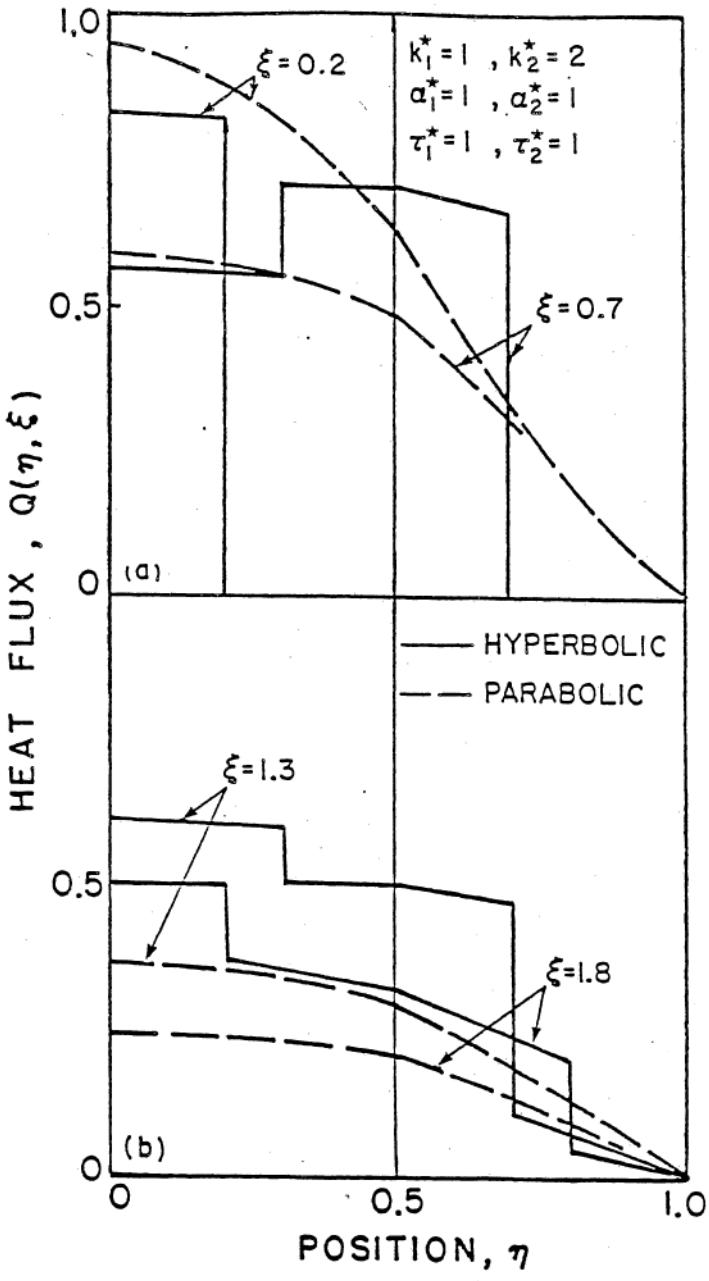


Figure 4.4.1 Comparison of Hyperbolic and Parabolic Heat Flux for a Sequence of Times with $k_2^* = 2$ when Composite is Subject to a Step Change in Wall Temperature.

plotting purposes. In general, the bilinear series representation for the heat flux is a slowly convergent series which requires a few hundred terms for plotting accuracy.

At $\xi = 0.7$, the energy entering the slab has incurred a partial reflection at the interface at $\eta = \eta_2 = 0.5$, while the remainder of energy is transmitted. Observe that the flux gradient is discontinuous at the interface at $\eta = \eta_2$ as predicted by the boundary condition expressed in Eq. (4.4.1c). Also observe that the partial reflection at the interface has given rise to two thermal fronts; one located at $\eta = 0.7$ moving in the positive direction and one located at $\eta = 0.3$ moving in the negative direction. Also at this time, the parabolic solution has decayed further in a continuous manner.

By $\xi = 1.3$ and 1.8, further reflections from the boundaries have occurred. Since this is linear theory, no interaction of wavefronts has occurred. This process of internal reflections will persist until the wave has damped out. The parabolic solution for the flux distribution is also decaying toward its steady state value.

Figure 4.4.2 shows the temperature distributions corresponding to Fig. 4.4.1 for the hyperbolic and the parabolic approximations. Again, the procedure of determining the integral transforms $\overline{Q}_m(\xi)$ numerically and then using the modified Fourier's law to obtain the temperature distribution proves to be numerically 'exact.' The plots do not possess the numerical oscillations associated with pure numerical (finite difference) solutions. At $\xi = 0.2$, an undisturbed region is ahead of the wavefront for the hyperbolic case whereas the parabolic solution has maintained a continuous distribution. Since the conductivities are

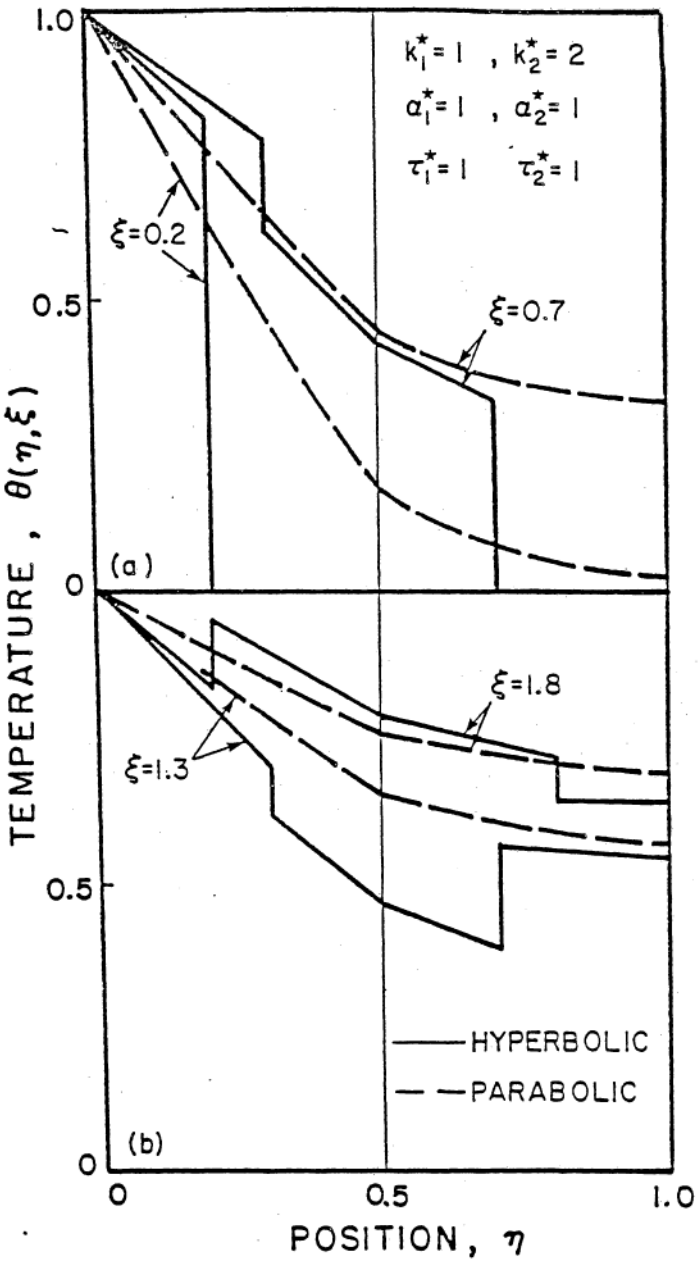


Figure 4.4.2 Comparison of Hyperbolic and Parabolic Temperature Distributions for a Sequence of Times with $k_2^* = 2$ when Composite is Subject to a Step Change in Wall Temperature.

different, $k_1^* \neq k_2^*$, while the relaxation times are equal, $\tau_1^* = \tau_2^*$, the usual parabolic boundary condition is valid at $\eta = \eta_2 = 0.5$. At $\xi = 0.7$, an internal reflection at the interface has occurred and the discontinuous temperature gradient is apparent. The parabolic temperature distribution is established and is tending toward its steady state value. As time increases, the hyperbolic and parabolic solutions each approach the steady state value of 1.

A parametric study is now included to show the effect of the various dimensionless properties $\tau_2^*$, $k_2^*$, $\alpha_2^*$ that can be adjusted in region 2. Figure 4.4.3 shows the effect of various conductivities $k_2^*$ on the temperature and heat flux, respectively, for times $\xi = 0.2$ and $\xi = 0.7$. At $\xi = 0.2$, all distributions are identical since the wave has not reached region 2 with different properties and has not experienced any reflection from the interface. Since $\tau_2^* = \alpha_2^* = 1$, the wave speed for the various profiles are identical and the wavefronts at any given time must coincide, regardless of the conductivity, $k_2^*$. For time $\xi = 0.7$, we observe that the transmitted and reflected portions of the thermal disturbance tend to decrease the temperature profiles but increase the flux profiles as $k_2^*$ increases. Figure 4.4.3a is interesting in this regard since the area under the temperature profile represents the total energy content in the region. For times $\xi < 1.0$, the energy content in the composite media must be the same for any value of $k_2^*$ at any given time since the surface of $\eta = 0$ is unaware of any energy due to reflection. Examining the temperature profiles at $\xi = 0.7$ in Fig. 4.4.3a gives the impression that this energy conservation principle has been violated since the area under the curves increases for smaller values

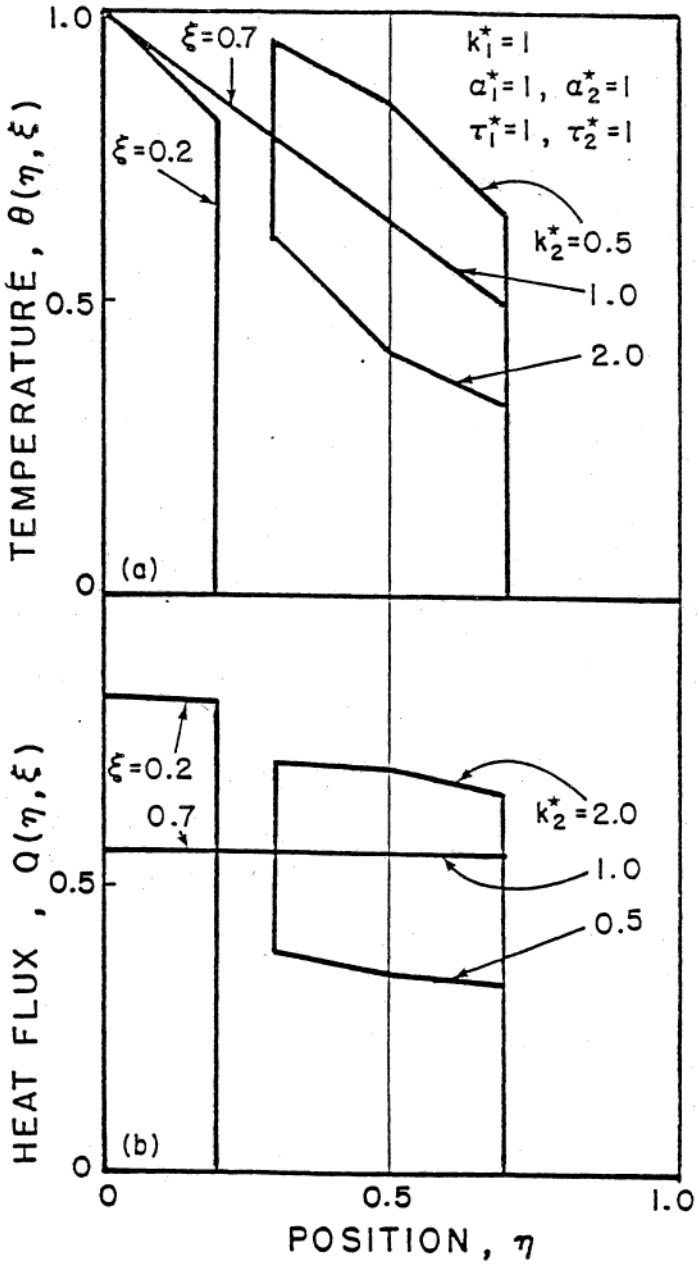


Figure 4.4.3 Effect of $k_2^*$ on Temperature and Heat Flux.

of $k_2^*$. However, since the total energy is actually the integral of the temperature times heat capacity, $\rho C_p$, the energy content represented by each curve is identical since $(\rho C_p)_2$ changes in direct proportion to $k_2^*$ when $\alpha_2^*$ is held constant. With $\tau_1^* = \tau_2^*$, the appropriate temperature interface condition is Eq. (4.2.6f) which gives rise to a discontinuous temperature gradient whenever $k_2^* \neq k_1^*$. The interface condition in flux given by Eq. (4.3.4c) gives rise to a discontinuous flux gradient when $k_2^* \neq k_1^*$.

In Fig. 4.4.4, the effect of varying the dimensionless diffusivities in region 2 is investigated with reference to the one region solution, represented by $\alpha_2^* = 1$. By varying the diffusivity, the wave speed in region 2 changes. Figure 4.4.4a shows the temperature distribution for times $\xi = 0.2$ and $\xi = 0.7$. Again at $\xi = 0.2$, all the distributions are identical. At $\xi = 0.7$, the different wave speeds in region 2 are clearly shown. Since $\sqrt{c_2^*} = \sqrt{\alpha_2^* / \tau_2^*}$, the larger the diffusivity the faster the wavefront travels. However, the reflected portion of the wavefront for the various cases still coincides in region 1 since the properties of region 1 have been used as the reference. Since the conductivities and relaxation times are the same in both regions, the temperature gradient in this case will appear continuous at the interface. The corresponding flux distribution shown in Fig. 4.4.4b, displays similar features to the temperature distribution. Notice, however that a discontinuous flux gradient appears at the interface when $\xi = 0.7$ since the products of density and specific heats are different $\alpha_2^*/k_2^* \neq \alpha_1^*/k_1^*$ in the two regions.

Finally, Fig. 4.4.5 shows the effect of various relaxation times.

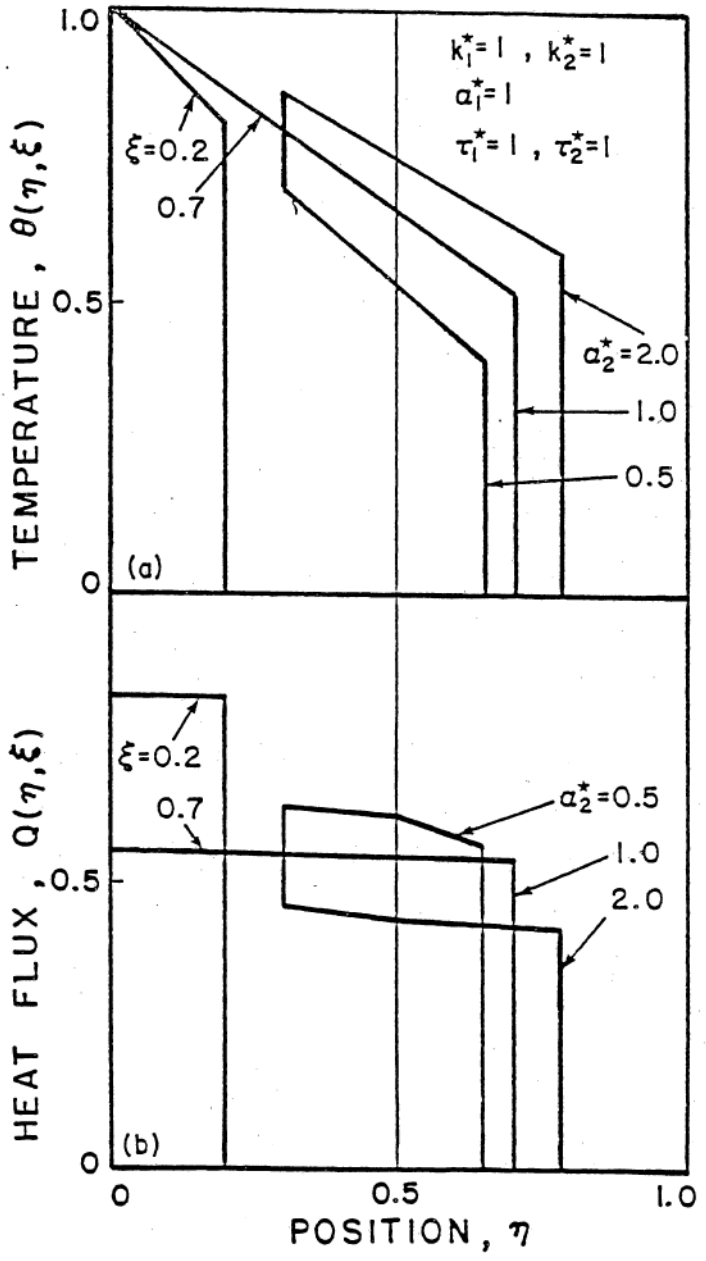


Figure 4.4.4 Effect of $\alpha_2^*$ on Temperature and Heat Flux.

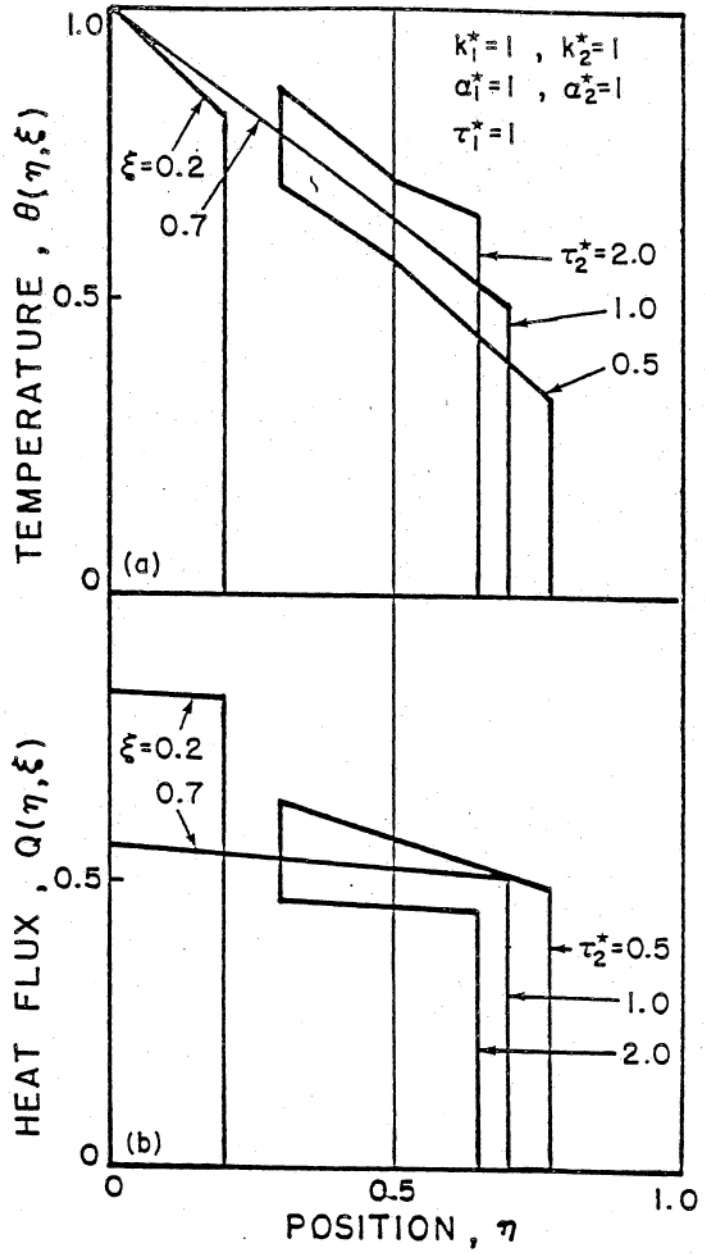


Figure 4.4.5 Effect of $\tau_2^*$ on Temperature and Heat Flux.

As stated previously, no exact analytical solution exists for the temperature and flux distributions since the governing field equations are nonseparable. Fig. 4.4.5 displays the usual result of identical profiles at $\xi = 0.2$. Since $\alpha_2^* = \alpha_1^*$ $k_2^* = k_1^*$ but $\tau_2^* \neq \tau_1^*$, we see that the wavespeed in region 2 at $\xi = 0.7$ is proportional to $1/\tau_2^*$. From Eq. (4.2.6e), the effect of this new interface boundary condition can now be investigated. The effect of the $\tau_i(\partial^2 T_{i+1}/\partial x \partial t)$ terms at the interface produces a discontinuous temperature gradient. Again we see similar results to that of Fig. 4.4.4 in terms of the location of the fronts and in terms of energy content considerations. The corresponding flux distribution behaves similarly to the temperature distribution. However, since $k_1^* = k_2^*$ and $\alpha_1^* = \alpha_2^*$, the flux gradient at the interface is continuous.

## 4.5 Two Region Slab Subjected to Pulsed Heat Source

Numerical results displaying the unusual nature of hyperbolic heat conduction in a two region (N = 2) slab (P = 0) are presented. The fundamental nature of hyperbolic heat conduction is best represented by considering a pulsed volumetric source of width $\Delta x$ emanating from region 1 adjacent to the exterior surface at x = 0. This source is described mathematically as

$$u_1(x,t) = \begin{cases} \dfrac{U_o \delta(t)}{\Delta x} & , \; x_1 = 0 < x \leq \Delta x \\ 0 & , \; \Delta x < x \leq x_2 \end{cases} \qquad (4.5.1a)$$

$$u_2(x,t) = 0 \quad , \; x_2 < x < x_3 \; ,$$

where

$$U_o = \int_{t=0}^{\infty} \int_{x=0}^{\Delta x} u_1(x,t) \, dxdt < \infty \; . \qquad (4.5.1b)$$

The term $U_o$ represents the total amount of energy generated by the source per area perpendicular to the x-direction for all space and time. By choosing the reference temperature as $T_{ref} = U_o c_1/k_1$, we obtain the dimensionless sources

$$S_1(\eta,\xi) = \begin{cases} \dfrac{\delta(\xi)}{\Delta\eta} & , \quad \eta_1 = 0 < \eta \leq \Delta\eta \\ 0 & , \quad \Delta\eta < \eta \leq \eta_2 \end{cases} \qquad (4.5.1c)$$

$$S_2(\eta,\xi) = 0 \quad , \quad \eta_2 < \eta < \eta_3 \; .$$

We consider the situation where the two external boundaries are insulated for all time $t > 0$. In this situation, the total energy content of the system is preserved. The corresponding boundary coefficients are $a_1 = a_2 = 1$, $b_1 = b_2 = 0$. While the dimensionless counterparts become $a_1^* = a_2^* = 1$ and $b_1^* = b_2^* = 0$. Now, all the necessary ingredients for determining a unique solution are present. The eigenfunctions $\psi_m(\eta)$, eigenvalues $\lambda_m$'s, and the evaluation of $B_{\ell m}$ are displayed in Appendix 5. The parameters $k_2^*$, $\alpha_2^*$ and $\tau_2^*$ are varied in order to study the consequences and features associated to heat conduction based on the modified Fourier's law. A standard fourth order Runge-Kutta [154] was considered in resolving $c_j(\lambda_m,\xi)$, $j = 1,2$, $m = 1,2,\ldots$ numerically when $\tau_2^* \neq \tau_1^*$. When $\tau_1^* = \tau_2^*$, the exact analytic solution (both flux and temperature formulation) are presented. Comparison of the two formulations show that the infinite series representing the flux and temperature distributions converge at different rates. The two formulations produce identical results in the limit, thus showing their equivalence and the correctness of the flux formulation. As is generally known, infinite series solutions for hyperbolic (wave) equations converge much slower than parabolic equations. The rate of convergence is related to the behavior of the terms in the bilinear series.

In Section 4.4, we obtain very accurate results when $\tau_1^* \neq \tau_2^*$ for the problem with a step change in wall temperature. This accuracy was in part due to the nature of the thermal disturbance, i.e., the boundary disturbance was continuous for all time $t > 0$ and the series converged more rapidly than in the case of a pulsed source.

Figure 4.5.1 displays the flux distributions for the case

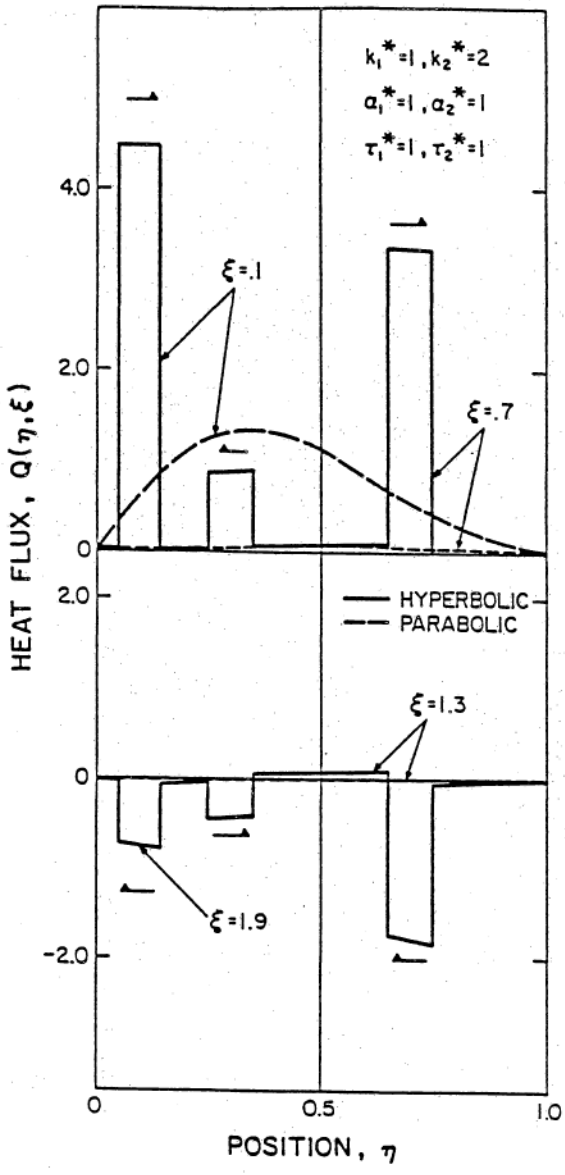


Figure 4.5.1 Comparison of Hyperbolic and Parabolic Heat Flux Distributions for a Sequence of Times with $k_2^* = 2$ when Composite is Subjected to a Pulsed Source.

where $k_2^* = 2$, $\tau_2^* = \alpha_2^* = 1$ for various times $\xi$ as predicted by the two approximations of heat conduction. The dimensionless pulse width of the source is initially $\Delta\eta = 0.05$ and is initially released in the interval $0 \leq \eta \leq \Delta\eta$. At $\xi = .1$, the definite wave-nature associated with hyperbolic heat conduction is evident. The inital pulse width doubles after being released at $t = 0^+$ since it initially has no preferred direction. This result is identical to the half space problem since an undisturbed region lies ahead of the wave. In contrast, the parabolic approximation shows a continuous distribution which is smaller in magnitude. By $\xi = .7$, the initial wavefront has split into two waves traveling in opposing directions. One represents a reflected wave (travelling left) and the other represents the transmitted wave (travelling right), both retain the initial wavelike features. This division initially occurred at $\xi = 0.45$ due to the impacting of the original wave into the interface at $\eta = .5$. In contrast, the parabolic approximation shows a monotonic decay toward steady state.

By $\xi = 1.3$, a pure reflection at the external boundaries has taken place. A pure reflection occurs because the insulated boundary conditions do not permit energy to leave the system. Each wavefront then approaches the interior interface at $\eta = .5$ at the same speed and will initially impact at $\xi = 1.45$. This impact appears to cancel the weaker of the two fronts as seen at $\xi = 1.9$. Meanwhile, the parabolic heat conduction approximation has attained its steady state value.

Figure 4.5.2 displays the temperature distributions corresponding to the situation described in Fig. 4.5.1. Hyperbolic heat conduction predicts higher temperatures and fluxes than the parabolic approxima-

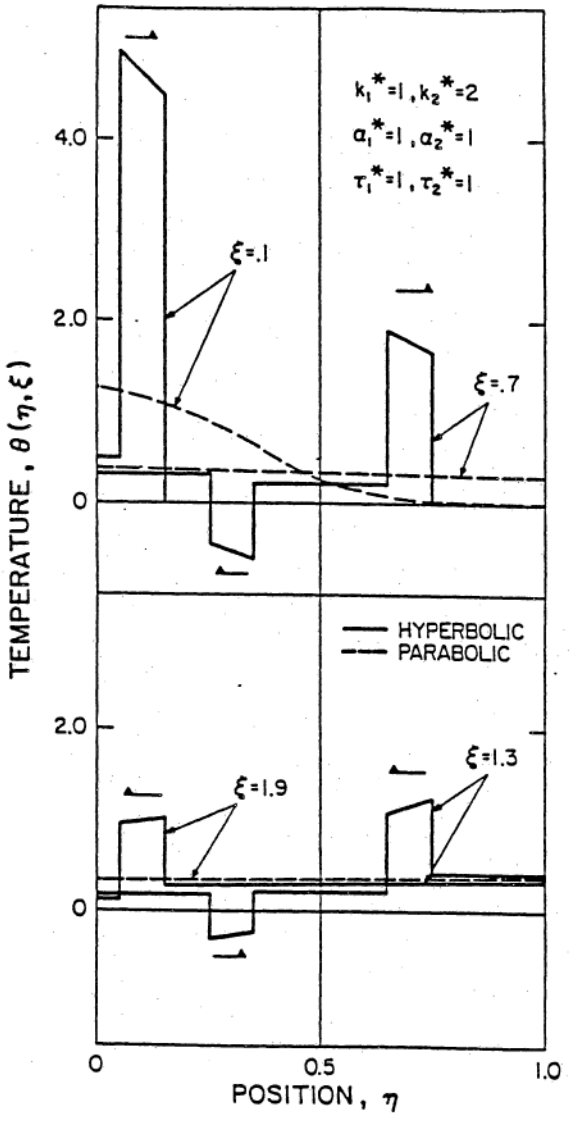


Figure 4.5.2 Comparison of Hyperbolic and Parabolic Temperature Distributions for a Sequence of Times with $k_2^* = 2$ when Composite is Subjected to a Pulsed Source.

tion. The wave front, of width $2\Delta\eta$, is preserved for all reflection-transmission effects when the wave speed in region 2 is unity, i.e., $c_2^* = c_1^* = 1$. At $\xi = .1$, the wave train shows the effects of diffusion in two ways; first, a residual temperature in the wake of the pulse and second, a slant across the top of the initially flat wave front. At $\xi = .7$, we see two distinct waves which result from the impacting of the initial wave at $\xi = .45$ into the interface at $\eta = .5$. Notice the wave front traveling to the left is negative corresponding to temperatures below the initial temperature. Since $k_2^* > k_1^*$, less resistance causes more energy to enter region 2, thus creating the temperature lull of the negative temperature wave front in order to preserve the energy content of the system. Since the total energy is the spatial integral of the temperature times the heat capacity $\rho C_p$, the energy content represented by each curve is identical since $(\rho C_p)_2$ changes in direct proportion to $k_2^*$ when $\alpha_2^*$ is held constant. Also, since the external boundaries are insulated for all time $\xi > 0$, the total energy content is constant. At $\xi = 1.3$, the wave fronts have reflected from the exterior insulated surfaces and are directed toward the interface at $\eta = .5$. The dominant wave emanating from region 2 later combines with the subdominant wave to form a single wave moving toward the origin as seen clearly at $\xi = 1.9$. This transmission-reflection-combination phenomena will persist until diffusion dominants.

The remaining figures help provide a fundamental understanding into the effects of the parameters $k_2^*$, $\alpha_2^*$ and $\tau_2^*$ on hyperbolic heat conduction in composites. Figure 4.5.3 shows the effect of $k_2^*$ on the temperature and flux distribution. The single region ($k_2^* = 1$) solution is

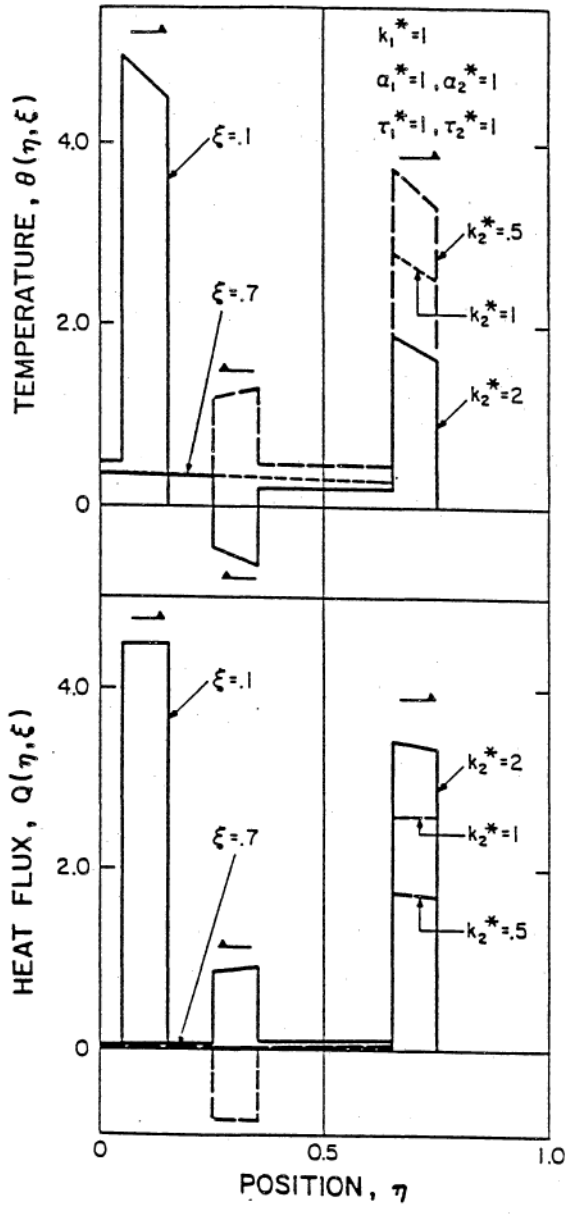


Figure 4.5.3 Effect of $k_2^*$ on Temperature and Heat Flux.

presented as a reference to judge the effect of a higher and lower conductivity in region 2. At =.1, the temperature distributions for all three cases considered are identical since the wavefront is unaware of region 2 at this time. At $\xi = .7$, the distinction between the three values of $k_2^*$ becomes clear. When $k_2^* = 2 > k_1^*$, the forward wave front is smaller in magnitude compared to the equivalent one region standard. The reflected portion, which initially encountered the interface at $\xi = .45$, shows a wave moving toward the origin but negative in magnitude. Again, this temperature lull is due to the enhanced ability of region 2 to transmit energy and the basic criteria of energy conservation. When $k_2^* = .5$, the forward temperature wave is greater than the one region ($k_2^* = 1$) counterpart, while a positive magnitude wave is reflected toward the origin. Again, this is consistent with energy considerations. The corresponding flux distributions display similar features.

The effect of various diffusivities in region 2 are displayed in Fig. 4.5.4. Since the wave speed ratio is $\sqrt{c_2^*} = \sqrt{\alpha_2^*/\tau_2^*}$, we expect different speeds in region 2 when $\alpha_2^* \neq 1$. At $\xi = .1$, all curves are again identical. At $\xi = .7$, the distinctions between the various diffusivities $\alpha_2^* = 0.5,1,2$ are evident. When $\alpha_2^* = 2$, the wave speed $c_2^*$ is greater than the one region ($c_2^* = 1$) standard, giving rise to a stretching of the width of the pulse disturbance. At $\xi = .45$, the leading edge of the pulse impacts the interface at $\eta = .5$, and the wave emerging from the interface in region 2 is pulling away faster ($c_2^* > c_1^*$) than the oncoming energy from region 1. Hence, the net effect is the stretching of the pulse width. This is evident in both the temperature and flux

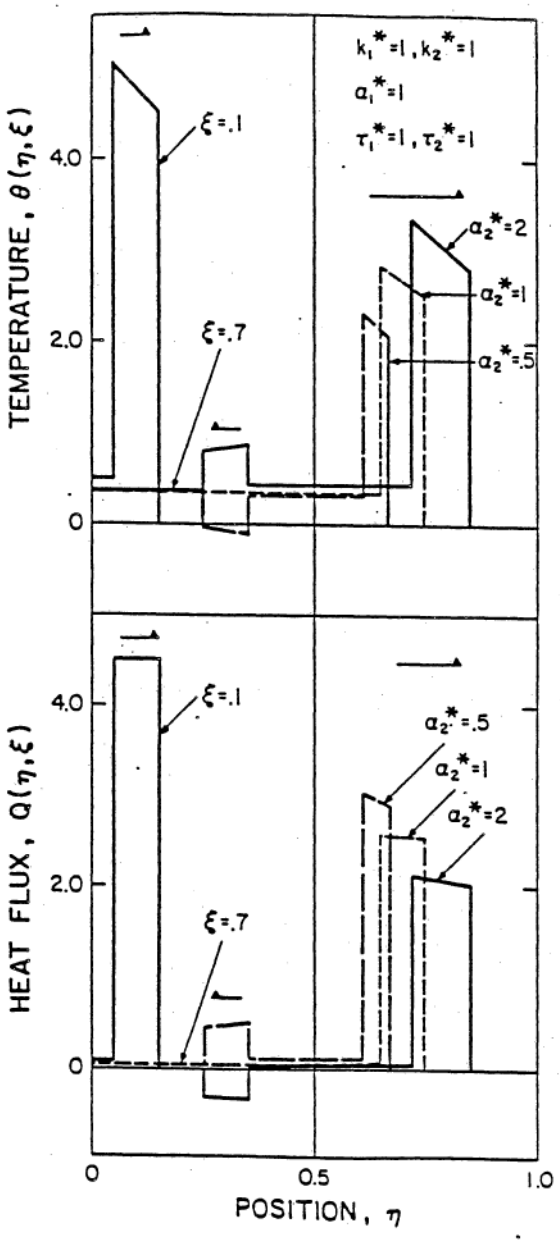


Figure 4.5.4 Effect of $\alpha_2^*$ on Temperature and Heat Flux.

distributions. The opposite occurs when $c_2^* < c_1^*$, as seen when $\alpha_1^* = .5$. As the energy leaves the interface when $\xi = .45$, a 'pile up' of energy occurs since the wave leaving the interface moves slower than that entering the interface, hence a thinner pulse width emerges. The reflected portion, when $\alpha_2^* = 2$, shows a temperature wave directed toward the origin consistent with the energy content of the system. Also, the reflected wave corresponding to $\alpha_2^* = .5$, displays a negative temperature wave directed toward the origin. This again is consistent with conservation of energy in the system.

Finally, the effect of various relaxation times in region 2 is studied. For fixed $k_2^* = \alpha_2^* = 1$, the wavespeed in region 2 should change for various relaxation times $\tau_2^*$. In Fig. 4.5.5, the distributions plotted are obtained from the numerical procedure outlined previously since no exact solution is available. Unlike Section 4.4, more terms of the infinite series solutions are required to obtain plotting accuracy. This is mainly due to the severity of the thermal disturbance. The numerical procedure was checked by comparing the exact results displayed in Figs. 4.5.3 and 4.5.4. This provided assurance to the procedure and accuracy of the proposed scheme. When $\xi = .7$, three distinct curves exist for the various relaxation times in region 2 for $\tau_2^* = 0.5,1,2$. When $\tau_2^* = 2$, the wavespeed in region 2 is less than the one region standard ($\tau_2^* = 1$). Again, a compressed pulse appears due to the dissimilar wavespeeds of the two regions. The wavespeed increases when $\tau_2^* = .5$ and the pulse width expands accordingly. The total energy content of the system is preserved for each temperature distribution.

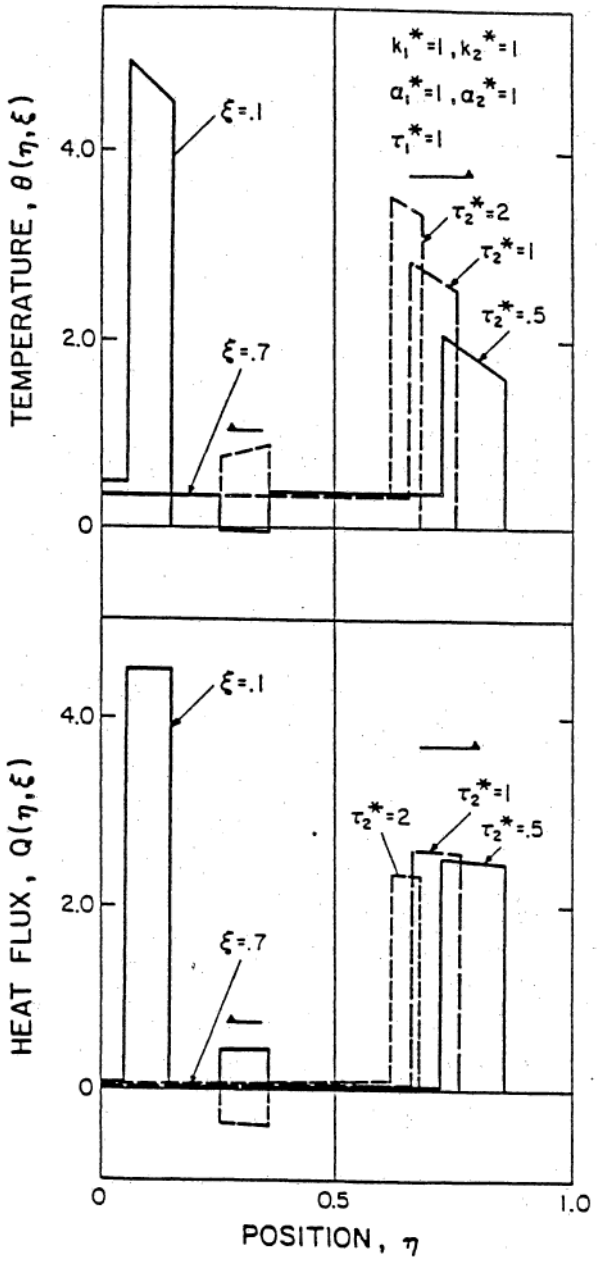


Figure 4.5.5 Effect of $\tau_2^*$ on Temperature and Heat Flux.

## 4.6 Conclusions

The general one-dimensional constant property heat flux and temperature formulation, based on the hyperbolic heat conduction approximation, has been developed for multiregion media. These new formulations produce a linear but nonseparable system. In addition, the temperature formulation produces a new nonseparable higher order boundary condition at the interface of two adjacent regions. These formulations recover the standard parabolic approximation as the relaxation times in each region approach zero. Since these systems of equations are nonseparable, a generalized finite integral transform technique is proposed which produces an infinite set of coupled, nonhomogeneous, constant coefficient ordinary differential equations (initial value problems) in the transformed variable. Since these equations may contain generalized functions and since a large number of terms of the infinite series are required, standard numerical solution techniques are not well suited. Thus we transform these ordinary differential equations into an infinite set of linear Volterra integral equations of the second kind. Since the kernels are exactly decomposable, the method of Bownds is applied in a unique and nonstandard manner to numerically solve for the transforms. Also, it should be mentioned that the analysis presented here has potential application to nonlinear problems. An exact analytical solution for the temperature and flux distributions is available when the relaxation times for each region are identical. The accuracy of the proposed flux formulation and numerical procedure may then be tested.

A detailed study in a two region slab provides evidence of the correctness of the flux formulation and numerical procedure outlined.

The contrast between the parabolic and hyperbolic heat conduction approximations in a two region slab exposed to a sudden change in surface temperature is displayed. The numerical procedure for finding the integral transform is shown to be numerically exact for the test cases where the relaxation times are identical in both regions. The figures displaying both the exact analytical and numerically exact profiles are identical. It is shown that internal reflections at the interface of two dissimilar media are present and the extent of the reflection varies with properties. For various combinations of material properties, the wave speed changes while the energy content on the first pass remains constant. Also, the temperature and flux gradients at the interface of two adjacent regions behave differently depending on the arrangement of material properties.

The contrast between the parabolic and hyperbolic heat conduction approximations in a two region slab exposed to a pulsed volumetric source is also displayed. The numerical procedure for finding the integral transform is shown to be numerically accurate for the test cases where the relaxation times are identical in both regions. The figures displaying both the exact analytical and numerically accurate profiles are identical. It is shown that internal reflections at the interface of two dissimilar media are present and the extent of the reflection varies with properties. For various combinations of material properties, the wave speed changes and deformation of the pulse width may occur. In light of some recent experiments involving reflections of thermal waves in superfluid helium [91,92] the results of this section will help to provide a sound theory for predicting this complex phenomenon.

# Chapter 5

# NONLINEAR THEORY-VARIABLE THERMAL CONDUCTIVITY

## 5.1 Introduction

In this chapter, we study the effects of temperature dependent thermal conductivity in hyperbolic heat conduction. Many problems occurring in engineering involve situations where the material properties vary significantly over temperature ranges of interest. In these circumstances, the most accurate results for the temperature distribution are obtained by accounting for the nonlinearities introduced by temperature dependent properties. Temperature dependent thermal conductivity may possibly be more important in hyperbolic heat conduction than in parabolic heat conduction since more severe temperature gradients exist.

In parabolic heat conduction, temperature dependent thermal conductivity is well-studied [158-164]. In these investigations, only a linear variation in temperature has been assumed for the thermal conductivity. Recently, Frankel and Vick [165] proposed a generalized thermal conductivity in the form of a Taylor series about a reference temperature for parabolic heat conduction. In addition, they developed an exact methodology for solving nonlinear diffusion equations using integral transforms.

In hyperbolic heat conduction, Glass, Ozisik, and Vick [74] developed numerical results assuming a linear variation in temperature for the thermal conductivity, namely

$$k(T) = k_o[1 + \beta'(T - T_o)] \tag{5.1.1}$$

where $k_o$ is the thermal conductivity at the reference temperature $T_o$. Since the thermal conductivity is a function of the temperature, the thermal wave speed is written as

$$c(T) = \sqrt{\frac{\alpha}{\tau}} = \sqrt{\frac{k(T)}{\rho C_p \tau}} , \tag{5.1.2}$$

where it can be seen that a variable thermal conductivity will effect the wave speed c.

By substituting Eq. (5.1.1) into Eq. (5.1.2), the wave speed becomes

$$c(T) = \sqrt{\frac{\alpha_o}{\tau}\left[1 + \beta'(T - T_o)\right]} , \tag{5.1.3}$$

where $\alpha_o \equiv \frac{k_o}{\tau C_p}$ and $\rho, C_p, \tau$, are assumed constant. Qualitatively, we see that positive $\beta'$ implies an increase in the thermal wave speed with respect to the linear ($\beta' = 0$) case. The opposite can be said for negative $\beta'$.

In the next sections, we introduce a generalized expression for the thermal conductivity as a function of temperature in terms of a Taylor series expansion about the reference temperature. In instances involving a large temperature range, the linear variation in k(T) may not be accurate. We then introduce the generalized thermal conductivity into the transient one-dimensional temperature field equation for the three standard orthogonal coordinate systems. The resulting form of this new

heat equation suggests that one may analytically remove the spatial coordinate prior to resorting to any numerical procedure.

To illustrate the method, we examine a special case of a slab. Our goal is to obtain an exact analytical representation for the temperature distribution of the nonlinear transient heat conduction equation using the finite integral transform technique [93]. In our procedure, the nonlinear terms arising in the governing field equation may be treated as an effective heat source and we may follow the usual methodology associated with the finite integral transform technique. It is shown that the spatial dependence may be removed analytically by integration, resulting in a nonlinear initial value problem (IVP) in the transform variable. This nonlinear IVP is converted to an equivalent nonlinear Volterra integral equation of the second kind for numerical evaluation. Unlike the equivalent parabolic heat conduction problem [165], the large system of equations and large number of internal operations requires us to develop an approximate analytical solution when using conventional mini and mainframe computers.

## 5.2 General One-Dimensional Temperature Formulation

In this section, the general one-dimensional temperature field equation, and boundary and initial conditions, are developed using a generalized temperature dependent thermal conductivity.

The usual temperature dependent representation for the thermal conductivity, k(T), appearing in heat conduction is

$$k(T) = k_o[\beta_o + \beta_1 (T - T_o)] , \qquad (5.2.1)$$

where $\beta_o \equiv 1$, and $k_o$ is the thermal conductivity at the reference temperature $T_o$. Equation (5.2.1) can be regarded as the first two terms of the Taylor series expansion of k(T) about the reference temperature $T_o$. In general, a higher order expansion is usually obtained when experimental data is fitted. Certainly, a linear variation in temperature is valid over various temperature ranges. A more universal expression for the thermal conductivity can be written in terms of a truncated Taylor series expansion about the reference temperature. That is, we let

$$k(T) = k_o \sum_{n=0}^{N} \beta_n (T - T_o)^n , \qquad (5.2.2)$$

where $\beta_o \equiv 1$ and the remaining $\beta_n$'s are obtained from experimental data. When N = 1, Eq. (5.2.2) reduces to the linear variation in temperature displayed in Eq. (5.2.1). Recalling Eq. (3.3.1), we write the mathematical expression for the conservation of energy as

$$-\frac{1}{x^p}\frac{\partial}{\partial x}(x^p q) + u(x,t) = \rho C_p \frac{\partial T}{\partial t} , \; x \in (x_i, x_o) \; t > 0 , \qquad (5.2.3a)$$

where

$$p = \begin{cases} 0 \text{ slab} \\ 1 \text{ cylinder} \\ 2 \text{ sphere} \end{cases} \qquad (5.2.3b)$$

The constitutive equation relating the heat flux to the temperature is the modified Fourier's law and is given as

$$\tau \frac{\partial q}{\partial t} + q = -k(T) \frac{\partial T}{\partial x} , \tag{5.2.4}$$

where the thermal conductivity k(T) is an explicit function of the temperature.

To obtain the temperature field equation, we eliminate q(x,t) between Eqs. (5.2.3a) and (5.2.4), where the thermal conductivity is given by Eq. (5.2.2) to get

$$k_o \beta_o \frac{1}{x^p} \frac{\partial}{\partial x} \left(x^p \frac{\partial T}{\partial x}\right) + \frac{k_o}{x^p} \sum_{n=1}^{N} \frac{\beta_n}{(n+1)} \cdot \left\{\frac{\partial^2}{\partial x^2} \left[x^p (T - T_o)^{n+1}\right]\right. \tag{5.2.5}$$

$$\left. - p \frac{\partial}{\partial x} \left[x^{p-1} (T - T_o)^{n+1}\right]\right\} +$$

$$+ u(x,t) = \rho C_p \left(\frac{\partial T}{\partial t} + \tau \frac{\partial^2 T}{\partial t^2}\right) , \quad x \in (x_i, x_o) , \quad t > 0 .$$

At this junction, we observe that the form of the temperature field equation suggests a methodology for the solution of the temperature distribution by an eigenfunction expansion technique. The Sturm-Liouville weight function associated with the linear heat equation appears in front of both the linear and nonlinear spatial operators. This suggests that an exact solution representation may be developed by the finite integral transform technique [93].

The boundary and initial conditions required to complete the mathematical formulation are presently developed. Referring to Fig. 3.3.1, the boundary conditions become

$$C^*_{2i}k(T)\frac{\partial T}{\partial x} + C^*_{1i}T = -C^*_{2i}\left[\frac{\tau dq_i}{dt} + q_i(t)\right] + C^*_{1i}T_i(t) \ , \ x = x_i \ , \qquad (5.2.6a)$$

and

$$C^*_{2o}k(T)\frac{\partial T}{\partial x} + C^*_{1o}T = C^*_{2o}\left[\frac{\tau dq_o}{dt} + q_o(t)\right] + C^*_{1o}T_o(t) \ , \ x = x_o \ , \qquad (5.2.6b)$$

where the boundary coefficients $C^*_{1j}$, $C^*_{2j}$, $j = i,o$ follow the previously described logic (see Section 3.3). Note that the general boundary conditions are nonlinear since the product of $k(T)\frac{\partial T}{\partial x}$ produces terms in higher powers of T.

Finally, equilibrium initial conditions are readily established as

$$T = T_o \ , \qquad (5.2.7a)$$

$$\frac{\partial T}{\partial t} = 0 \ , \ x\varepsilon[x_i,x_o] \ , \ t > 0 \ . \qquad (5.2.7b)$$

## 5.3 Solution in Slab by the Finite Integral Transform Technique

In this section, we propose a methodology for solving nonlinear heat conduction problems using analytical developments based on the finite integral transform technique. For purposes of illustration and clarity in the procedure, we consider a slab ($p = 0$) where the thermal conductivity varies linearly with temperature ($N = 1$). The temperature distribution is developed for a slab subject to a step change in wall temperature $T_w$ at its front face at $x = x_i = 0$ while the back surface at $x = x_o$ remains insulated for all time $t > 0$. In this example, the finite integral transform technique is utilized in obtaining the exact

analytical representation for the temperature distribution. In this approach, direct parametric relationships are explicitly available.

For convenience in the subsequent analysis, we introduce the dimensionless quantities expressed by Eq. (3.4.1a-c) into Eq. (5.2.5) where p = 0, N = 1, and u(x,t) = 0 to get

$$M_0[\theta(\eta,\xi)] = -\frac{\beta_1^*}{2}\frac{\partial^2}{\partial\eta^2}[\theta^2(\eta,\xi)] \ , \ \eta\varepsilon(\theta,\eta_o) \ , \ \xi > 0 \ , \qquad (5.3.1)$$

where $\alpha_o \equiv k_o/\rho C_p$ is the thermal diffusivity at the initial temperature $T_o$, and $T_{ref} = T_w - T_o$ and $\beta_1^* = \beta_1(T_w - T_o)$. The linear conduction operator $M_0$ is defined by Eq. (3.4.3). For this particular problem, the dimensionless boundary conditions reduce to

$$\theta(0,\xi) = 1, \qquad (5.3.2a)$$

$$\frac{\partial\theta}{\partial\eta}(\eta_o,\xi) = 0 \ , \ \xi > 0 \ , \qquad (5.3.2b)$$

since the boundary coefficients expressed in dimensional form from Eq. (5.2.6) are $C_{2i}^* = 0$ , $C_{1i}^* = 1$ and $C_{2o}^* = 1$, $C_{1o}^* = 0$. Finally, the initial conditions are

$$\theta(\eta,0) = 0 \ , \qquad (5.3.3a)$$

$$\frac{\partial\theta}{\partial\xi}(\eta,0) = 0 \ , \ \eta\varepsilon[0,\eta_o] \ . \qquad (5.3.3b)$$

Equations (5.3.1)-(5.3.3) constitute the complete mathematical formula-

tion required to uniquely determine the temperature distribution. If desired, the heat flux distribution may be resolved by either the conservation of energy or by the modified Fourier's law.

The finite integral transform technique [93], a generalized eigenfunction expansion method, is now utilized in determining the temperature distribution, $\theta(\eta,\xi)$. In our approach, we view the nonlinear contribution to the heat equation, as expressed in Eq. (5.3.1) as an effective heat source or nonhomogeneity. The associated eigenvalue problem is developed from considering the linear homogeneous version of Eqs. (5.3.1)-(5.3.3). The eigenvalue problem can be readily established as

$$\frac{d^2\psi_m}{d\eta^2} + \lambda_m^2 \psi_m(\eta) = 0 \quad , \tag{5.3.4}$$

subject to

$$\psi_m(0) = 0 \quad , \quad \frac{d\psi_m(\eta_o)}{d\eta} = 0 \quad . \tag{5.3.5a,b}$$

The solution to this problem gives the eigenfunctions

$$\psi_m(\eta) = \sin\lambda_m\eta \tag{5.3.6a}$$

where the eigenvalues are

$$\lambda_m = \frac{(2m - 1)\,\pi}{2\eta_o} \quad , \; m = 1, 2, \ldots \tag{5.3.6b}$$

The orthogonality relation for the eigenfunctions are

$$\int_{\eta=0}^{\eta_o} \psi_m(\eta)\, \psi_n(\eta)\, d\eta = \begin{cases} 0 & , \ m \neq n \\ N(\lambda_m) & , \ m = n \end{cases} , \tag{5.3.7a}$$

where $N(\lambda_m)$ is the normalization integral given by

$$N(\lambda_m) = \frac{\eta_o}{2} . \tag{5.3.7b}$$

Using the orthogonality relation, we can develop the integral transform pair as

Inversion Formula:

$$\theta(\eta,\xi) = \sum_{m=1}^{\infty} \frac{\psi_m(\eta)}{N(\lambda_m)}\, \bar{\theta}_m(\xi) \tag{5.3.8a}$$

Integral Transform:

$$\bar{\theta}_m(\xi) = \int_{\eta=0}^{\eta_o} \psi_m(\eta)\, \theta(\eta,\xi)\, d\eta \quad . \tag{5.3.8b}$$

We now remove all spatial dependence analytically from our original nonlinear dimensionless temperature field equation. We operate on Eq. (5.3.1) with

$$\int_{\eta=0}^{\eta_o} \psi_m(\eta)\, d\eta \tag{5.3.9}$$

to obtain

$$\int_{\eta=0}^{\eta_o} M_0[\theta(\eta,\xi)]\ \psi_m(\eta)\ d\eta = -\frac{\beta_1^*}{2} \int_{\eta=0}^{\eta_o} \frac{\partial^2}{\partial\eta^2}[\theta^2(\eta,\xi)]\ \psi_m(\eta)\ d\eta\ . \qquad (5.3.10)$$

Integrating Eq. (5.3.10) by parts and using the boundary conditions, as expressed in Eqs. (5.3.2) and (5.3.5), and finally using the definition of the integral transform as expressed in Eq. (5.3.8b) we obtain the following ordinary differential equation

$$\frac{d^2\bar{\theta}_m(\xi)}{d\xi^2} + 2\frac{d\bar{\theta}_m(\xi)}{d\xi} + \lambda_m^2\,\bar{\theta}_m(\xi) = \psi_m'(0)\ [1 + \frac{\beta_1^*}{2}] - \frac{\beta_1^*}{2}\lambda_m^2 \int_{\eta=0}^{\eta_o} \psi_m(\eta)\ \theta^2(\eta,\xi)\ d\eta\ , \qquad (5.3.11a)$$

$$m = 1, 2, \ldots$$

We now substitute the inversion formula Eq. (5.3.8a) with a new dummy index $\ell$ into Eq. (5.3.11a) to get the system of nonlinear initial value problems

$$\frac{d^2\bar{\theta}_m(\xi)}{d\xi^2} + 2\frac{d\bar{\theta}_m(\xi)}{d\xi} + \lambda_m^2\,\bar{\theta}_m(\xi) = \psi_m'(0)\cdot[1 + \frac{\beta_1^*}{2}] - \frac{\lambda_m^2\,\beta_1^*}{2} \int_{\eta=0}^{\eta_o} \psi_m(\eta)\ [\sum_{\ell=1}^{\infty} \frac{\psi_\ell(\eta)\bar{\theta}_\ell(\xi)}{N(\lambda_\ell)}]^2\ d\eta\ , \qquad (5.3.11b)$$

subject to the transformed initial condition

$$\bar{\theta}_m(0) = 0\ , \qquad (5.3.12a)$$

$$\frac{d\bar{\theta}_m(0)}{d\xi} = 0 \ , \ m = 1,2,... \qquad (5.3.12b)$$

At this point, we convert Eq. (5.3.11b) and (5.3.12a,b) into an equivalent system of nonlinear Volterra integral equations of the second kind. This conversion permits us to take advantage of the exact analytic solution for the linear case ($\beta_1^* = 0$) in a general purpose computer program. In other words, the equivalent integral equation automatically accommodates for the exact linear solution when $\beta_1^* = 0$. Using the Laplace transform and incorporating convolution, we arrive at

$$\bar{\theta}_m(\xi) = \frac{\left(1 + \frac{\beta_1^*}{2}\right)}{\lambda_m} \cdot \left[1 - e^{-\xi}\left(\frac{\sin\sqrt{\lambda_m^2 - 1}\ \xi}{\sqrt{\lambda_m^2 - 1}} + \cos\sqrt{\lambda_m^2 - 1}\ \xi\right)\right]$$

(5.3.13a)

$$- \frac{\lambda_m^2 \beta_1^*}{2} \int_{\xi_o=0}^{\xi} \frac{e^{-(\xi-\xi_o)} \sin\sqrt{\lambda_m^2 - 1}(\xi-\xi_o)}{\sqrt{\lambda_m^2 - 1}} \sum_{\ell=1}^{\infty} \frac{\bar{\theta}_\ell(\xi_o)}{N(\lambda_\ell)} \cdot \sum_{k=1}^{\infty} \frac{A_{m\ell k}\bar{\theta}_k(\xi_o)d\xi_o}{N(\lambda_k)} \ ,$$

$$m = 1, 2, \ldots$$

where $A_{m\ell k}$ is defined as

$$A_{m\ell k} \equiv \int_{\eta=0}^{\eta_o} \psi_m(\eta)\ \psi_\ell(\eta)\ \psi_k(\eta)\ d\eta \ . \qquad (5.3.13b)$$

First, we notice that when $\beta_1^* = 0$, Eq. (5.3.13a) reduces to the exact analytic solution for the transform. Second, the sums have formally been expanded explicity and the constants $A_{m\ell k}$ have been introduced.

The $A_{m\ell k}$'s can be evaluated analytically using the eigenvalue problem, as given by Eqs. (5.3.4) and (5.3.5) in a similar manner as one obtains the orthogonality relation (see Appendix 6). Since $A_{m\ell k}$ can be resolved analytically, we have reduced the dimensionality of the original field equation by one independent variable before employing any numerical approximations. It should be mentioned that the numerical evaluation of $A_{m\ell k}$ may be performed very accurately if one notes the oscillatory nature of the integrand. In either case, we have removed the necessity of incorporating any finite difference scheme (which generally associates a lower truncation error). Once the integral transforms have been resolved numerically, all the ingredients for the exact analytical representation for the temperature distribution are available.

The 'kernel' of the integral equation, as expressed in Eq. (5.3.13a) is degenerate or separable. We came across a similar kernel in Chapter 4, although without the exponential portion which came about from the damping term.

The kernel can be written as a finite sum of products of two linearly independent functions in the form

$$K(\xi,\xi_o;\ \lambda_m) = e^{-(\xi-\xi_o)}\sin\sqrt{\lambda_m^2 - 1}\ (\xi-\xi_o) = \sum_{j=1}^{2} a_j(\lambda_m,\xi)b_j(\lambda_m,\xi)\ , \tag{5.3.14}$$

where we choose the following

$$a_1(\lambda_m,\xi) = e^{-\xi}\sin\sqrt{\lambda_m^2 - 1}\ \xi \quad , \quad a_2(\lambda_m,\xi) = -e^{-\xi}\cos\sqrt{\lambda_m^2 - 1}\ \xi\ ,$$

(5.3.15a-d)

$$b_1(\lambda_m,\xi_o) = e^{\xi_o}\cos\sqrt{\lambda_m^2 - 1}\,\xi_o \quad , \quad b_2(\lambda_m,\xi_o) = e^{\xi_o}\sin\sqrt{\lambda_m^2 - 1}\,\xi_o \ .$$

The method of Bownds [144,145,150-152] can again be utilized in obtaining an exact analytical form for resolving the integral transforms, $\bar{\theta}_m(\xi)$. As mentioned in Chapter 4, this procedure introduces a new smoother variable which is resolved numerically, then the integral transform may be reconstructed. We substitute the functional form of the kernel expressed in Eq. (5.3.14) into Eq. (5.3.13a) to get

$$\bar{\theta}_m(\xi) = G_m(\xi) - \frac{\lambda_m^2\beta_1^*}{2\sqrt{\lambda_m^2 - 1}} \sum_{j=1}^{2} a_j(\lambda_m,\xi)c_j(\lambda_m,\xi) \ , \qquad (5.3.16a)$$

where

$$c_j(\lambda_m,\xi) = \int_{\xi_o=0}^{\xi} b_j(\lambda_m,\xi_o)\Big[\sum_{\ell=1}^{\infty}\frac{\bar{\theta}_\ell(\xi_o)}{N(\lambda_m)} \cdot \sum_{k=1}^{\infty}\frac{A_{m\ell k}\bar{\theta}_k(\xi_o)}{N(\lambda_m)}\Big]d\xi_o \ , \qquad (5.3.16b)$$

and

$$\bar{G}_m(\xi) = \frac{\left(1 + \frac{\beta_1^*}{2}\right)}{\lambda_m}\left\{1 - e^{-\xi}\left(\frac{\sin\sqrt{\lambda_m^2 - 1}\,\xi}{\sqrt{\lambda_m^2 - 1}} + \cos\sqrt{\lambda_m^2 - 1}\,\xi\right)\right\} \ , \qquad (5.3.16c)$$

$$m = 1,2,\ldots$$

Once the $c_j(\lambda_m,\xi)$ functions have been resolved numerically, the integral transform $\bar{\theta}_m(\xi)$ is known, as shown in Eq. (5.3.16a). We next construct a system of equations, in the $c_j(\lambda_m,\xi)$ variable, to be solved numerically. To this end, we differentiate Eq. (5.3.16b) and substitute Eq. (5.3.16a) into the result to get

$$\frac{dc_j(\lambda_m,\xi)}{d\xi} = \sum_{\ell=1}^{\infty} \frac{1}{N(\lambda_\ell)} \{G_\ell(\xi) - \frac{\lambda_\ell^2 \beta_1^*}{2\sqrt{\lambda_\ell^2 - 1}} \sum_{i=1}^{2} a_i(\lambda_\ell,\xi) c_i(\lambda_\ell,\xi)\} \cdot$$

(5.3.17a)

$$\sum_{k=1}^{\infty} \frac{A_{m\ell k}}{N(\lambda_k)} \{G_k(\xi) - \frac{\lambda_k^2 \beta_1^*}{2\sqrt{\lambda_k^2 - 1}} \sum_{n=1}^{2} a_n(\lambda_k,\xi) c_n(\lambda_k,\xi)\} \cdot b_j(\lambda_m,\xi) \ ,$$

$$j = 1,2,...$$

subject to the initial conditions

$$c_j(\lambda_m,0) = 0 \quad , \quad j = 1,2, \quad , \quad m = 1,2,... \qquad (5.3.17b)$$

The initial conditions can be developed by evaluating Eq. (5.3.16b) at $\xi = 0$ to obtain the trivial initial conditions. The problem is reduced to solving a set of initial value problems in $c_j(\lambda_m,\xi)$, $j = 1,2$, $m = 1,2,...$ Once these have been resolved, the transform can be obtained which in turn completes the temperature distribution.

## 5.4 Approximate Solution in Slab

In this section, we display some approximate results for the temperature distribution. From experience, we realize that it will take hundreds of terms of the infinite series describing $\theta(\eta,\xi)$ for convergence to 3-4 significant figures. Since the nonlinearity is $\theta^2(\eta,\xi)$, we will need approximately $O(mmax^3)$ operations, where mmax is the actual number of terms in the infinite series, at each $\Delta\xi$ time step. A supercomputer would be capable of performing these computations. However, we

may obtain a reasonably accurate solution by examining the various contributions to the series solution of the temperature $\theta(\eta,\xi)$. In this way, the computational task is minimal and may be performed on either a mini or conventional mainframe computer.

The lowest order approximation would be to let $\bar{\theta}_m(\xi) = G_m(\xi)$ in Eq. (5.3.16a) and the temperature distribution may then be calculated analytically. This solution would either raise or lower the temperatures uniformly about the linear solution ($\beta_1^* = 0$). A better procedure would be to investigate the terms in the system of equations for $C_j(\lambda_m,\xi)$.

An <u>approximate analytical</u> solution for the $c_j(\lambda_m,\xi)$ functions can be obtained by rewriting Eq. (5.3.17a) as

$$\frac{dc_j(\lambda_m,\xi)}{d\xi} = \int_{\eta=0}^{\eta_o} \psi_m(\eta) \sum_{\ell=1}^{\infty} \frac{\psi_\ell(\eta)G_\ell(\xi)}{N(\lambda_m)} \cdot \sum_{k=1}^{\infty} \frac{\psi_k(\eta)G_k(\xi)}{N(\lambda_m)} \cdot b_j(\lambda_m,\xi)d\eta \ ,$$

$$j = 1,2, \qquad (5.4.1)$$

where we have neglected the coupling in the $c_j$'s. The $G_\ell(\xi)$ and $G_k(\xi)$ terms represent $(1 + \beta_1^*/2)$ times the linear transform. The linear temperature distribution may be accurately described by a truncated Taylor series expansion in two variables (space, time) of the form

$$\theta_{LIN}(\eta,\xi) = 1 + (d_o + d_1\xi)\eta \ , \qquad 0 \leq \eta < \xi \leq \eta_o \qquad (5.4.2)$$

on the first pass. The coefficients $d_o$ and $d_1$ may be determined by various methods. Expressions similar to Eq. (5.4.2) may be developed on each pass in the medium. The $c_j(\lambda_m,\xi)$ functions are then readily avail-

able and $\overline{\theta}_m(\xi)$ may be reconstructed using Eq. (5.3.16a). In this procedure, we did not make use of $A_{m\ell k}$ for the hyperbolic solution; however, Frankel and Vick [165] developed the solution to the corresponding parabolic problem using $A_{m\ell k}$ to obtain exact numerical results. Using Eq. (5.4.1) to obtain the $c_j(\lambda_m,\xi)$ functions approximately provides understanding to the various contributions in Eq. (5.3.16).

Figure 5.4.1a displays the contrasting temperature distributions of the two heat conduction approximations where $\eta_o = 1$. The hyperbolic temperature distribution was obtained using the approximate procedure outlined in this section. The parabolic solution follows [165] in which an exact methodology, based on integral transforms, was developed. This methodology follows that of Chapter 5.3 and makes use of $A_{m\ell k}$ as defined in Eq. (5.3.13b) to obtain numerically exact values for the temperature distribution. The approximate hyperbolic solution displays the usual dissipative wave nature while the parabolic solution displays the usual continuous distribution. It is apparent that the approximate analytical solution for hyperbolic heat conduction produces some error in predicting the correct location of the wavefront since the wave speed c must change in accordance to Eq. (5.1.3). We may determine the degree of error in the front location and temperatures by comparing our results to a purely numerical scheme. Glass, Ozisik, and Vick [74] have addressed this particular problem using the McCormick's predictor-corrector method and we shall make use of their results.

Figure 5.4.1b displays the approximate analytical solution and the purely numerical solution of [74]. Using the simple approach proposed here, the temperatures match to three significant figures behind the

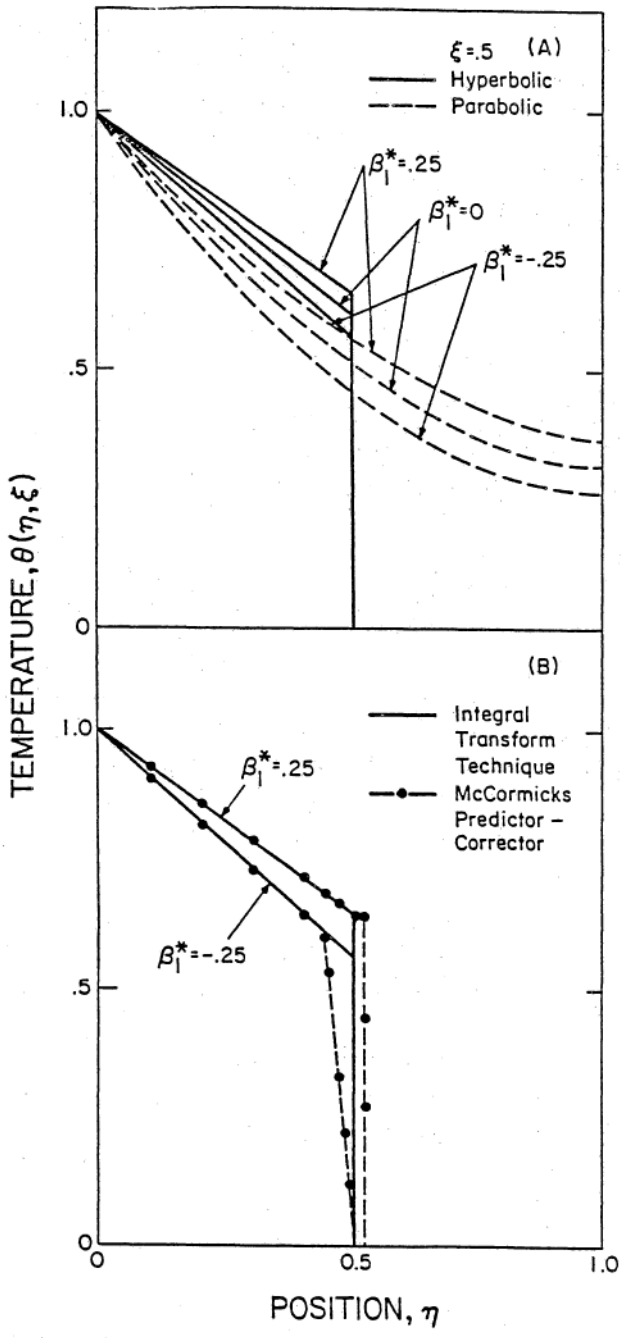


Figure 5.4.1 Comparison of Hyperbolic and Parabolic Temperature Distributions for k(T).

wavefront. However, in the neighborhood of the discontinuity, McCormick's method must predict more accurate results and indeed predicts the correct physical response for $\pm\beta_1^*$. We can venture to say that the contribution of coupling the $c_j$ functions, as shown in Eq. (5.3.17a) is extremely important in predicting the location of the wave front. However, by uncoupling the system, we still obtain an accurate account of the temperature away from the front.

Another point is that the approximate analytical solution developed here may be integrated and differentiated analytically since a functional form of the temperature solution is present. The series representation for the temperature also permits direct parametric relationships to be studied.

## 5.5 Conclusions

Though the results presented in this chapter do not yield exact values of the temperature, it does provide additional insight to the nature of the solution based on integral transforms. The methodology for constructing an exact representation for the temperature distribution in terms of an infinite series has produced exact numerical results [165] in parabolic equations. Since hyperbolic solutions require so many terms, it appears that a slight modification in this approach is warranted.

An integral equation approach which may yield accurate results is now being considered by the author. This method is based on a direct conversion of the original partial differential equation, Eq. (5.3.1), to

$$\theta(\eta,\xi) = M_0^{-1}\left[-\frac{\beta_1^*}{2}\frac{\partial^2}{\partial\eta^2}\theta^2(\eta,\xi)\right] , \tag{5.5.1}$$

where $M_0^{-1}$ is the inverse operator associated with the differential operator $M_o$. The inverse operator $M^{-1}_0$ is the integral operator whose kernel will be Green's function associated with the linear operator $M_o$, i.e.

$$\theta(\eta,\xi) = \int_{\xi_o=0}^{\xi} G_{\eta_o}(\eta,\xi/0,\xi_o)d\xi_o$$

$$- \frac{\beta_1^*}{2}\int_{\xi_o=0}^{\xi}\int_{\eta_o=0}^{1} G(\eta,\xi/\eta_o,\xi_o)\frac{\partial^2}{\partial\eta_o^2}[\theta^2(\eta_o,\xi_o)]d\eta_o d\xi_o , \tag{5.5.2a}$$

$$\eta\varepsilon[0,1] , \xi \geq 0 ,$$

where

$$G(\eta,\xi/\eta_o,\xi_o) = \sum_{m=1}^{\infty}\frac{\psi_m(\eta)\psi_m(\eta_o)}{N(\lambda_m)\sqrt{\lambda_m^2-1}}\cdot e^{-(\xi-\xi_o)}\sin\sqrt{\lambda_m^2-1}\,(\xi-\xi_o) ,$$

$$\xi > \xi_o , \tag{5.5.2b}$$

which is the equivalent integral equation for Eqs. (5.3.1)-(5.3.3). The eigenfunctions $\psi_m(\eta)$, eigenvalues $\lambda_m$, and normalization integrals $N(\lambda_m)$ are the same as defined in Section 5.3.

The two-dimensional nonlinear integral equation may be resolved by various block-by-block methods. The bilinear series representation for

the Green's function may be accelerated using the Kummers transform [95,103]. The number of terms required for convergence drops radically to that of an equivalent parabolic system. This approach and others are presently under investigation by the author.

Finally, though this approach provides only discrete values of temperature in space and time, it may be a better solution method than the standard numerical schemes which discretize the governing partial differential equations immediately.

# Chapter 6

# SUMMARY AND RECOMMENDATIONS

## 6.1 Summary

This dissertation addressed various theoretical aspects concerning hyperbolic heat conduction as developed through the modified Fourier's law. A unified approach has been undertaken in order to systematically address the basic physics and mathematical aspects associated with hyperbolic systems. The unusual and controversial features attributed to hyperbolic heat conduction have been demonstrated through numerous examples with various thermal sources and configurations.

Chapter 2 began by clarifying the relationships between temperature and heat flux in heat conduction. The general linear temperature and flux formulations for the three standard orthogonal coordinate systems were developed. Taitel's problem was revisited to introduce the basic physics and mathematics associated with hyperbolic heat conduction. The controversial behavior of linear hyperbolic heat conduction in radially dependent geometries was then investigated where the general temperature distribution was developed by the finite integral transform technique. Once the temperature distribution had been established, the flux distribution was resolved from the modified Fourier's law. Examples were presented for various thermal disturbances in a solid cylinder and sphere. These examples clearly showed that linear one-dimensional hyperbolic heat conduction predicts temperature singularities as a wave front approaches the center of a cylindrical or spherical region. These singularities occur as a result of a wave of finite energy content

packing into a region of zero volume. The utility of the flux formulation and the unusual nature of heat conduction based on the hyperbolic formulation are demonstrated by developing analytical expressions for the heat flux and temperature distributions in a finite slab exposed to a pulsed surface heat flux.

In light of some recent experimental results showing the existence of reflections of thermal waves at the interface of dissimilar materials in superfluid helium, a theoretical investigation of thermal waves in composite media was necessary to provide a theoretical foundation to the observed phenomenon. In Chapter 3, the general one-dimensional temperature and heat flux formulation for hyperbolic heat conduction in a composite medium was presented. Also, the general solution, based on the flux formulation, was developed for the standard three orthogonal coordinate systems. Unlike classical parabolic heat conduction, heat conduction based on the modified Fourier's law produces nonseparable field equations for both the temperature and flux. Therefore standard analytical techniques cannot be applied in these situations. A generalized finite integral transform technique was proposed in the flux domain and a general solution was developed for the standard three orthogonal coordinate systems. This technique led to an infinite set of coupled initial value problems in the transform variable. The set of ordinary differential equations was then transformed into an equivalent set of linear Volterra integral equations of the second kind with degenerate kernels. These integral equations are more amenable to numerical approximation than the original differential equation. The method of Bownds was incorporated to determine the transforms numerically. The

flux and temperature distributions were then determined uniquely. Two examples were presented to display the unusual and controversial nature associated with heat conduction based on the modified Fourier's law in composite regions.

Chapter 5 considered the problem of temperature dependent thermal conductivity in hyperbolic heat conduction. Unlike previous works with variable thermal conductivity, a generalized expression in terms of a Taylor series expansion about a reference temperature was developed. Using this expression, in conjunction with the modified Fourier's law, produced a new nonlinear hyperbolic temperature field equation for the three standard orthogonal coordinate systems. An approximate analytical solution, based on the integral transform technique, was applied to a slab problem. The contribution of the various terms in the solution of the temperature distribution was studied.

## 6.2 Recommendations

Recommendations concerning areas requiring further examination and clarification are now presented.

Taitel [26] and Van Kampen [28] felt that higher order approximations in the hierarchy of field equations [16] should be investigated. These approximations will contain higher derivatives in space and time in the governing temperature field equation. Additional boundary and initial conditions must be constructed to complete the mathematical formulation. This problem needs to be addressed to verify at what point one may truncate the temperature field equation without losing any important information.

Experimental verification of focusing in radially dependent systems and accurate measurements of the relaxation times $\tau$ must be sought. The effects of temperature dependent properties on radial dependent systems should be studied to see in what circumstances focusing is inhibited or promoted. Also, the neighborhood about the origin must be clarified in the cylindrical and spherical geometries since temperature singularities are predicted. Should one abandon the continuum in the vicinity of the origin and connect a microscopic theory when approaching a few mean free radii of the origin?

New approximate analytical and purely numerical schemes should be developed which may accurately predict the temperature and flux distributions. An integral equation approach, as proposed at the end of Chapter 5, may lead to an accurate numerical scheme as an alternative to standard numerical schemes based on differential equations.

REFERENCES


1. Arpaci, V., Conduction Heat Transfer, Addison-Wesley, California, 1966.

2. Kao, Tsai-tse, "On Thermally Induced Non-Fourier Stress Waves in a Semi-Infinite Medium," AIAA Journal, Vol. 14, #6, 818-820, 1976.

3. Kaliski, S., "Wave Equation of Heat Conduction," Bulletin De L'Academie Polonaise Des Sciences: Serie des sciences techniques, Vol. 13, #4, 211-219, 1965.

4. Maxwell, J. C., "On the Dynamical Theory of Gases," Philosophical Transactions of the Royal Society of London, Vol. 157, 49-88, 1867.

5. Vernotte, M. P., "la veritable equation de la chateur," Comptes Rendus, Vol. 247, 2103-2105, 1958

6. Vernotte, M. P., Les Paradoxes de la theorie continue de l'equation de la chaleur," Comptes Rendus, Vol. 246, 3154-3155, 1958.

7. Vernotte, M. P., "Sur Quelques Complications Possibles Dans les Phenomenes de Conduction de la Chaleur," Comptes Rendus, Vol. 252, #15, 2190-2191, 1961.

8. Cattaneo, "Sur une forme de l'equation de la chaleur e'liminant le paradoxe d'une propagation instantanee ", Comptes Rendus, Vol. 246, 431-433, 1958.

9. Morse, P. M., and Feshbach, H., Methods of Theoretical Physics, I, McGraw-Hill, New York, 1953.

10. Tye, R. P. (ed.), Thermal Conductivity, Academic Press, N.Y., 1969.

11. Ulbrich, C. W., "Exact Electric Analogy to the Vernotte Hypothesis," Physical Review, Vol. 123, #6, 2001-2002, 1961.

12. Lumsdaine, E., "Thermal Resonance," Mechanical Engineering News, Vol. 9, #3, 34-37, 1972.

13. Luikov, A. V., "Applications of the Methods of Thermodynamics of Irreversible Processes to the Investigation of Heat and Mass Transfer," Journal of Engineering Physics, Vol. 9, #3, 189-202, 1965.

14. Kreith, F., Principles of Heat Transfer, 3rd ed., Harper and Row, N.Y., 1973.

15. Hughes, W. F., An Introduction to Viscous Flow, McGraw-Hill, N.Y., 1979.

16. Simons, S., "On the Differential Equation for Heat Conduction," Transport Theory and Statistical Physics, Vol. 2, 117-128, 1972.

17. Peshkov, V., "Second Sound in Helium II," Journal of Physics, Vol. VIII, #6, 381, 1944.

18. Peshkov, V., "Determination of the Velocity of Propagation of the Second Sound in Helium II," Report of an International Conference on Fundamental Particles and Low Temperatures (the Physical Society, London) 1947.

19. Atkin, R. J., N. Fox and M. W. Vasey, "A Continuum Approach to the Second Sound Effect," J. of Elasticity, Vol. 5, #3,4, 237-248, 1975

20. Ackerman, C. C., B. Bertman, H. A. Fairbank and R. A. Guyer, "Second Sound in Solid Helium," Physical Review Letters, Vol. 16, #18, 789-791, 1966

21. Chester, M., "Second Sound in Solids," Physical Reviews, Vol. 131, #5, 2013-2015, 1963.

22. Maurer, M. J., "Relaxation Model for Heat Conduction in Metals," Journal of Applied Physics, Vol. 40, #13, 5123-5130, 1969

23. Nettleton, R. E., "Relaxation Theory of Thermal Conduction in Liquids," Physics of Fluids, Vol. 3, #2, 216-225. 1960.

24. Luikov, A. V. Analytical Heat Diffusion Theory, Academic Press, New York, 1968.

25. Weyman, H. D., "Finite Speed of Propagation in Heat Conduction Diffusion, and Viscous Shear Motion," American Journal of Physics, Vol. 36, #6, 488-496, 1967.

26. Taitel, Yehuda, "On the Parabolic, Hyperbolic and Discrete Formulation of the Heat Conduction Equation," Int. J. Heat Mass Transfer, Vol. 15, 369-371, 1972.

27. Temkin, A. G., "Discrete Formulation of Heat Conduction and Diffusion Equations," Int. J. Heat and Mass Transfer, Vol. 19, 785-789, 1976.

28. Van Kampen, N. G., "A Model for Relativistic Heat Transport," Physica, Vol. 46, 315-332, 1970.

29. Kelly, D. C., "Diffusion: A Relativistic Appraisal," American Journal of Physics, Vol. 36, #7, 585-591, 1968.

30. Bubnov, V. A., "Wave Concepts in the Theory of Heat," Int. J. Heat Mass Transfer, Vol. 19, 175-184, 1976.

31. Berkovsky, B. M., and V. G. Bashtovoi, "The Finite Velocity of Heat Propagation from the View Point of Kinetic Theory," Int. J. Heat Mass Transfer, Vol. 20, 621-626, 1977.

32. Chernyshov, A. D. "Theory of Thermal Conduction When the Rate of Heat Propagation is Finite," Journal of Engineering Physics, Vol. 28, #3, 387-391, 1975.

33. Domanski, R., "Establishing Application Limits for Classical Fourier and Wave Heat Conduction Equations for Metals on the Basis of Analytical Solution and Calculated Temperature Distribution in Case of Giant Heat Pulse," 6th International Heat Transfer Conference, Toronto, Ont., Aug. 7-11, 1978.

34. Gurtin, M. E. and A. C. Pipkin, "A General Theory of Conduction with Finite Wave Speeds," Arch. Rational Mech. Anal., Vol. 31, 113-126, 1968.

35. Amos, D. E., and P. J. Chen, "Transient Heat Conduction with Finite Wave Speeds," Journal of Applied Mechanics, Vol. 37, Dec. 1145-1146, 1970.

36. Maccamy, R. C., "An Integro-Differential Equation with Application in Heat Flow," Quarterly of Applied Mathematics, Vol. 35, #1, 1-19, 1977.

37. Coleman, B. D., and V. J. Mizel, "Thermodynamics and Departures from Fourier's Law of Heat Conduction," Arch. Rational Mech. Anal., Vol. 13, 245-261, 1963.

38. Coleman, B. D., and M. E. Gurtin, " On the Growth and Decay of One-Dimensional Acceleration Waves," Arch. Rational Mech. Anal., Vol. 19, 1965, 239-265.

39. Hermann, R. P. and R. R. Nachlinger, "On Uniqueness and Wave Propagation in Nonlinear Heat Conductors with Memory," Journal of Mathematical Analysis and Applications, Vol. 50, 530-547, 1975.

40. Chen, P. J., and M. E. Gurtin, "On Second Sound in Materials with Memory," ZAMP, Vol. 21, 1970, 232-241.

41. Chen, P. J., "On the Growth and Decay of Temeprature Rate Waves of Arbitrary Form," ZAMP, Vol. 20, 448-453, 1969.

42. Norwood, F. R., "Transient Thermal Waves in the General Theory of Heat Conduction with Finite Wave Speeds," Journal of Applied Mechanics, Vol. 94, 673-676, 1972.

43. Norwood, F. R., "A Note on Heat Conduction with Memory," Journal of Applied Mechanics, Vol. 95, 1124-1125, 1973.

44. Nunziato, J. W., "On Heat Conduction in Materials with Memory," Quarterly of Applied Mathematics, Vol. 29, 187-204, 1971.

45. Lindsay, K. A., and B. Straughan, "Temperature Waves in a Rigid Heat Conductor," Journal of Applied Mathematics and Physics, (ZAMP), Vol. 27, 653-662, 1976.

46. Lord, H. W. and Y. Shulman, "A Generalized Dynamical Theory of Thermoelasticity," Journal Mech. Phys. Solids, Vol. 15, 299-309, 1967.

47. Kaliski, S., "Wave Equations of Thermoelasticity," Bulletin De L'Academie Plolnaise Des Sciences:Serie des sciences techniques, Vol. 13, #5, 253-260, 1965.

48. Maccamy, R. C., "A Model for One Dimensional, Nonlinear Viscoelasticity," Quarterly of Applied Mathematics, 21-33, 1977.

49. Lockett, F. J., "Effect of Thermal Properties of a Solid on Velocity of Rayleigh Waves," J. of the Mechanics and Physics of Solids, Vol. 7, 71-75, 1958.

50. Chadwick, P. and I. N. Sneddon, "Plane Waves in an Elastic Conducting Heat," Journal of Mechanics and Physics of Solids, Vol. 6, 223-230, 1958.

51. Puri, Pratrap, "Plane Waves in Generalized Thermoelasticity," Int. J. Eng. Sci., Vol. 11, 735-744, 1973.

52. Polov, E. B., "Dynamic Coupled Problem of Thermoelasticity for Half-Space Taking Account the Finiteness of the Heat Propagation Velocity," J. of Applied Mathematics and Mechanics, Vol. 31, 349-356, 1967.

53. Nayfeh, A. and S., Nemat-Nasser, "Thermoelastic Waves in Solids with Thermal Relaxation," Acta Mechanica, Vol. 12, 53-69, 1971.

54. Achenback, J. D., "The Influence of Heat Conduction on Propagating Stress Jumps," J. Mech. Phys. Solids, Vol. 16, 273-282, 1968.

55. Ivanov, T. and Y. K. Engel'brekht, "Thermoelasticity Models Taking Account of a Finite Heat Propagation Rate," Journal of Engineering Physics, Vol. 35, #2, 986-991, 1978.

56. Batra, R. C., "On Heat Conduction and Wave Propagation in Non-Simple Rigid Solids," Letters in Applied and Engineering Sciences, Vol. 3, 97-107, 1975.

57. Shashov, A. G. and S. Yu. Yarovskii, "Structure of Unidimensional Temperature Stresses," J. Eng. Physics, Vol. 33, #5, 1363-1369, 1977.

58. Koninski, W., and K. Szmit, "On Waves in Elastic Materials at Low Temperatures, I. Hyperbolicity in Thermoelasticity," Bulletin de L'Academie Plolnaise Des Sciences:Serie des Sciences techniques, Vol. 25, 17-31, 1977.

59. Boley, B. A., and J. H. Weiner, Theory of Thermal Stresses, John Wiley & Sons, Inc., New York, 1960.

60. Baumeister, K. J. and T. D. Hamill, "Hyperbolic Heat Conduction Equation - A Solution for the Semi-Infinite Body Problem," J. of Heat Transfer, Vol. 91, 543-548, 1969.

61. Baumeister, K. J. and T. D. Hamill, "Hyperbolic Heat Conduction Equation - A Solution for the Semi-Infinite Body Problem," J. of Heat Transfer, Vol. 93, 126-127, 1971.

62. Brazel, J. P. and E. J. Nolan, "Non-Fourier Effects in the Transmission of Heat," Conf. On Thermal Conductivity (6th), 238-254, Oct. 1966.

63. Maurer, M. J. and H. A. Thompson, "Non-Fourier Effects at High Heat Flux," Journal of Heat Transfer, Vol. 95, 284-286, May 1973.

64. Chan, S. H., J. D. Low and W. K. Mueller, "Hyperbolic Heat Conduction in Catalytic Supported Crystallites," AIChE, Vol. 17, #6, 1499-1501, Nov. 1971.

65. Lorenzini, E., and M. Spiga, "Temperature in Heat Generating Solids with Memory," Warme-und Stoffubertragung, Vol. 16, 113-118, 1982.

66. Vick, B., and M. N. Ozisik, "Growth and Decay of a Thermal Pulse Predicted by the Hyperbolic Heat Conduction Equation," Journal of Heat Transfer, Vol. 105, 902-907, 1983.

67. Ozisik, M. N., and B. Vick, "Propagation and Reflection of Thermal Waves in a Finite Medium," Int. J. Heat Mass Transfer, Vol. 27, #10, 1845-1854, 1984.

68. Kao, Tsai-tse, "Non-Fourier Heat Conduction in Thin Surface Layers," Journal of Heat Transfer, Vol. 99, 343-345, May 1977.

69. Anderson, D. A., J. C. Tannehill, and R. H. Pletcher, Computational Fluid Mechanics and Heat Transfer, Hemisphere, New York, 1984.

70. Warren, M. D., "Calculation of the Reflected Wave from a Pipe with a Nozzle End by the Lax-Wendroff Method," J. Heat and Fluid Flow, Vol. 6, #3, 205-211, 1985.

71. Harten, A., and H. Tal-Ezer, "On a Fourth Order Accurate Implicit Finite Difference Scheme for Hyperbolic Conservation Laws II: Five Point Schemes," J. of Comp. Phys., Vol. 41, 329-356, 1981.

72. Glass, D. E., M. N. Ozisik, D. S. McRae, And B. Vick, "On the Numerical Solution of Hyperbolic Heat Conduction," Numerical Heat Transfer, Vol. 8, #4, 497-504, 1985.

73. Glass, D. E., M. N. Ozisik, and B. Vick, "Hyperbolic Heat Conduction with Surface Radiation," Int. J. Heat Mass Transfer, Vol. 28, #10, 1823-1830, 1985.

74. Glass, D. E., M. N. Ozisik, and B. Vick, "Hyperbolic Heat Conduction with Temperature Dependent Thermal Conductivity," (accepted in J. Applied Physics)

75. Wiggert, D. C., "Analysis of Early-Time Transient Heat Conduction by Method of Characteristics," J. of Heat Transfer, Vol. 99, 35-40, Feb. 1977.

76. Carey, G. F. and M. Tsai, "Hyperbolic Heat Transfer with Reflection," Numerical Heat Transfer, Vol. 5, 309-327, 1982.

77. Finkel'shtein, A. V, "Solution of the Hyperbolic Heat-Conduction Equation by Expansion in a Small Parameter," J. of Eng. Phys., Vol. 44, #5, 555-559, 1983.

78. Shablovskii, O. N., "A Study of Temperature Waves Based on the Generalized Heat-Transfer Equation," Journal of Engineering Physics, Vol. 40, #2, 218-223, 1979.

79. Shablovskii, O. N., "Analytic Solutions of Parabolic and Hyperbolic Heat-Transfer Equations for Nonlinear Media," Journal of Engineering Physics, Vol. 40, #3, 319-324, 1981.

80. Bubnov, V. A., "Remarks on Wave Solutions of the Nonlinear Heat-Conduction Equation," Journal of Engineering Physics, Vol. 40, #5, p. 565-571, 1981.

81. Sadd, M. H. and J. E. Didlake, "Non-Fourier Melting of a Semi-Infinite Solid," Journal of Heat Transfer, Vol. 99, 25-28, 1981.

82. deScocio, L. M. and G. Gualtieri, "A Hyperbolic Stefan Problem," Quarterly of Applied Mathematics, 253-259, 1983.

83. Solomon, A. D., V. Alexiades, D. G. Wilson, and J. Drake, "The Formulation of a Hyperbolic Stefan Problem," (in press).

84. Novikov, N. A., "Hyperbolic Equation of Thermal Conductivity, Solution of the Direct and Inverse Problems for a Semiinfinite Rod," Journal of Engineering Physics, Vol. 35, #4, 1253-1257, 1978.

85. Novikov, N. A., "Solution of the Linear One-Dimensional Inverse Heat-Conduction Problems on the Basis of a Hyperbolic Equation," Journal of Engineering Physics, Vol. 40, #6, 668-671, 1980.

86. Ackerman, C. C. and R. A. Guyer, "Temperature Pulses in Dielectric Solids," Annals of Physics, Vol. 50, 128-185, 1968.

87. Bertman, B. and D. J. Sandiford, "Second Sound in Solid Helium," Scientific American, Vol. 222, #5, 92-101, 1970.

88. Ward, J. C. and J. Wilkes, "The Velocity of Second Sound in Liquid Helium near Absolute Zero," Phil. Mag., Vol. 42, 314-317, 1951.

89. Bertman, B. and R. A. Guyer, "Solid Helium," Scientific American, 84-101, Aug. 1967.

90. Enz, C. P., "One-Particle Densities, Thermal Propagation and Second Sound in Dielectric Crystals," Annals of Physics, Vol. 46, 114-173, 1968.

91. Torczynski, J. R., "On the Interaction of Second Shock Waves and Vorticity in Superfluid Helium," Phys. Fluids, Vol. 27, #11, 2636-2644, 1984.

92. Torczynski, J. R., D. Gerthsen, and T. Roesgen, "Schlieren Photography of Second-Sound Shock Waves in Superfluid Helium," Phys. Fluids, Vol. 27, #10, 2418-2423, 1984.

93. Ozisik, M. N., Heat Conduction, Wiley, New York, 1980.

94. Frankel, J. I., B. Vick, and M. N. Ozisik, "Propagation of Thermal Waves in Radial Systems," (to be submitted).

95. Frankel, J., B. Vick, and M. N. Ozisik, "Flux Formulation of Hyperbolic Heat Conduction," J. Appl. Physics, Vol. 58, #9, 3340-3345, 1985.

96. Wheelon, A. D., Tables of Summable Series and Integrals Involving Bessel Functions, Holden-Day, San Francisco, 1968.

97. Schwatt, I. J., An Introduction to the Operations with Series, 2nd. Chelsea Publ., New York, 1962.

98. Markushevich, A. I., Infinite Series, D. C. Heath Co., Boston, 1967.

99. Mathews, J., and R. L. Walker, Mathematical Methods of Physics, 2nd ed., Benjamin/Cummings Publ. Co., London, 1970.

100. Carrier, G. F., M. Krook, and C. E. Pearson, Functions of a Complex Variable, McGraw-Hill, New York, 310-312, 1966.

101. Shanks, D., "Nonlinear Transformations of Divergent and Slowly Convergent Sequences," J. Math. Phys., Vol. 34, 1-42, 1955.

102. Bromwich, T. J., An Introduction to the Theory of Infinite Series, Macmillan and Co., London, 1931.

103. Knopp, K. K., Infinite Sequences and Series, Dover, New York, 1956.

104. Mangulis, V., Handbook of Series for Scientists and Engineers, Academic Press, New York, 1965.

105. Jolley, L. B. W., Summation of Series, Dover, New York, 1961.

106. Hansen, E. R., A Table of Series and Products, Prentice-Hall Inc., Englewood Cliffs, N.J., 1975.

107. Perry, R. W., and A. Kantrowitz, "The Production and Stability of Converging Shock Waves," J. Appl. Physics, Vol. 22, #7, 8787-886, 1959.

108. Chisnell, R. F., "The Motion of a Shock Wave in a Channel, with Applications to Cylindrical and Spherical Shock Waves," J. Fluid Mech., Vol. 2, 286-298, 1957.

109. Payne, R. B., "A Numerical Method for a Converging Cylindrical Shock," J. Fluid Mech., Vol. 2, 185-200, 1957.

110. Abarbanel, S., and M. Goldberg, "Numerical Solution of Quasi-Conservative Hyperbolic Systems - The Cylindrical Shock Problem," J. Comp. Physics, Vol. 10, 1-21, 1972.

111. Bers, L., F. John, M. Schecter, Partial Differential Equations, Wiley & Sons, Inc. New York, 1974.

112. Greenberg, M. D., Application of Green's Functions in Science and Engineering, Prentice-Hall Inc., New Jersey, 1971.

113. Roach, G. F., Green's Functions, 2nd ed., Cambridge University Press, London, 1982.

114. Hildebrand, F. B., Advanced Calculus for Applications, 2nd ed., Prentice Hall, New Jersey, 1976.

115. Bellman, R., and G. Adomian, Partial Differential Equations, D. Reidel Publishing Co., Boston, 1983.

116. Brysk, H., "Determinantal Solution of the Fredholm Equation with Green's Function Kernel," J. Math. Phys., Vol. 4, #12, 1536-1538, 1963.

117. Brysk, H., "Fredholm Equations and Green's Functions," Transport Theory and Statistical Physics, Vol. 4, #2, 87-95, 1975.

118. Beck, J. V., "Green's Function Solution for Transient Heat Conduction Problems," Int. J. Heat Mass Transfer, Vol. 27, #8, 1235-1244, 1984.

119. Beck, J. V., and N. R. Keltner, "Green's Function Partitioning Procedure Applied to Foil Heat Flux Gages," ASME, paper #85-ht-56.

120. Beck, J. V., "Transient Temperatures in a Semi-Infinite Cylinder heated by a Disk Heat Source," Int. J. Heat Mass Transfer, Vol. 24, #10, 1631-1640, 1981.

121. Patera, A. T., "A Finite-Element/Green's Function Embedding Technique Applied to One-Dimensional Change-of-Phase Heat Transfer," Numerical Heat Transfer, Vol. 7, 241-147, 1984.

122. Chuang, Y. K., and J. Szekely, "On the Use of Green's Functions for Solving Melting of Solidification Problems," Int. J. Heat Mass Transfer, Vol. 14, 1285-1294, 1971.

123. Chuang, Y. K., and J. Szekely, "The Use of Green's Functions for Solving Melting or Solidification Problems in the Cylindrical Coordinate System," Int. J. Heat Mass Transfer, Vol. 15, 1171-1174, 1972.

124. Budhia, H., and F. Kreith, "Heat Transfer with Melting or Freezing in a Wedge," Int. J. Heat Mass Transfer, Vol. 16, 195-211, 1973.

125. Baker-Jarvis, James, and R. Inguva, "Heat Conduction in Layered, Composite Materials, J. Appl. Phys., Vol. 57, #5, 1569-1573, 1985.

126. Feijoo, L., H. T. Davis, and D. Ramkrishna, "Heat Transfer in Composite Solids with Heat Generation," J. Heat Transfer, Vol. 101, 137-143, 1979.

127. Huang, S. C., and Y. P. Chang, "Heat Conduction in Unsteady, Periodic and Steady States in Laminated Composites," J. of Heat Transfer, Vol. 102, 742-748, 1980.

128. Chang, Y. P., C. S. Kang, and D. J. Chen, "The Use of Fundamental Green's Functions for the Solution of Problems of Heat Conduction in Anisotropic Media," J. Heat Mass Transfer, Vol. 16, 1905-1918, 1971.

129. Horway, G., R. Mani, M. A. Veluswami, and G. E. Zinsmeister, "Transient Heat Conduction in Laminated Composites," J. Heat Transfer, Vol. 5, 309-316, 1973.

130. Chu, H. S., C. Weng, and C. Chen, "Transient Response of a Composite Straight Fin," J. Heat Transfer, Vol. 105, 307-311, 1983.

131. Kostoff, R. H., "Temperature Prediction and Control in Pulsed Fusion-Hybrid Neutron Multipliers," J. of Fusion Energy, Vol. 4, #4, 277-287, 1985.

132. Coppari, L. A. and J. R. Thomas, Jr., "Temperature Decay in a Composite Geometry Reactor Vessel Subjected to Thermal Shock: Two-Dimensional Solution," Nuclear Engineering and Design, Vol. 44, #2, 211-225, 1977.

133. Coppari, L. A. and J. R. Thomas, Jr., "Two-Dimensional Steady Temperature Distribution in a Composite Geometry Reactor Vessel Subjected to Nuclear Radiation: An Analytical Solution," Nuclear Engineering and Design, Vol. 41, #3, 361-373, 1977.

134. Calder, K. D., R. Sue, and E. Aly, "Modelling of CW Laser Annealing of Multilayer Structures," Laser and Electron-Beam Interactions, Elsevier Publ. Co., 489-494, 1982.

135. Ramkrishna, D., and N. R. Amundson, "Transport in Composite Materials: Reduction to a Self Adjoint Formalism," Chem. Eng. Sci. Vol. 29, 1457-1464, 1974.

136. Mulholland, G. P., and M. H. Cobble, "Diffusion Through Composite Media," J. Heat Mass Transfer, Vol. 15, 147-160, 1972.

137. Yener, Y., and M. N. Ozisik, "On the Solution of Unsteady Heat Conduction in Multi-Region Finite Media with Time Dependent Heat Transfer Coefficient," Proc. 5th Int. Heat Transfer Conf., Tokyo, 188-192, 1974.

138. Tittle, C. W., "Boundary Value Problems in Composite Media: Quasi-Orthogonal Functions," J. Appl. Phys., Vol. 36, #4, 1486-1488, 1965.

139. Cobble, M. H., "Heat Transfer in Composite Media Subject to Distributed Sources, and Time-Dependent Discrete Sources and Surroundings," J. of the Franklin Institute, Vol. 290, #5, 453-465, 1970.

140. Mikhailov, M. D., M. N. Ozisik, and N. L. Vulchanov, "Diffusion in Composite Layers with Automatic Solution of the Eigenvalue Problem," Int. J. Heat Mass Transfer, Vol. 26, #8, 1131-1141, 1983.

141. Mikhailov, M. D., "General Solutions of the Diffusion Equations Coupled at Boundary Conditions," Int. J. Heat Mass Transfer, Vol. 16, 2155-2164, 1973.

142. Bulavin, P. E., and V. M. Kasheev, "Solution of the Non-Homogeneous Heat Conduction Equation for Multilayered Bodies, Int. Chem. Eng., Vol. 5, #1, 112-115, 1965.

143. Mikhailov, M. D., "General Solutions of the Coupled Diffusion Equations," Int. J. Engng. Sci., Vol. 11, 235-241, 1973.

144. Frankel, J., B. Vick, M. N. Ozisik, "Hyperbolic Heat Conduction in Composite Regions," Eighth International Heat Transfer Conference, San Francisco, August 1986.

145. Frankel, J., B. Vick, and M. N. Ozisik, "General Formulation and Analysis of Hyperbolic Heat Conduction in Composite Media," (In review, Int. J. Heat Mass Transfer).

146. Tricomi, F. G., Integral Equations, Dover, New York, 1985.

147. Hochstadt, H., Integral Equations, Wiley-Interscience, New York, 1973.

148. Mikhlin, S. G., Linear Integral Equations, Hindustan Publishing Co., Delhi, 1960.

149. Green, C. D., Integral Equations Methods, Barnes and Noble, New York, 1969.

150. Bownds, J. M., and B. Wood, "On Numerically Solving Nonlinear Volterra Integral Equations with Fewer Computations," SIAM J. Numer. Anal., Vol. 13, #5, 705-719, 1976.

151. Bownds, J. M., "A Modified Galerkin Approximation Method for Volterra Equations wtih Smooth Kernels," Applied Math. and Computations, Vol. 4, 67-79, 1978.

152. Golberg, M. N., ed., Solution Methods for Integral Equations, Plenum Press, New York, 1978.

153. Atkinson, K. E., A Survey of Numerical Methods for the Solution of Fredholm Integral Equations of the Second Kind, SIAM, Philadelphia, 1976.

154. Lambert, J. D., Computational Methods in Ordinary Differential Equations, Wiley and Sons, New York, 1977.

155. Burden, L. B., J. D. Faires, and A. C. Reynolds, Numerical Analysis, 2nd ed., Prindle, Weber and Schmidt, Boston, 1981.

156. Butcher, J. C., "Implicit Runge-Kutta Processes," Math. Comp., Vol. 18, 50-64, 1964.

157. James, M. L., G. M. Smith, and J. C. Wolford, Applied Numerical Methods for Digital Computation with Fortran and CSMP, 2nd ed., Harper and Row, Publ., New York, 1977.

158. Patankar, S. V., Numerical Heat Transfer, Wiley, New York, 1981.

159. Myers, G. E., Analytical Methods in Conduction Heat Transfer, McGraw-Hill, New York, 1971.

160. Aziz, A., and J. Y. Benzies, "Applications of Perturbation Techniques to Heat Transfer Problems with Variable Thermal Properties," Int. J. Heat Mass Transfer, Vol. 19, 271-276, 1976.

161. Aziz, A., and S. M. Enamul Huq, "Perturbation Solution for Convecting Fin with Variable Thermal Conductivity," J. Heat Transfer, Vol. 7, 300-301, 1975.

162. Vujanovic, B., "Application of the Optimal Linearization Method to the Heat Transfer Problem," Int. J. Heat Mass Transfer, Vol. 16, 1111-1117, 1973.

163. Imber, M., "Thermally Symmetric Nonlinear Heat Transfer in Solids," J. Heat Transfer, Vol. 103, 745-752, 1981.

164. Muzzio, A., "Approximate Solution for Convective Fins with Variable Thermal Conductivity," J. Heat Transfer, Vol. 8, 680-682, 1976.

165. Frankel, J. I., and B. Vick, "An Exact Methodology for Solving Nonlinear Diffusion Equations Based on Integral Transforms," (in review J. Comp. Phys.).

166. Berg, P. W., and J. L. McGregor, Elementary Partial Differential Equations, Holden-Day, San Francisco, 366, 1966.

APPENDIX 1: Development of Transform Pair in Composites

Briefly, we develop the orthogonality relation, normalization integral and the integral transform pair following similar argument as presented in [93].

First, the orthogonality relation can be derived by considering two different eigenfunctions $\psi_{im}$, $\psi_{in}$ and the associated eigenvalue problem, namely

$$[\frac{1}{\eta^p}(\eta^p\psi_{im})']' + \frac{\lambda_m^2}{c_i^*}\psi_{im}(\eta) = 0 , \tag{A.1.1}$$

$$[\frac{1}{\eta^p}(\eta^p\psi_{in})']' + \frac{\lambda_n^2}{c_i^*}\psi_{in}(\eta) = 0 . \tag{A.1.2}$$

Multiplying (A.1.1) by $\eta^p\psi_{in}$ and (A.1.2) by $\eta^p\psi_{im}$ and subtracting yields

$$\eta^p\psi_{in}[\frac{1}{\eta^p}(\eta^p\psi_{im})']' - \eta^p\psi_{im}[\frac{1}{\eta^p}(\eta^p\psi_{in})']' = \frac{(\lambda_n^2 - \lambda_m^2)}{c_i^*}\eta^p\psi_{im}\psi_{in}. \tag{A.1.3}$$

From considering the boundary condition, Eq. (4.3.8c) we multiply (A.1.3) by $\frac{\alpha_i^*}{k_i^*}$, integrate over each region, manipulate and sum to get

$$\sum_{i=1}^{N}\frac{\alpha_i^*}{k_i^*}\left[\psi_{in}(\eta^p\psi_{im})' - \psi_{im}(\eta^p\psi_{in})'\right]_{\eta=\eta_i}^{\eta_{i+1}} =$$

(A.1.4)

$$(\lambda_n^2 - \lambda_m^2) \sum_{i=1}^{N} \frac{\alpha_i^*}{k_i^* c_i^*} \int_{\eta=\eta_i}^{\eta_{i+1}} \eta^p \psi_{im} \psi_{in} d\eta \ .$$

After evaluating the LHS of (A.1.4), using the homogeneous boundary conditions expressed in Eqs. (4.3.8.b-e) we get

$$(\lambda_n^2 - \lambda_m^2) \sum_{i=1}^{N} \frac{\alpha_i^*}{k_i^* c_i^*} \int_{\eta=\eta_i}^{\eta_{i+1}} \eta^p \psi_{im} \psi_{in} d\eta = 0 \quad , \lambda_n \neq \lambda_m \ . \tag{A.1.5}$$

Finally, from our construction, we arrive at the orthogonality relation

$$\sum_{i=1}^{N} \frac{\alpha_i^*}{k_i^* c_i^*} \int_{\eta_i=\eta_i}^{\eta_{i+1}} \eta^p \psi_{im} \psi_{in} d\eta = \begin{cases} 0 & , \ m \neq n \\ N(\lambda_m) & , \ m = n \ . \end{cases} \tag{A.1.6}$$

We now construct our transform pair by assuming

$$Q_i(\eta,\xi) = \sum_m \psi_{im}(\eta) \, \Gamma_m(\xi) \ . \tag{A.1.7}$$

We operate on (A.1.7) with

$$\int_{\eta=\eta_i}^{\eta_{i+1}} \frac{\alpha_i^*}{k_i^* c_i^*} \eta^p \psi_{ip}(\eta) d\eta \ , \tag{A.1.8}$$

and sum over all regions i to get

$$\sum_{i=1}^{N} \frac{\alpha_i^*}{k_i^* c_i^*} \int_{\eta=\eta_i}^{\eta_{i+1}} \eta^p Q_i(\eta,\xi) \psi_{ip}(\eta) d\eta = \tag{A.1.9}$$

$$\sum_m \Gamma_m(\xi) \sum_{i=1}^{N} \frac{\alpha_i^*}{k_i^* c_i^*} \int_{\eta=\eta_i}^{\eta_{i+1}} \eta^p \psi_{im} \psi_{ip} d\eta \ .$$

But from the orthogonality relation (A.1.6), we find

$$\Gamma_m(\xi) = \frac{1}{N(\lambda_m)} \sum_{i=1}^{N} \frac{\alpha_i^*}{k_i^* c_i^*} \int_{\eta=\eta_i}^{\eta_{i+1}} \eta^p \psi_{im}(\eta)\, Q_i\,(\eta,\xi) d\eta \ . \qquad \text{(A.1.10)}$$

For convenience, we define our integral transform pair as

Inversion Formula:

$$Q_i(\eta,\xi) = \sum_m^{\infty} \frac{\psi_{im}(\eta)\overline{Q}_m(\xi)}{N(\lambda_m)} \ , \ i = 1,2,\ldots,N \qquad \text{(A.1.11)}$$

Integral Transform:

$$\overline{Q}_m(\xi) = \sum_{i=1}^{N} \frac{\alpha_i^*}{k_i^* c_i^*} \int_{\eta=\eta_i}^{\eta_{i+1}} \eta^p \psi_{im}(\eta)\, Q_i(\eta,\xi) d\eta \ . \qquad \text{(A.1.12)}$$

APPENDIX 2: General Expression for $A_m(\xi)$

The expression for $A_m(\xi)$ is given in Eq. (4.3.12b) as

$$A_m(\xi) = \sum_{i=1}^{N} \frac{\alpha_i^*}{k_i^*} \left[\psi_{im} \frac{\partial}{\partial\eta}(\eta^p Q_i) - Q_i(\eta^p \psi_{im})'\right]_{\eta=\eta_i}^{\eta_{i+1}}$$

$$- \frac{1}{2} \sum_{i=1}^{N} \frac{\alpha_i^*}{k_i^*} \int_{\eta=\eta_i}^{\eta_{i+1}} \frac{\partial S_i}{\partial\eta} \eta^p \psi_{im}(\eta) d\eta \ . \qquad (A.2.1)$$

Incorporating the boundary conditions expressed in Eqs. (4.3.4a-d) will give an explicit expression for $A_m(\xi)$ in terms of thermal disturbances. We find

$$A_m(\xi) = \sum_{i=1}^{N-1} \psi_{im} \frac{\eta^p}{2} \left[\frac{\alpha_i^*}{k_i^*} S_i - \frac{\alpha_{i+1}^*}{k_{i+1}^*} S_{i+1}\right]_{\eta=\eta_{i+1}}$$

$$+ \frac{\alpha_1^*}{k_1^*} \left[b_1^* \psi_{im} \eta^p \left(-\frac{S_1}{2} + \frac{k_1^*}{\alpha_1^*} \frac{d\theta_{w,1}}{d\xi}\right) + a_1^* Q_{w,1} (\eta^p \psi_{im})'\right]_{\eta=\eta_1}$$

$$- \frac{\alpha_N^*}{k_N^*} \left[b_{N+1}^* \psi_{Nm} \eta^p \left(-\frac{S_i}{2} + \frac{k_N^*}{\alpha_N^*} \frac{d\theta_{w,N+1}}{d\xi}\right) - a_{N+1}^* Q_{w,N+1} (\eta^p \psi_{Nm})'\right]_{\eta=\eta_{N+1}}$$

$$- \frac{1}{2} \sum_{i=1}^{N} \frac{\alpha_i^*}{k_i^*} \int_{\eta=\eta_i}^{\eta_{i+1}} \frac{\partial S_i}{\partial\eta} \eta^p \psi_{im}(\eta) d\eta \ . \qquad (A.2.2)$$

APPENDIX 3: Development of $B_{\ell m}$ and $B_{mm}$

In Eq. (4.3.14) we defined $B_{\ell m}$ as

$$B_{\ell m} \equiv \sum_{i=1}^{2} \frac{\alpha_i^*}{k_i^* c_i^* \tau_i^*} \int_{\eta=\eta_i}^{\eta_{i+1}} \psi_{i\ell}(\eta)\psi_{im}(\eta)d\eta \ . \qquad (A.3.1)$$

Observe that (A.3.1) is very similar to the orthogonality relation (A.1.6) except for the appearance of $\tau_i^* = \alpha_i^*/c_i^*$. The $\tau_i^*$ is the term which essentially made the flux field equation Eq. (4.3.3a) nonseparable. Two cases should be considered when developing analytical expressions for $B_{\ell m}$, namely $\ell = m$ and $\ell \neq m$.

Starting from the associated eigenvalue problem, and following a similar procedure as before (Appendix I), we get

$$\psi_i'' + \frac{\lambda^2}{c_i^*} \psi_i = 0 \ , \qquad (A.3.2)$$

$$\psi_{im}'' + \frac{\lambda_m^2}{c_i^*} \psi_{im} = 0, \ i = 1,2,\ldots,N. \qquad (A.3.3)$$

where $\lambda$ in (A.3.2) is not necessarily an eigenvalue [166].

Multiplying (A.3.2) by $\psi_{im}$ and (A.3.3) by $\psi_i$, subtracting and multiplying by $\frac{\alpha_i^*}{\tau_i^* k_i^*}$, integrating over each region i and finally summing over all regions, we get

$$\sum_{i=1}^{2} \frac{\alpha_i^*}{\tau_i^* k_i^* c_i^*} \int_{\eta=\eta_i}^{\eta_{i+1}} \psi_i(\eta)\psi_{im}(\eta)d\eta$$

(A.3.4)

$$= \frac{1}{\lambda_m^2 - \lambda^2} \cdot \sum_{i=1}^{2} \frac{\alpha_i^*}{k_i^* c_i^*} \left[\psi_i' \psi_{im} - \psi_{im}' \psi_i\right]_{\eta=\eta_i}^{\eta_{i+1}},$$

where $\alpha_i^*/c_i^* = \tau_i^*$. For $\ell \neq m$, we let $\lambda \to \lambda_\ell$ and find

$$B_{\ell m} = \frac{1}{\lambda_\ell^2 - \lambda_m^2} \cdot \sum_{i=1}^{2} \frac{\alpha_i^*}{k_i^* \tau_i^*} \left[\psi_{im}' \psi_{i\ell} - \psi_{i\ell}' \psi_{im}\right]_{\eta=\eta_i}^{\eta_{i+1}}, \quad \ell \neq m. \tag{A.3.5}$$

The special case where $m = \ell$ is a bit more complicated. In (A.3.4), if $\lambda = \lambda_m$, a division by zero would occur, that is, the RHS of (A.3.4) is indeterminate as $\lambda \to \lambda_m$. We must therefore apply L'Hopital's rule and take the limit as $\lambda \to \lambda_m$ to get

$$B_{mm} = \lim_{\lambda \to \lambda_m} \sum_{i=1}^{2} \frac{\alpha_i^*}{\tau_i^* k_i^* c_i^*} \int_{\eta=\eta_i}^{\eta_{i+1}} \psi_i(\eta) \psi_{im}(\eta) d\eta$$

(A.3.6)

$$= \lim_{\lambda \to \lambda_m} \left\{ -\frac{1}{2\lambda} \sum_{i=1}^{2} \frac{\alpha_i^*}{k_i^* \tau_i^*} \left[\frac{d\psi_i'}{d\lambda} \psi_{im} - \psi_{im}' \frac{d\psi_i}{d\lambda}\right]_{\eta=\eta_i}^{\eta_{i+1}} \right\}.$$

APPENDIX 4: Determination of eigenfunctions, eigenvalues, and $B_{\ell m}$ for composite problem with step change in wall temperature

We can evaluate (A.3.5) and (A.3.6) using the eigenfunctions

$$\psi_{1m}(\eta) = \cos \frac{\lambda_m \eta}{\sqrt{c_1^*}} \tag{A.4.1a}$$

$$\psi_{2m}(\eta) = R(\lambda_m) \sin \frac{\lambda_m(\eta_3-\eta)}{\sqrt{c_2^*}} \tag{A.4.1b}$$

where

$$R(\lambda_m) = \cos \frac{\lambda_m \eta_2}{\sqrt{c_1^*}} \Big/ \sin \frac{\lambda_m(\eta_3 - \eta_2)}{\sqrt{c_2^*}} , \tag{A.4.1c}$$

whose eigenvalues are defined as the positive roots of

$$\frac{\alpha_2^*}{k_2^*\sqrt{c_2^*}} \cos \frac{\lambda_m \eta_2}{\sqrt{c_1^*}} \cos \frac{\lambda_m(\eta_3-\eta_2)}{\sqrt{c_2^*}} - \frac{\alpha_1^*}{k_1^*\sqrt{c_1^*}} \sin \frac{\lambda_m \eta_2}{\sqrt{c_1^*}} \sin \frac{\lambda_m(\eta_3-\eta_2)}{\sqrt{c_2^*}} = 0 , \tag{A.4.2}$$

to get

$$B_{mm} = \frac{1}{2\lambda_m} \left\{ \frac{\alpha_1^*}{\tau_1^* k_1^*} \left[ \frac{1}{\sqrt{c_1^*}} \cos \frac{\lambda_m \eta_2}{\sqrt{c_1^*}} \sin \frac{\lambda_m \eta_2}{\sqrt{c_1^*}} + \frac{\lambda_m \eta_2}{c_1^*} \right] \right.$$

$$+\frac{\alpha_2^*}{\tau_2^* k_2^*} R^2(\lambda_m)\left[\frac{\lambda_m(\eta_3-\eta_2)}{c_2^*}-\frac{1}{\sqrt{c_2^*}}\sin\frac{\lambda_m(\eta_3-\eta_2)}{\sqrt{c_2^*}}\cos\frac{\lambda_m(\eta_3-\eta_2)}{\sqrt{c_2^*}}\right]\Big\}\,,$$

$$m=\ell\,,$$

and

$$B_{\ell m}=\frac{1}{\lambda_\ell^2-\lambda_m^2}\left\{\frac{\alpha_1^*}{\tau_1^* k_1^* \sqrt{c_1^*}}\left[-\lambda_m \sin\frac{\lambda_m \eta_2}{\sqrt{c_1^*}}\cos\frac{\lambda_\ell \eta_2}{\sqrt{c_1^*}}+\lambda_\ell \sin\frac{\lambda_\ell \eta_2}{\sqrt{c_1^*}}\cos\frac{\lambda_m \eta_2}{\sqrt{c_1^*}}\right]\right.$$

(A.4.4)

$$+\frac{\alpha_2^*}{\tau_2^* k_2^* \sqrt{c_2^*}}\left[R(\lambda_m)R(\lambda_\ell)\lambda_m \cos\frac{\lambda_m(\eta_3-\eta_2)}{\sqrt{c_2^*}}\sin\frac{\lambda_\ell(\eta_3-\eta_2)}{\sqrt{c_2^*}}\right.$$

$$\left.\left.-R(\lambda_m)R(\lambda_\ell)\lambda_\ell \cos\frac{\lambda_\ell(\eta_3-\eta_2)}{\sqrt{c_2^*}}\sin\frac{\lambda_m(\eta_3-\eta_2)}{\sqrt{c_2^*}}\right]\right\}\,,\quad m\neq\ell\,.$$

APPENDIX 5: Determination of eigenfunctions, eigenvalues, and $B_{\ell m}$ for composite problem with pulsed heat source.

We evaluate (A.3.5) and (A.3.6) using the eigenfunctions

$$\psi_{1m}(\eta) = \sin \frac{\lambda_m \eta}{\sqrt{c_1^*}} , \tag{A.5.1a}$$

$$\psi_{2m}(\eta) = R(\lambda_m) \sin \frac{\lambda_m(\eta_3-\eta)}{\sqrt{c_2^*}} , \tag{A.5.1b}$$

where

$$R(\lambda_m) = \sin \frac{\lambda_m \eta_2}{\sqrt{c_1^*}} \Big/ \sin \frac{\lambda_m(\eta_3 - \eta_2)}{\sqrt{c_2^*}} , \tag{A.5.1c}$$

whose eigenvalues are defined as the positive roots of

$$\frac{\alpha_2^*}{k_2^*\sqrt{c_2^*}} \sin \frac{\lambda_m \eta_2}{\sqrt{c_1^*}} \cos \frac{\lambda_m(\eta_3-\eta_2)}{\sqrt{c_2^*}} + \frac{\alpha_1^*}{k_1^*\sqrt{c_1^*}} \cos \frac{\lambda_m \eta_2}{\sqrt{c_1^*}} \sin \frac{\lambda_m(\eta_3-\eta_2)}{\sqrt{c_2^*}} = 0 , \tag{A.5.2}$$

to get

$$B_{\ell m} = \frac{1}{\lambda_\ell^2-\lambda_m^2} \cdot \Big\{ \frac{\alpha_1^*}{k_1^*\tau_1^*\sqrt{c_1^*}} \cdot \Big[ \lambda_m \cos \frac{\lambda_m \eta_2}{\sqrt{c_1^*}} \sin \frac{\lambda_\ell \eta_2}{\sqrt{c_1^*}} - \lambda_\ell \cos \frac{\lambda_\ell \eta_2}{\sqrt{c_1^*}} \sin \frac{\lambda_\ell \eta_2}{\sqrt{c_1^*}} \Big]$$

$$+ \frac{\alpha_2^*}{k_2^*\tau_2^*\sqrt{c_2^*}} R(\lambda_m)R(\lambda_\ell)\Big[\lambda_m \cos \frac{\lambda_m(\eta_3-\eta_2)}{\sqrt{c_2^*}} \sin \frac{\lambda_\ell(\eta_3-\eta_2)}{\sqrt{c_2^*}} \tag{A.5.3}$$

$$-\lambda_\ell \cos \frac{\lambda_\ell(\eta_3-\eta_2)}{\sqrt{c_2^*}} \sin \frac{\lambda_m(\eta_3-\eta_2)}{\sqrt{c_2^*}} ]\} \ , \ \ell \neq m \ ,$$

and

$$B_{mm} = -\frac{1}{2\lambda_m} \{\frac{\alpha_1^*}{k_1^*\tau_1^*\sqrt{c_1^*}} [\cos \frac{\lambda_m\eta_2}{\sqrt{c_1^*}} \sin \frac{\lambda_m\eta_2}{\sqrt{c_1^*}} - \frac{\lambda_m\eta_2}{\sqrt{c_1^*}}] \tag{A.5.4}$$

$$+ \frac{\alpha_2^*}{k_2^*\tau_2^*\sqrt{c_2^*}} \cdot R^2(\lambda_m) [\cos \frac{\lambda_m(\eta_3-\eta_2)}{\sqrt{c_2^*}} \sin \frac{\lambda_m(\eta_3-\eta_2)}{\sqrt{c_2^*}} - \frac{\lambda_m(\eta_3-\eta_2)}{\sqrt{c_2^*}} ]\}$$

where $R(\lambda_m)$ is defined in (A.5.1c).

APPENDIX 6: Development of $A_{m\ell k}$

In Eq. (5.3.13b) the constants $A_{m\ell k}$ were defined as

$$A_{m\ell k} = \int_{\eta=0}^{\eta_o} \psi_m(\eta)\, \psi_\ell(\eta)\, \psi_k(\eta)\, d\eta \ . \qquad (A.6.1)$$

This integral may be evaluated analytically from the associated eigenvalue problem in a similar manner as one develops the orthogonality relation. Consider

$$\psi_m'' + \lambda_m^2\, \psi_m = 0 \ , \qquad (A.6.2a)$$

$$\psi_\ell'' + \lambda_\ell^2\, \psi_\ell = 0 \ , \qquad (A.6.2b)$$

$$\psi_k'' + \lambda_k^2\, \psi_k = 0 \ , \qquad (A.6.2c)$$

We multiply (A.6.2a) by $\frac{\psi_\ell\, \psi_k}{\lambda_m}$, (A.6.2b) by $\frac{\psi_m\, \psi_k}{\lambda_\ell}$, (A.6.2c) by $\frac{\psi_m\, \psi_\ell}{\lambda_k}$, to get

$$\frac{\psi_\ell\, \psi_k\, \psi_m''}{\lambda_m} + \lambda_m\, \psi_m\, \psi_\ell\, \psi_k = 0 \ , \qquad (A.6.3a)$$

$$\frac{\psi_m\, \psi_k\, \psi_\ell''}{\lambda_\ell} + \lambda_\ell\, \psi_m\, \psi_\ell\, \psi_k = 0 \ , \qquad (A.6.3b)$$

$$\frac{\psi_m\, \psi_\ell\, \psi_k''}{\lambda_k} + \lambda_k\, \psi_m\, \psi_\ell\, \psi_k = 0 \ . \qquad (A.6.3c)$$

We now incorporate addition and subtraction of various combinations of (A.6.3a-c). Adding Eqs. (A.6.3a-c) gives

$$-(\lambda_m + \lambda_\ell + \lambda_k)\ \psi_m\ \psi_\ell\ \psi_k = \frac{\psi_m''\ \psi_\ell\ \psi_k}{\lambda_m} + \frac{\psi_\ell''\ \psi_m\ \psi_k}{\lambda_\ell} + \frac{\psi_m\ \psi_\ell\ \psi_k''}{\lambda_k} . \qquad \text{(A.6.4a)}$$

Adding Eqs. (A.6.3a,b) and subtracting (A.6.3c)

$$-(\lambda_m + \lambda_\ell - \lambda_k)\ \psi_m\ \psi_\ell\ \psi_k = \frac{\psi_m''\ \psi_\ell\ \psi_k}{\lambda_m} + \frac{\psi_\ell''\ \psi_m\ \psi_k}{\lambda_\ell} - \frac{\psi_k''\ \psi_m\ \psi_\ell}{\lambda_k} . \qquad \text{(A.6.4b)}$$

Adding Eqs. (A.6.3a,c) and subtracting Eq. (A.6.3b)

$$-(\lambda_m - \lambda_\ell + \lambda_k)\ \psi_m\ \psi_\ell\ \psi_k = \frac{\psi_m''\ \psi_\ell\ \psi_k}{\lambda_m} - \frac{\psi_\ell''\ \psi_m\ \psi_k}{\lambda_\ell} + \frac{\psi_k''\ \psi_m\ \psi_\ell}{\lambda_k} . \qquad \text{(A.6.4c)}$$

Adding Eqs. (A.6.3b,c) and subtracting Eq. (A.6.3a)

$$-(-\lambda_m + \lambda_\ell + \lambda_k)\ \psi_m\ \psi_\ell\ \psi_k = \frac{-\psi_m''\ \psi_\ell\ \psi_k}{\lambda_m} + \frac{\psi_\ell''\ \psi_m\ \psi_k}{\lambda_\ell} + \frac{\psi_k''\ \psi_m\ \psi_\ell}{\lambda_k} . \qquad \text{(A.6.4d)}$$

Dividing Eqs. (A.6.4a-d) by eigenvalues in front of $\psi_m\ \psi_\ell\ \psi_k$ then adding, we find after a lengthy but straightforward set of manipulations

$$\begin{aligned}\psi_m\ \psi_\ell\ \psi_k = -\frac{1}{4}\Bigg\{ & \frac{1}{\lambda_m + \lambda_\ell + \lambda_k}\left[\frac{\psi_m'\ \psi_\ell\ \psi_k}{\lambda_m} + \frac{\psi_\ell'\ \psi_m\ \psi_k}{\lambda_\ell} + \frac{\psi_k'\ \psi_m\ \psi_\ell}{\lambda_k} - \frac{\psi_m'\ \psi_\ell'\ \psi_k'}{\lambda_m\ \lambda_\ell\ \lambda_k}\right]' \\ & + \frac{1}{\lambda_m + \lambda_\ell - \lambda_k}\left[\frac{\psi_m'\ \psi_\ell\ \psi_k}{\lambda_m} + \frac{\psi_\ell'\ \psi_m\ \psi_k}{\lambda_\ell} - \frac{\psi_k'\ \psi_m\ \psi_\ell}{\lambda_k} + \frac{\psi_m'\ \psi_\ell'\ \psi_k'}{\lambda_m\ \lambda_\ell\ \lambda_k}\right]' \qquad \text{(A.6.5)} \\ & + \frac{1}{\lambda_m - \lambda_\ell + \lambda_k}\left[\frac{\psi_m'\ \psi_\ell\ \psi_k}{\lambda_m} - \frac{\psi_\ell'\ \psi_m\ \psi_k}{\lambda_\ell} + \frac{\psi_k'\ \psi_m\ \psi_\ell}{\lambda_k} + \frac{\psi_m'\ \psi_\ell'\ \psi_k'}{\lambda_m\ \lambda_\ell\ \lambda_k}\right]'\end{aligned}$$

$$+\frac{1}{-\lambda_m+\lambda_\ell+\lambda_k}\left[\frac{-\psi_m'\,\psi_\ell\,\psi_k}{\lambda_m}+\frac{\psi_\ell'\,\psi_m\,\psi_k}{\lambda_\ell}+\frac{\psi_k'\,\psi_m\,\psi_\ell}{\lambda_k}+\frac{\psi_m'\,\psi_\ell'\,\psi_k'}{\lambda_m\,\lambda_\ell\,\lambda_k}\right]'\Big\}$$

Straightfoward integration of Eq. (A.6.5) produces $A_{m\ell k}$ when $\lambda_m + \lambda_\ell - \lambda_k^{\circ} \neq 0$ and $\lambda_m - \lambda_\ell + \lambda_k \neq 0$ and $-\lambda_m + \lambda_\ell + \lambda_k \neq 0$. Otherwise, we incorporate L'Hopital's rule on Eq. (A.6.5), then integrate to obtain the desired integral.

**The vita has been removed from the scanned document**